

MALDI Mass Spectrometry and Ionic Liquids

Applications in Functional Protein Analysis

Dissertation
zur Erlangung des Grades
des Doktors der Naturwissenschaften
der Naturwissenschaftlich-Technischen Fakultät III
Chemie, Pharmazie, Bio- und Werkstoffwissenschaften
der Universität des Saarlandes

von
Masoud Zabet Moghaddam

Saarbrücken, Germany

2006

Tag des Kolloquiums

13. Nov. 2006

Dekan

Kaspar Hegetschweiler

Berichterstatter

Prof. Dr. Elmar Heinzle

Prof. Dr. Christian Huber

Acknowledgements

This dissertation is the result of three and a half years of work during which I have been supported by many people. It is with great thanks to God and much pleasure that I now have the chance to express my gratitude to all of them.

My first thanks must go to my advisor Prof. Elmar Heinzle whose support and stimulating suggestions helped me significantly during my research. He is not only a great scientist with deep vision but also and most importantly a kind person.

To my official referee Prof. Christian Huber, warmest thanks to you for the reviewing of this dissertation.

I would also like to thank my supervisor Dr. Andreas Tholey who kept an eye on my progress and was always available when I needed his advice. I am deeply indebted to him for all of our monthly, weekly and even daily discussions which shaped my ideas in the best way. It was a great pleasure for me to complete this project under his supervision.

Special thanks to my colleagues at the Technische Biochemie. You all gave me the feeling of being at home. I especially wish to thank our functional proteomics group (Ditte Bungert, Nathalie Selevsek and Maria Lasasosa) with whom I had invaluable discussions. Additionally, I would like to thank Ditte Bungert for reading parts of my dissertation and providing me with helpful comments.

I owe my sincere gratitude to my colleague Rahul Deshpande for his unconditional support and inspiration during my research. Thank you Rahul for your meticulous attention to the small details of this dissertation – you are the best.

I wish to thank Nathanael Delmotte (Department of Instrumental Analysis and Bioanalysis, University of Saarland) for the help with LC-UV analysis.

I would like to thank Bundesministerium für Bildung und Forschung (BMBF) for their financial assistance. I am grateful for their support during this process.

I humbly extend my most heartfelt appreciation to my parents who taught me love and patience. I must acknowledge my mother whose prayers were the most protecting of all that I am as a son, young man, friend and scholar – thank you very much Maman. I am equally grateful to my father who showed me the value of hard work by his own example. I wish to thank my sisters (Malihe and Mansooreh) and my brother-in-law (Ali agha Mousavi) for their encouraging words that always made me hopeful. I also owe a huge debt of gratitude to my

dear brother Majid whose loyalty to me and my family made situation easier for me to pursue my studies.

This acknowledgement would be incomplete if I did not mention the name of my two lovely friends, Abji and Khanum jane aziz (Ali and Mitra), without whom I would have never achieved this success.

I am indebted to you all. Thank you.

Contents

1	Abstract.....	1
1	Zusammenfassung	3
2	Introduction.....	5
2.1	Application of ionic liquids.....	6
2.1.1	Analytical application of ionic liquids.....	6
2.1.2	Ionic liquids as solvent for chemical reaction.....	7
2.1.3	Biocatalysis in ionic liquids.....	7
2.2	Mass Spectrometry.....	8
2.2.1	MALDI-TOF-MS	9
2.2.2	Sample homogeneity, a rate limiting step in application of MALDI for qualitative and quantitative analysis.....	10
2.2.2.1	Liquid Matrices.....	12
2.2.2.2	Ionic Liquid Matrices (ILMs).....	13
2.3	Goals of the work	14
2.3.1	Ionic Liquid Matrices (ILMs).....	14
2.3.2	MALDI-MS for Analysis of Ionic Liquids Containing Samples.....	14
2.3.3	Ion Formation in MALDI	15
3	Materials and Methods.....	16
3.1	Materials	16
3.2	Methods.....	17
3.2.1	MALDI instrumentation	17
3.2.2	Protein digestion protocol.....	17
3.2.3	Ionic Liquid Matrices (ILMs).....	18
3.2.3.1	MALDI sample preparation.....	18
3.2.3.2	Calibration curves with internal standard (for low molecular weight analytes).....	19
3.2.3.3	Calibration curves without internal standard (for peptides and proteins).....	20
3.2.3.4	Enzyme kinetic.....	20

3.2.3.5	Derivatization of peptides	21
3.2.3.6	MALDI-TOF analysis.....	22
3.2.3.7	Database search.....	23
3.2.4	Ionic Liquid (IL)	23
3.2.4.1	Sample preparation	23
3.2.4.2	Monitoring of D-amino acid oxidase activity	25
3.2.4.3	MALDI-ToF analysis.....	25
4	Ionic Liquid Matrices (ILMs).....	27
4.1	Qualitative analysis and stability of ILMs	27
4.2	Sample homogeneity	31
4.3	Analysis of low molecular weight compounds in ILMs	32
4.3.1	Quantification of low molecular weight compounds applying internal standards	36
4.4	Qualitative analysis of peptides and proteins in ILMs	39
4.5	Quantification of peptides using isotopically labeled internal standard.....	42
4.6	Influence of the molar matrix-to-analyte ratio on the ion response in ILM... 	43
4.6.1	Quantification of a mixture of peptides without IS	47
4.6.2	Monitoring of enzyme catalyzed reactions without IS	48
4.6.2.1	Monitoring of the tryptic digest of single peptide.....	48
4.6.2.1.1	Enzyme kinetic study	51
4.6.2.2	Semi-quantitative monitoring of multi-substrate conversions	52
4.6.3	Quantification of proteins without IS	57
4.6.3.1	Monitoring of tryptic digest of BSA as model protein	59
4.7	Pyridinium-based ionic liquid matrices for proteome analysis	60
4.7.1	Properties of the pyridinium-based ionic liquid matrices, analysis of model peptides and optimization of molar acid-base ratios	61
4.7.2	Analysis of tryptic protein digests in pyridinium-based ILM.....	66
5	MALDI-MS for Analysis of Ionic Liquids (ILs) Containing Samples	75
5.1	Characterization of ILs.....	75

5.1.1	LDI-mode analysis.....	75
5.1.2	MALDI-mode analysis	76
5.2	Analysis of small molecules dissolved in ILs.....	78
5.2.1	Quantification of low molecular weight compounds in IL	82
5.3	Analysis of peptides and proteins in IL.....	83
5.4	Monitoring of the enzymatic reaction of D-amino acid oxidase in the presence of IL	86
6	Ion Formation in MALDI	90
6.1	Comparison of IL with ILM.....	93
6.2	Ion formation in LDI and MALDI analysis of ILs.....	95
6.2.1	Adduct formation between IL-cations and IL-anions.....	95
6.2.2	Absence of metal ion adducts	96
6.2.3	Absence of Adducts between IL-cations/anions and analytes.....	96
6.2.4	Laser threshold and peak broadening in dependence of analyte size	97
6.2.5	Matrix dependent formation of [Cat+H] ⁺ -ions	98
6.2.6	Influence of IL water miscibility on analyte response.....	98
7	Conclusions and Outlook	100
7.1	ILMs	100
7.2	ILs	103
8	References.....	104
9	Appendix.....	118
9.1	Abbreviations.....	118
9.2	Publications.....	120

1 Abstract

The use of ionic liquids as matrices for matrix assisted laser desorption/ionization-mass spectrometry (MALDI-MS) was investigated. Traditionally used ionic liquids are unsuitable as matrices in MALDI analysis. A new class of ionic liquids was explored, the so-called *ionic liquid matrices* (ILMs) that show great promise as matrices. ILMs are equimolar mixtures of solid MALDI-matrices, 2,5-dihydroxybenzoic acid (DHB), α -cyano-4-hydroxycinnamic acid (CCA), sinapinic acid (SA) or indoleacrylic acid (InAA) with organic bases. These allowed the formation of a thin liquid layer on the target having negligible vapour pressure. The main advantage of using ILMs was found in remarkable enhancement in sample homogeneity leading to increase spot-to-spot and shot-to-shot reproducibility.

The ILMs were used for the analysis of low molecular weight compounds such as amino acids, sugars and vitamins, and also large biomolecules like peptides and proteins. The high sample homogeneity achieved using ILMs facilitated the measurement by eliminating the laborious searching for the analyte on the target spot. In conjunction with the use of a proper internal standard, the relative quantification of amino acids was improved using ILM when compared to using crystallized matrixes. An additional advantage was the significantly reduced measurement time in an automated measurement.

The ability of ILMs to perform quantification of peptides and proteins without using internal standards was also investigated. It was found that there is a linear correlation between the amount of analyte on the target and their signal intensities when increased molar matrix-to-analyte ratios are used. The dynamic range of linearity was about one order of magnitude. The method was further applied successfully for screening of the trypsin-catalyzed reaction of single peptide. Moreover, semi-quantitative monitoring of multi-substrate (peptide mixtures) cleavage catalyzed by trypsin was shown.

Pyridinium-based ILM in substoichiometric amount of pyridine (Py) with CCA (molar ratio of CCA:Py = 2:1) improved the measurement of peptides compared to using CCA in terms of signal-to-noise ratios, reduction of chemical noise and reduced formation of alkali adducts and matrix-clusters. This optimized ILM was used for the measurement of tryptic in-solution as well as in-gel digests of the model proteins. As a result, the identification of proteins by peptide mass fingerprint (PMF) was facilitated compared to using CCA in database search engine, yielding higher scores and increased sequence coverage.

In the second part of work, MALDI-MS was applied for the characterization of five different ionic liquids and the analysis of amino acids, peptides and proteins dissolved in ionic liquids. The ionic liquids were characterized both by laser desorption/ionization (LDI) and by MALDI-MS. The signals of both cations and anions of ionic liquids could be observed in both methods. In the latter case, adduct formations between cations and anions of ionic liquids were identified. Analysis of the amino acids, peptides and proteins dissolved in ionic liquids could be performed after addition of matrix molecules. Interestingly, no sodium or potassium adducts could be observed for any analyte tested here. Typically, low molecular weight compounds and peptides could be analyzed better in water-immiscible ionic liquids whereas proteins gave the better results in water-miscible ionic liquids. The homogeneity of samples was reduced in the presence of ionic liquids when compared to classical MALDI preparations. However relative quantification of amino acids using isotope-labeled internal standard was possible. Thus D-amino acid oxidative reaction catalyzed by D-amino acid oxidase which was carried out in ionic liquids could be monitored by MALDI-MS.

In the last part of work basic MALDI mechanistic principles by the use of ILMs was investigated and theoretical aspects of ion formation in the presence of ionic liquids both in LDI and MALDI analysis are discussed.

1 Zusammenfassung

In der vorliegenden Arbeit wurde die Anwendung von ionischen Lösungen als Matrix für die Matrix unterstützte Laser-Desorption/Ionisation (Matrix Assisted Laser Desorption/Ionization-Mass Spectrometry; MALDI-MS) untersucht. Da die traditionellen ionischen Lösungen als Matrix für MALDI Analysen unbrauchbar sind, wurde hier eine neue Klasse von Ionischen Lösungen untersucht, die so genannten *Ionic Liquid Matrices* (ILMs). ILMs sind equimolare Mixturen von festen MALDI Matrices, wie etwa 2,5-Dihydroxybenzoesäure (DHB), α -Cyano-4-hydroxymizsäure (CCA), 3-Hydroxy-4-methoxymizsäure (Sinapinic Acid; SA) oder 3-(1-H-Indol-3-yl)-2-propionsäure (Indoleacrylic Acid; InAA), mit organischen Basen. Diese Anwendung ermöglichte die Ausbildung von dünnen Schichten der Lösungen auf der Probenplatte mit vernachlässigbarem Dampfdruck. Der hauptsächliche Vorteil in der Nutzung von ILMs verdeutlichte sich in der bemerkenswerten Verbesserung der Probenhomogenität und in einer erhöhten spot-to-spot und shot-to-shot Reproduzierbarkeit.

Die ILMs wurden für die Analyse von Komponenten mit niedrigen molekularen Massen, wie etwa Aminosäuren, Zuckern und Vitaminen, aber auch von grossen Biomolekülen, wie Peptide und Proteine benutzt. Die durch die Anwendung von ILMs erhaltene hohe Probenhomogenität erleichterte die Messungen durch die Eliminierung der mühsamen Suche nach den Analyten auf den Spots der Probenplatte. Im Vergleich zu kristallisierten Matrices konnte durch die Anwendung von ionischen Lösungen mit geeigneten internen Standards die relative Quantifizierung von Aminosäuren verbessert werden. Ein zusätzlicher Vorteil in dieser Methodik war die signifikante Reduzierung der Messdauer bei automatisierten Messungen.

Des Weiteren wurde die Eignung von ILMs untersucht um Peptide und Proteine ohne interne Standards zu quantifizieren. Hierbei zeigte sich dass die Menge des Analyts auf der Probenplatte mit den Signalintensitäten linear korreliert, nachdem erhöhte molare Matrix:Analyt Verhältnisse benutzt wurden. Der dynamische Bereich der Linearität betrug hierbei eine Zehnerpotenz. Diese Methode wurde des Weiteren erfolgreich zum *Screening* von Trypsin katalysierten Reaktionen von einzelnen Peptiden benutzt und darüber hinaus ebenfalls zur semi-quantitativen Kontrolle von Multi-Substrat (Peptid Mixturen) Verdau durch Trypsin.

Auf Pyridinium basierte ILMs mit substöchiometrischen Mengen von Pyridin (Py) und CAA (CCA:Py=2:1) verbesserten die Messungen von Peptiden bezüglich des Signal- Rausch Verhältnisses, der Reduktion des chemischen Rauschen und der Reduktion von Alkali Addukt-Bildung und Matrix-Clustern im Vergleich zu Messungen nur mit CCA. Diese optimierten ILMs wurden für die Messung von tryptischen Spaltungen in Lösung wie auch In-Gel-Trypsinisierungen von Modell-Proteinen benutzt. Es konnte gezeigt werden, dass im Vergleich zu CCA die Identifikation der Proteine durch Peptide Mass Fingerprint (PMF) per Datenbanksuche deutlich verbessert wurde. Im Detail konnten höhere Score's in der Datenbanksuche und eine erhöhte Sequenzabdeckung erreicht werden.

Im zweiten Teil der Arbeit wurde MALDI-MS zur Charakterisierung von fünf unterschiedlichen ionischen Lösungsmitteln und der Analyse von in ionischen Lösungsmitteln gelösten Aminosäuren, Peptiden und Proteinen untersucht. Die ionischen Lösungsmitteln wurde sowohl durch Laser Desorbition/Ionisation (LDI) als auch per MALDI-MS charakterisiert. Die Signale der Kationen und Anionen der ionischen Lösungsmittel konnten durch beide Methoden verfolgt werden. Im letzteren Fall konnte die Bildung von Addukten zwischen den Kationen und Anionen der ionischen Lösungsmittel beobachtet werden. Die Zugabe von Matrix-Molekülen erlaubte die Analyse von in ionischen Lösungsmittel gelösten Aminosäuren, Peptiden und Proteinen. Bei keinem der getesteten Analyten konnten interessanterweise Natrium- oder Kalium-Addukte nachgewiesen werden. Typischerweise konnten Komponenten mit niedrigen molekularen Massen und Peptide in Wasser abweisenden ionischen Lösungsmittel analysiert werden. Im Vergleich zur klassischen MALDI Probenpräparation war die Homogenität der Proben in der Anwesenheit von ionischen Lösungsmittel verringert. Nichtsdestotrotz war eine relative Quantifizierung von Aminosäuren mit Hilfe von isotopisch markierten internen Standards möglich. Folglich konnten durch D-Aminosäureoxidase katalysierte oxidative Reaktionen von D-Aminosäuren mit MALDI-MS verfolgt werden.

Im letzten Teil dieser Arbeit wurden grundsätzliche mechanistische Prinzipien der MALDI in der Anwendung von ILMs untersucht und theoretische Aspekte der Ionenbildung in Anwesenheit von ionischen Lösungsmitteln sowohl in der LDI als auch MALDI diskutiert.

2 Introduction

Ionic liquids are salts having melting points below 100 °C. In fact, an ionic liquid is a liquid containing exclusively ions. Thus it theoretically includes all molten salts, for e.g. sodium chloride at temperatures higher than 800 °C. However, the term is now generally associated with salts in which the ions are poorly coordinated and thus have relatively low melting points, less than 100 °C. At least one ion has a delocalized charge and one component is organic, which prevents the formation of a stable crystal lattice (Holbrey and Rogers, 2003). Due to their potential to replace hazardous, flammable and environmentally damaging volatile organic solvents in many fields, they have attracted much attention in the recent years (Figure 2.1). Ionic liquids have been called *designer solvents* (Freemantle, 1998) as their physical properties such as melting point, viscosity, density, hydrophobicity and water miscibility can be modified according to the desired applications by tuning their component cation and anion (Hagiwara and Ito, 2000). Frequently used cations are pyridinium- or imidazolium derivatives, ammonia-compounds or phosphonium ions. Inorganic or organic anions like nitrate, tetrafluoroborate, hexafluorophosphate, tosylate and triflate are frequently used as counterions (Figure 2.2). A variety of features make them attractive alternatives for the currently used solvents:

- i) They have negligible or no vapour pressure. Thus, they do not emit hazardous volatile organic compounds.
- ii) They possess good thermal stability and do not decompose over a wide range of temperature (0-250 °C) making it possible to perform reactions at high temperatures if required.
- iii) They are non-flammable, non-explosive and can be stored without decomposition for an extended period of time.

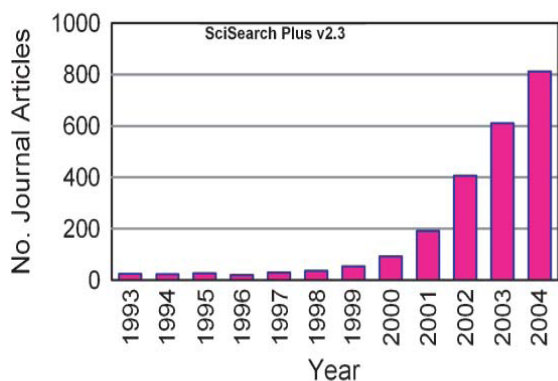


Figure 2.1: Number of journal articles dealing with ionic liquids appearing annually during the last decade. The figure was taken from reference (Baker et al., 2005).

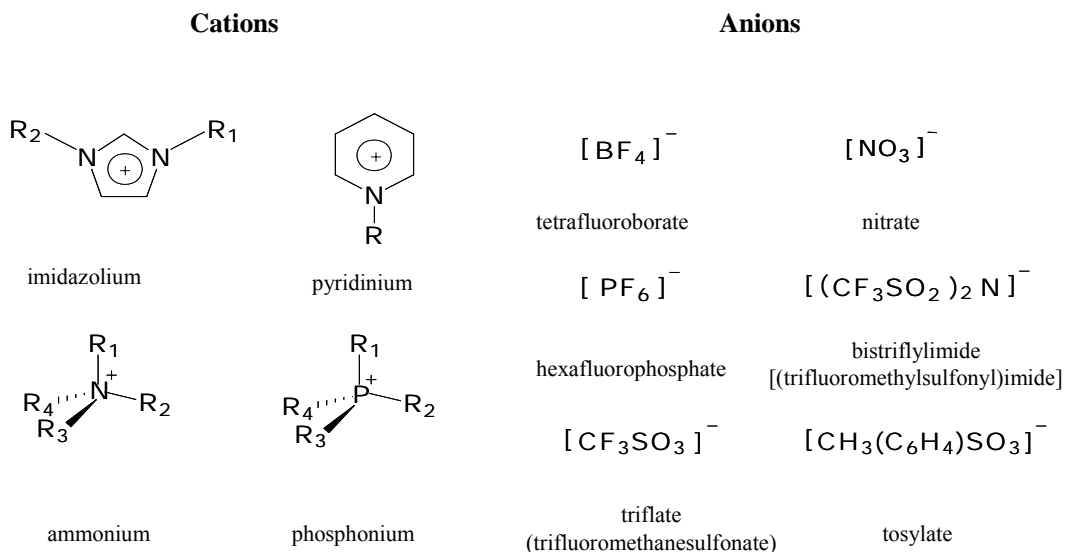


Figure 2.2: Typical cation-anion combinations for ionic liquids

iii) They can be synthesized from relatively inexpensive precursor materials. However, the synthesis of very pure ionic liquid is still expensive.

2.1 Application of ionic liquids

The applications of ionic liquids can be divided in three major groups:

- i) Analytical applications
- ii) As solvents for chemical reactions
- iii) As solvents for biocatalytic processes

2.1.1 Analytical application of ionic liquids

Ionic liquids have been used in a variety of chromatographic methods. Examples of these include their use as stationary phase in gas chromatography (GC) (Anderson and Armstrong, 2003; Armstrong et al., 1999), as additives for the mobile phase in high performance liquid chromatography (HPLC) (Xiaohua et al., 2004; Zhang et al., 2003) and as running electrolytes in capillary electrophoresis (CE) (Jiang et al., 2003; Yanes et al., 2001).

They have been also reported as suitable candidates for the replacement of volatile organic solvents in liquid-liquid extraction processes (Fadeev and Meagher, 2001; Huddleston and

Rogers, 1998; Visser et al., 2000). Ionic liquids are comprised of ions, which makes them to be potential solvents for electroanalytical applications (McEwen et al., 1999). Their potential as electrolytes in rechargeable cells, in electrodeposition of metals and their use in photochemical solar cells as well as double-layer capacitors have been described (Buzzeo et al., 2004). The use of ionic liquid for matrix-assisted laser desorption/ionization mass spectrometry (MALDI-MS) was first reported shortly by Armstrong et al. (2001).

In this work, the application of ionic liquids as matrices for MALDI-MS is intensively investigated.

2.1.2 Ionic liquids as solvent for chemical reaction

The application of ionic liquids as solvents for organic chemical synthesis and chemical reactions involving either catalysis or biocatalysis has been intensively studied (Jain et al., 2005). Diels-Alder reaction (Fischer et al., 1999), Friedel-Crafts reaction (Earle et al., 1998; Surette et al., 1996) and esterification of alcohols (Deng et al., 2001) are some of the examples of organic chemical reactions performed in ionic liquids. The transition metal-catalyzed reactions, e.g. hydrogenations (Chauvin et al., 1996), Heck reaction (Kaufmann et al., 1996) and oxidations (Song and Roh, 2000), are the major class of catalytic chemical reactions carried out in ionic liquids (Wasserscheid and Keim, 2000).

2.1.3 Biocatalysis in ionic liquids

In recent years, ionic liquids gained increasing attention in the field of enzyme-catalyzed reaction (Kragl et al., 2002). For this purpose, ionic liquids are used in three different methods in the enzyme systems, i) as a co-solvent in the aqueous phase, ii) as a pure solvent and iii) as two-phase system in combination with other solvents.

The formation of *Z*-aspartame by thermolysin (Erbeldinger et al., 2000), conversions using lipases and esterases (Kim et al., 2001; Madeira Lau et al., 2000; Park and Kazlauskas, 2001; Schöfer et al., 2001), transesterifications of short peptides and protected amino acids catalyzed by chymotrypsin (Laszlo and Compton, 2001), hydrolysis of *N*-acylamino esters by the protease subtilisin (Zhao and Malhotra, 2002), galactosidase catalyzed conversions of sugars and derivatives (Kaftzik et al., 2002) and oxidative reactions using glucose oxidase and peroxidase (Okrasa et al., 2003) are some examples of enzymatic reactions performed in

ionic liquids. Additionally, biocatalysis using whole cells in ionic liquids have been also reported (Cull et al., 2000; Pfründer et al., 2004).

For the analysis of compounds dissolved in ionic liquids, either the analytes can be separated from the ionic liquids and investigated by suited methods or they are investigated directly in the ionic liquids. A number of articles have been published in recent years reporting the analysis of reactants in these solvents. Most common methods are based on separation by HPLC (Cull et al., 2000), analysis of UV/VIS-absorption or fluorescence or NMR (Durazo and Abu-Omar, 2002). These methods can be subject to several restrictions. The separation of mixtures involving ionic liquids by HPLC is time consuming and is in many cases still a challenge. Spectroscopic techniques can suffer from background absorption/fluorescence of the ionic liquids and are difficult to perform in more complex reaction mixtures. Moreover, another problem is the need of substrates carrying chromophoric or fluorophoric groups, which are not readily available for each kind of biocatalytic conversion (Tholey and Heinzle, 2002).

The techniques used for characterization of ionic liquids include electrochemical methods, ion chromatography, reversed phase-liquid chromatography (Stepnowski et al., 2003), water determination, thermal analysis, rheology (Bonhote et al., 1996), NMR (Oxley et al., 2003) and methods for the determination of linear free energy characterizing the interactions with dissolved analytes (Anderson et al., 2002). Fast atom bombardment (FAB) (Abdul-Sada et al., 1992) and electrospray ionization (ESI) mass spectrometry (Alfassi et al., 2003) have also been used for characterization of ionic liquids and the determination of water solubility of these solvents.

Mass spectrometry is one possible alternative method for analysis of compounds dissolved in ionic liquids. The method does not need pre-purification of sample in many cases, thus, can offer direct analysis of substrates and products of enzyme-catalyzed reactions carried out in ionic liquids. Additionally, it can be used for characterization of ionic liquids. Therefore, application of mass spectrometry for these purposes is the subject of the investigations here.

2.2 Mass Spectrometry

The application of mass spectrometry (MS) for the analysis of compounds of biological relevance has been accelerated by introduction of two major ionization techniques, the matrix assisted laser desorption ionization (MALDI) (Karas and Hillenkamp, 1988; Tanaka et al.,

1988) and the electrospray ionization (ESI) (Fenn et al., 1989). These two methods have been primarily applied for the accurate determination of the molecular mass of biomolecules. Subsequent applications have been also oriented towards quantitative analysis in the field of biochemistry and biotechnology. The broad mass range of analysis (1 Da to 1000 kDa), high sensitivity (femtomole or atomole quantities) and high throughput capability have made these methods attractive alternative to the more traditional bioanalytical methods. The tolerance of MALDI against non-volatile salts is higher than ESI. Additionally, the ESI spectra include many signals of multiply charged ions, which complicate their interpretation in the case of complex samples whereas the singly or doubly charged ions (for compounds above ~10,000 Da) obtained in MALDI spectra are easier to interpret.

2.2.1 MALDI-TOF-MS

MALDI-mass spectrometry has now become the most popular method in the analysis of biomolecules such as peptides, proteins, oligonucleotides (Hillenkamp et al., 1991; Karas et al., 1987) and low molecular weight compounds of biological interest (Cohen and Gusev, 2002). Figure 2.3 illustrates the principle of MALDI-TOF-MS. The general strategy for sample preparation and analysis involves the mixing of matrix solution with the analyte solution and then depositing the matrix/analyte mixture on the target (dried droplet method). After evaporation of the solvent, the co-crystallized matrix/analyte mixture is introduced into the high vacuum of the mass spectrometer. The matrix is an organic molecule, which absorbs the laser light and then promotes desorption and ionization of the analyte. The ionized analytes are then accelerated in a high voltage region (acceleration region) and further ion separation based on the mass-to-charge ratio occurs in a field-free tube (mass analyzer). This analyzer is called Time of Flight (TOF). Since all ions receive the same energy, the lighter ions arrive earlier at the detector than heavier ones.

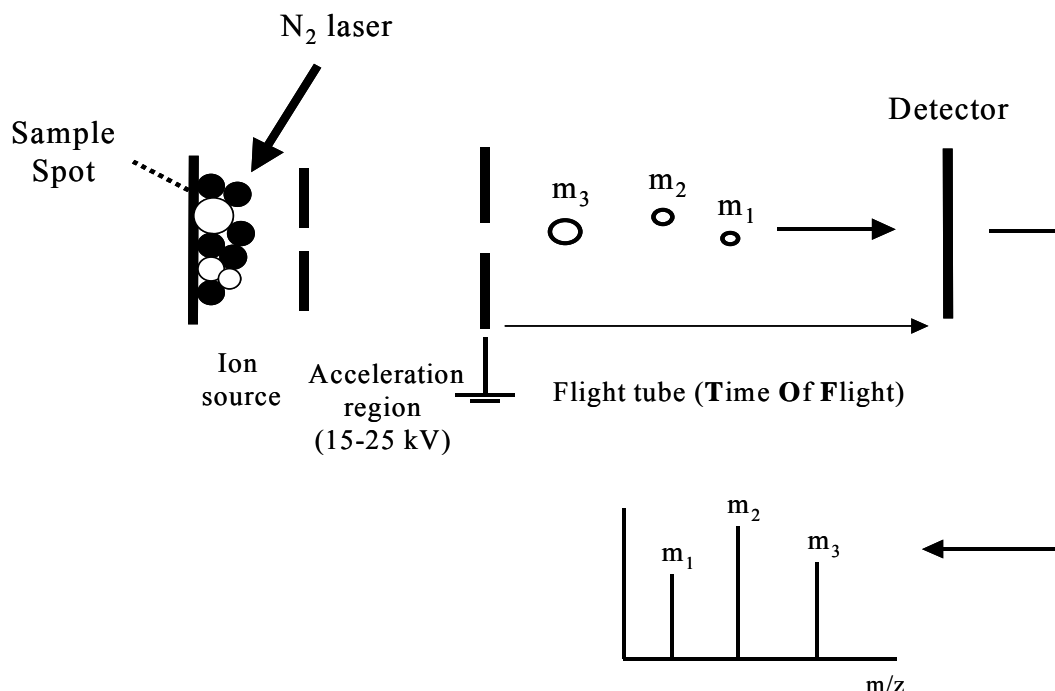


Figure 2.3: The schematic of a MALDI-TOF-MS.

2.2.2 Sample homogeneity, a rate limiting step in application of MALDI for qualitative and quantitative analysis

Sample homogeneity is one of the major concerns in MALDI analysis. The efficiency of MALDI has been shown to be highly sensitive to the sample preparation procedure. The oldest sample preparation method used in MALDI analysis is the dried-droplet method (Karas and Hillenkamp, 1988) in which the formation of analyte/matrix crystals takes place throughout the droplet as the solvent evaporates. The crystals formed upon evaporation of the solvent are usually inhomogeneous and irregularly dispersed. Hence, this inhomogeneous distribution of analyte/matrix co-crystals leads to the formations of *hot spots*. This means that not at all positions over a spot sufficient analyte signal can be found, whereas at other positions strong signals of analyte can be detected. This sample inhomogeneity forces the MALDI users to search for these hot spots to get a better analyte signal. It is also often observed the points on the sample spot with no crystals and thus no signal. This hot spot formation causes a poor shot-to-shot reproducibility and sample-to-sample reproducibility (Garden and Sweedler, 2000). Dai and coworkers applied confocal fluorescence microscope imaging to investigate the analyte distribution in the matrix crystals after the crystallization

process (Dai et al., 1996). In a similar study, more detailed investigations in this regard were reported by Horneffer and coworkers (Horneffer et al., 2001). They compared analyte localization in the matrix crystals in different sample preparation methods such as dried-droplet and thin-layer preparations. The heterogeneity within MALDI samples in two different crystallized MALDI-matrices have also been shown using mass spectrometric imaging (Garden and Sweedler, 2000). The phenomenon leading to hot spot formations is still not fully understood. However, a potential explanation can be that during co-crystallization of analyte/matrix, the analyte would be entrained in the bulk of the crystal, where it is not accessible for laser desorption. Also, the variation of the analyte signal intensity can potentially be due to the difference in the relative orientation of the matrix-analyte crystals to the spectrometric axis.

Inhomogeneity of the sample is the most serious problem hampering the use of MALDI-MS for quantitative measurements. Nevertheless, a number of publications describe the use of MALDI-MS for quantitative measurements (Nelson et al., 1994; Tang et al., 1996; Yan et al., 2002) for example for the measurement of enzyme activities (Bungert et al., 2004b; Kang et al., 2001). The hot-spot formation leads to a large variation of signal intensities from shot to shot as well as from spot to spot. As a consequence, there is little correlation of signal intensity with the amount of sample analyzed. In this regard, the use of an isotope labeled internal standard can reduce these problems. It has molecular properties similar to that of the analytes thus ensuring comparable crystallization behaviour on the target as well as similar ionization efficiency. Whereas for low molecular weight substrates and products, e.g. amino acids and sugars, the corresponding internal standards are available in many cases, this situation changes when peptides or proteins are the substrates of the enzymes. In the latter case, an internal standard must be created by stable isotope tagging of amino acids of peptides or proteins (Gygi et al., 1999; Munchbach et al., 2000; Niwayama et al., 2003; Ross et al., 2004). Another strategy is the use of non-isotope-labelled internal standards applying structurally modified compounds (Bungert et al., 2004b; Duncan et al., 1993). For example, single amino acid exchanges (Wang et al., 2004) or peptides with high molecular similarity (Helmke et al., 2004; Muddiman et al., 1994) were successfully used as internal standards for the relative quantitation of peptides.

However, despite of using an internal standard making the quantification possible, the problem of sample inhomogeneity still remains critical. That is especially true for high throughput quantitative screening process using an automated measurement, where hot spot formation leads to significant increase of measurement time. The inhomogeneities can be

partially overcome by integral measurement over the preparation with an averaging of the collected signals (Kang et al., 2001) but this procedure is also time consuming even in automated form.

Improved sample homogeneity can circumvent some of these problems. As a result, higher sensitivity can be achieved for qualitative MALDI analyses and better measurement accuracy within a shorter time is obtained in quantitative MALDI analyses. Several techniques have been developed to improve sample homogeneity in crystalline sample preparations, e.g., adding of co-matrices like fucose to form a binary matrix (Gusev et al., 1995), fast evaporation methods using highly volatile solvents (Vorm et al., 1994; Xiang and Beavis, 1994), deposition of droplets (Miliotis et al., 2002; Onnerfjord et al., 1999), by electrospray based sample deposition processes (Hensel et al., 1997), sol-gel based systems (Lin and Chen, 2002a), aerospray sample deposition using CCA-thin layer preparation (Dally et al., 2003) or the use of solvent-free sample preparations (Trimpin et al., 2001).

2.2.2.1 *Liquid Matrices*

Another alternative to improve the sample homogeneity is the employment of liquid matrices. Liquid matrices do not produce hot spots, refresh continuously their surfaces (Cramer and Burlingame, 2000), exhibit higher signal reproducibility and are miscible with polar and nonpolar analytes. Liquid matrices like glycerol have been frequently used in IR-MALDI-MS. However, due to poor absorption efficiency of these liquid matrices in the wavelength employed in UV-MALDI-MS (337 nm), their use is restricted herein. To bring forth the advantage of liquid matrices to UV-MALDI, chemical doped-liquid matrices have been developed (Sze et al., 1998; Turney and Harrison, 2004). In these, an organic compound that is able to absorb the laser light of the applied wavelength (337 nm) is added to a liquid support. In this respect, the particle suspension in a liquid medium has also been shown to meet the advantages of liquid matrices for analysis (Schürenberg et al., 1999). Nevertheless, the use of these liquid matrices is still associated with low mass resolution, extensive adduct formation and high chemical background (Schürenberg et al., 1999; Turney and Harrison, 2004).

2.2.2.2 *Ionic Liquid Matrices (ILMs)*

Ionic liquids are potential matrices for MALDI-MS due to their previously mentioned specific properties. The first attempt of using ionic liquids as matrices for MALDI-MS analysis of peptides and proteins was done by Armstrong and co-workers (Armstrong et al., 2001). It was shown that the class of ionic liquids described above is not suitable for the use as MALDI-matrices, possibly due to poor laser absorption capacity and the lack of transferable protons (Armstrong et al., 2001). In the same study they introduced a new class of ionic liquids, formed by the combination of commonly used solid MALDI-matrices with a variety of organic bases as counter ions. These substances were shown to hold the potential to be used as MALDI-matrices as they possess both, the outstanding properties of ionic liquids as well as the capability to perform the ionization and desorption process necessary for MALDI-MS. Additional to a higher signal intensity observed in some cases, the most important improvement was regarding *sample homogeneity*. Subsequently, the applications of ionic liquid matrices (ILMs) have been reported in number of publications. For example, they have been used for the improved analysis of DNA oligomers (Carda-Broch et al., 2003), oligosaccharides, peptides and proteins (Mank et al., 2004), phospholipids (Li et al., 2005), and fragmentation studies of peptides and oligonucleotides (Jones et al., 2005). They have also been employed for quantitative analysis of peptides and proteins (Li and Gross, 2004) and screening of enzymatic reactions (Bungert et al., 2004a).

2.3 Goals of the work

The major part of this work deals with the analytical application of ionic liquids as matrices for the MALDI-MS. In second part of the work, the employment of MALDI-MS as a new analytical technique for the analysis of ionic liquids and the monitoring of enzymatic reactions performed in ionic liquids is discussed. A brief discussion regarding MALDI-ionization mechanisms in ILMs as well as ionic liquids is presented in the last chapter.

2.3.1 Ionic Liquid Matrices (ILMs)

ILMs composed of solid MALDI-matrices with a variety of bases were tested with respect to their suitability for qualitative and quantitative analysis of different biologically interesting small molecules (< 500 Da) such as amino acids, sugars and vitamins. The homogeneity of samples using ILMs was compared with that achieved applying solid matrices. Additionally, the application of ILMs to achieve the goal of absolute quantification for peptides and proteins without the need for an internal standard was investigated. In this regard, parameters like matrix-to-analyte ratios necessary for the design of experiments, the dynamic range for linear correlation in the ion signal for model peptides and the limitations of the method were evaluated. ILMs were further applied for the determination of enzyme activities in protease-catalyzed reactions without internal standard. ILMs were also tested for their ability in qualitative analysis of peptides. It is shown that the use of the ILMs composed of CCA and pyridine could facilitate the identification of proteins by improving the quality of spectra and increased signal-to-noise ratios of the peptides obtained from the protein digest.

2.3.2 MALDI-MS for Analysis of Ionic Liquids Containing Samples

The aim of the latter part of work was to examine whether MALDI mass spectrometry can be used as a tool for the characterization of ionic liquids and of different biologically interesting compounds dissolved in these solvent systems. Five ionic liquids were tested and analyzed either by laser desorption ionization (LDI) mass spectrometry or after addition of MALDI-matrices. In case of analyses of compounds dissolved in ionic liquids, the method was first evaluated with amino acids as model analytes, which are interesting compounds for conversions in ionic liquids, and was then applied to the analysis of proteins and peptides.

Analysis conditions, molar matrix-to-analyte ratios, limits of detection as well as the sample homogeneity of the MALDI sample preparations were investigated and compared with preparations without ionic liquids.

The quantitative analysis directly from ionic liquid-containing solutions is highly demanded, e.g. for enzyme kinetic studies. Using a proper internal standard, the quantification of amino acids was feasible in the presence of considerable amounts of ionic liquids. Moreover, the applicability of MALDI-MS for the monitoring of an enzymatic reaction carried out in the presence of ionic liquids was shown.

2.3.3 Ion Formation in MALDI

The high sample homogeneity achieved using ILMs can allow a reliable comparison of signal intensities of analytes in different ILMs. In this regard, experiments were performed to explain the potential of the ILMs to ionize analyte molecules.

The investigations concerning the applicability of MALDI analysis to ionic liquid-containing solutions revealed some characteristic deviations compared to spectra obtained from classical MALDI preparations. These differences as well as their mechanistic implications are discussed, because they could cast some light on ion formation and adduct formation in MALDI, which is still only partially understood (Karas and Kruger, 2003).

3 Materials and Methods

3.1 Materials

All amino acids, fructose, pyridine (Py), ascorbic acid, β -D (+) glucose, α -ketoglutarate, adenosine 5-triphosphate (ATP), N, N-dimethylethylenediamine (DMED), 3-dimethylamino-1-propylamine (DMAPA), trimethylamine (TEA); MALDI-matrices α -cyano-4-hydroxycinnamic acid (CCA), 3,5-dimethoxy-4-hydroxycinnamic acid (sinapinic acid, SA), and 2,5-dihydroxybenzoic acid (DHB), 4-hydroxy-3-methoxycinnamic acid (ferulic acid, FA); peptides angiotensin II, substance P, neurotensin, ACTH (1-17), ACTH (18-39), Leu-enkephalin; proteins insulin, lysozyme (chicken egg white), cytochrome C (horse heart), bovine serum albumin (BSA), carbonic anhydrase (bovine erythrocytes), glucose oxidase (*Aspergillus niger*); buffers used for standard tryptic digestion and chemicals for polyacrylamide gel electrophoresis were provided from Sigma-Aldrich Chemical Co. (Taufkirchen, Germany). Trp¹¹-Neurotensin was from Bachem (Weil a.R., Germany). Trifluoroacetic acid (TFA), 3-indoleacrylic acid (InAA), N-acetylglucosamine, sodium D-gluconate, L-phenylglycine, 2-fluoro-DL-phenylglycine, D-phenylalanine, 1-methylimidazole (MI), arabinose, biotin, thiamine, nicotinamide adenine dinucleotide (NAD), 2-mercaptoethanol, sodium dithionite, alcohol dehydrogenase (*S. cerevisiae*) and L-lactate dehydrogenase (rabbit muscle) were purchased from Fluka (Neu-Ulm, Germany). Bradykinine was from Calbiochem (Bad Soden, Germany). Tributyl amine (TBA) was purchased from Acros Organics (Geel, Belgium). Fully ¹³C-labeled glutamine (98% L-5 ¹³C-glutamine, U¹³C-Gln), 1, 2, 3, 4, 5, 6-[ring]-¹³C-phenylalanine (6-¹³C-phenylalanine), 1-¹³C-alanine were supplied by Euroisotop (Gif-sur-Yvette, France). D₂O and NaOD were obtained from Deutero GmbH (Kastellaun, Germany). Immobilized D-amino acid oxidase enzyme (DAAO) was provided by Prof. Fischer, Institute for Food Technology, University of Hohenheim.

Ionic liquids 1-butyl-3-methyl-imidazolium-hexafluorophosphate ([BMIM][PF₆]), 1-butyl-3-methyl-imidazolium-octylsulfate ([BMIM][OctSO₄]), 1-butyl-3-methyl-imidazolium-tetrafluoroborate ([BMIM][BF₄]), 1-butyl-3-methyl-imidazolium-bis-trifluoromethanesulfonimide ([BMIM][(CF₃SO₂)₂N]) and 1,3-dimethyl-imidazolium-dimethylphosphate ([MMIM][(CH₃)₂PO₄]) were provided by Solvent Innovation GmbH (Köln, Germany).

Water was purified with a Millipore water purification system (Bedford, MA, USA). Organic solvents were all of HPLC grade.

3.2 Methods

3.2.1 MALDI instrumentation

Analyses were performed using a Bruker Reflex III™ time-of-flight mass spectrometer (Bruker Daltonics, Bremen, Germany) equipped with a SCOUT 384™ probe ion source. The system was equipped with a pulsed nitrogen laser (337 nm, Model VSL-337ND; Laser Science Inc., Boston, MA) with an energy of 400 μJ/ pulse. The ions were accelerated under delayed extraction conditions with an acceleration voltage of 20 kV. A reflector voltage of 22.5 kV was applied. A LeCroy 9384C, 4 GHz digital storage oscilloscope was used for data acquisition (LeCroy corp., Chestnut Ridge, NY, USA). Data were collected using either XACQ or FlexControl software (Bruker Daltonics, Bremen, Germany) and processed with the XMASS 5.1 program (Bruker Daltonics, Bremen, Germany). Alternatively, data were processed using FlexAnalysis software (Bruker Daltonics, Bremen, Germany).

External mass calibration was achieved using SA, DHB and CCA (analysis of low molecular weight compounds), standard peptides (analysis of peptides) and BSA (analysis of proteins) in standard matrices.

3.2.2 Protein digestion protocol

Stock solutions of the standard proteins (0.2 mg/ml for lysozyme, carbonic anhydrase and bovine serum albumin (BSA), 1 mg/ml for lactate dehydrogenase, alcohol dehydrogenase and glucose oxidase) were prepared by dissolving in ammonium bicarbonate (NH₄HCO₃) buffer (25 mM, pH 8).

Tryptic in-solution digest of the model proteins was performed by adding 10 μl dithiothreitol (10 mM in 25 mM NH₄HCO₃, pH 8) to 20 μl of the protein stock solutions and incubated for 5 minutes at 90°C. Cysteins were not alkylated. Modified trypsin was added to a final ratio of 1:20 (g/g, protease: substrate), digestion was performed overnight at 37°C.

Tryptic in gel-digestion of the model proteins was performed without prior alkylation of cysteine residues. 500 fmol of each model protein (reduction prior to electrophoresis) was

loaded onto the gel (one dimensional SDS-gel). To visualize the proteins, the gel was stained using coomassie staining. Tryptic in-gel digestion of a coomassie-stained two-dimensional SDS-gel sample (pI-range 4-7, alkylation by iodoacetamide) was done for a spot previously identified as the protein fructose-bisphosphate aldolase obtained from the cytosolic proteome fraction (100 µg total protein) of the bacterium *Corynebacterium glutamicum* (strain ATCC 13032, exponential growth phase). The corresponding bands were excised and digested with modified trypsin in 40 mM NH₄HCO₃-buffer at 37°C overnight following standard protocols.

3.2.3 Ionic Liquid Matrices (ILMs)

Ionic liquid matrices were prepared by dissolving of the particular amount of acids (DHB, CCA....) in a mixture of acetonitrile and water (2:1, v/v, 0.1% TFA). The ILM of InAA was prepared in 80% of acetonitrile/water mixture. Then equimolar amount of organic base (TBA, Py....) was added and the mixture was sonicated for 5 minutes. The solutions were used directly as MALDI-matrices. The solvent was evaporated on the target during sample preparation process without the additional steps of removing the solvent in a vacuum oven and re-dissolving the ionic liquid afterwards (Armstrong et al., 2001). The corresponding solid matrices (DHB, CCA...) were prepared in the same solvents as the ILMs.

3.2.3.1 MALDI sample preparation

Stock solutions of low molecular weight compounds (amino acids, vitamins, ATP and NAD) were prepared in 50% acetonitrile. Matrix stock solutions of 50 mM were prepared for analysis of the above low molecular weight analytes. Samples were prepared by mixing of matrix solution with test analyte to obtain a molar matrix-to-analyte-ratio (M/A) between 1:1 and 10:1.

For the preparation of the pyridinium based ionic liquid matrices, an appropriate amount of pyridine (Py) was added to the stock solution (50 mM) of the solid matrices CCA or SA in acetonitrile:water (2:1, v/v, 0.1% TFA) to result in a final molar ratio of 5:1, 2.5:1, 1.6:1, 1.25:1 and 1:1 (CCA:Py or SA:Py). These ILM mixtures were used for sample preparation without further treatment.

A mixture of model peptides containing 1 µl of stock solutions of angiotensin II, substance P, neurotensin and ACTH (18-39) (all stocks: 0.4 mg/ml) and 2 µl of a stock solution of ACTH (1-17) (0.1 mg/ml) were prepared in water. 0.5 µl of this peptide mixture was mixed with 20

μl of matrix solutions. For the analysis of protein digests, 0.5 μl of the diluted digest was mixed with 20 μl of the matrix solution and placed on the stainless steel target to result in a final amount of digest on target of 30 fmol or 100 fmol, respectively. The samples were measured (i) without further treatment or (ii) after washing of the dried sample spots with 2 μl 0.1% TFA (deposition of the washing solvent on the target-spot, removal after 30 seconds by blowing off from the target). Alternatively, the protein digests were desalted on ZipTip-microcolumns (ZipTip-C₁₈, Millipore, Schwalbach, Germany) according to supplier's recommendations and eluted with matrix solution.

3.2.3.2 *Calibration curves with internal standard (for low molecular weight analytes)*

Calibration curves were obtained using DHB-Py as ILM and DHB as the corresponding solid matrix. Glutamine and U¹³C-glutamine were selected as analyte (A) and internal standard (IS), respectively. Stock solutions of DHB-Py and DHB (30 mM) were prepared as described earlier. 0.025 mmol/ml stock solutions of glutamine and U¹³C-glutamine were prepared in 50% acetonitrile. From these stock solutions various final molar ratios of glutamine/U¹³C-glutamine (0.25-2.5) were prepared. The molar ratio of the matrix to the total amount of analytes (analyte plus internal standard) was kept at 30 in order to allow comparison between solid matrices and ionic liquid matrices. For each A/IS-ratio, 5 spots were placed on the MALDI target. For both matrices, [M+H]⁺ signals were selected for data analysis. For each A/IS-ratio, the arithmetic mean and standard deviation was calculated. Outliers were identified using the equation 1,

$$|X_m - \bar{X}| \geq 4 \cdot \frac{|X_1 - \bar{X}| + |X_2 - \bar{X}| + |X_3 - \bar{X}| + |X_4 - \bar{X}|}{n-1} \quad (\text{eq. 1})$$

where X_m is the data point to be validated, n is the number of measurements, \bar{X} is the mean of the values X_1 , X_2 , X_3 and X_4 , and rejected (Massart et al., 1997).

3.2.3.3 *Calibration curves without internal standard (for peptides and proteins)*

Quantification of peptides and proteins without internal standard proceeded using CCA-DMAPA or InAA-DMAPA (for peptides) and SA-DMED (for proteins) as matrices. Stock solutions of each peptide (angiotensin II, substance P, neurotensin, ACTH (1-17)) were prepared in 70% acetonitrile with concentration of 0.5 mM. Calibration curves were obtained for both single peptide (neurotensin) and mixture of peptides. The mixture of peptides was prepared by solving the same volume of each peptide stock solution in order to get the same amount of each peptide in the mixture. 4 μ L of different concentrations of the peptide solutions (0.02-0.002 mM) was mixed with 4 μ L of matrix solution (500 mM) to obtain a ratio of matrix to analyte between 250000-25000 (mol/mol). 1 μ L of this mixture was applied for measurement. For each concentration, 5 spots were prepared on the target.

Protein stock solutions of 0.05 mM were prepared in water. The same procedure described above for peptides was used for proteins. For the large proteins (carbonic anhydrase and BSA) a higher concentration of matrix solution (800 mM) was applied.

All the samples were dried in room temperature.

3.2.3.4 *Enzyme kinetic*

For the model protein, BSA was used as substrate. The stock solution of BSA was prepared at concentration of 4 mg/ml (25 mM NH_4HCO_3 buffer, pH = 8). 30 μ L of BSA stock solution (30 μ L = 120 μ g) was mixed with 30 μ L of NH_4HCO_3 buffer, and followed by 10 minutes incubation (100 $^\circ\text{C}$). No reduction and alkylation was carried out before the experiments. Modified trypsin was added to a final ratio of 1:120 (g/g, protease: substrate), and digestion was performed at 37 $^\circ\text{C}$. 3 μ L sample was taken from the tryptic digest solution every 30 seconds and directly mixed with 3 μ L of matrix solution. SA-DMED was used as ILM with concentration of 800 mM.

Tryptic digest of model peptide was performed using neurotensin as substrate. Three sets of experiments were performed with initial substrate concentration of 100, 200 and 300 μ M (25 mM NH_4HCO_3 buffer, pH=8) for the kinetic study. The reactions were initiated by adding 130 ng of modified trypsin to 50 μ L of substrate solution and incubated at 37 $^\circ\text{C}$. Tryptic digestion of a peptide mixture containing angiotensin II, substance P, neurotensin, ACTH (1-17) and ACTH (18-39) was performed at initial concentration of 100 μ M for each peptide in

the mixture. The reaction was carried out at a ratio of 200 [total peptides/trypsin (W/W)] in a solution containing 25 mM NH_4HCO_3 buffer, pH=8 and incubated at 37°C.

For the analysis of the model peptide InAA-DMED was used. Analysis of the mixture of peptides was performed using CCA-DMAPA. 2 μL of tryptic digest solutions were taken after a certain intervals of time and diluted 20 times with 80% acetonitrile. 3 μL of diluted sample was mixed with 3 μL of matrix solutions and 1 μL of this mixture was placed on the target. Control experiments using internal standard (Trp^{11} -Neurotensin) were performed as described earlier (Li and Gross, 2004). K_M -value was determined using the Lineweaver-Burk-plot.

3.2.3.5 Derivatization of peptides

Acetylation of model peptides

Substance P was used as a model peptide for the acetylation. Stock solution of 0.1 mM of peptide was prepared in NH_4HCO_3 buffer (50 mM, pH=8). N-hydroxysuccinimid-acetate (D_0) (NHS-acetate) and N-hydroxysuccinimid-acetate (D_3) were synthesized as described before (Bungert, 2004). Stock solutions of NHS-acetate (D_0) and deuterated NHS-acetate (D_3) were prepared at concentrations of 10 mM (dissolved in 40% acetonitrile+60% NaHCO_3 buffer). Derivatization was achieved by mixing equal volumes of peptide stock solutions with stock solutions of derivatization reagents in order to get a final molar ratio of 100 (NHS-acetate/peptide) (Figure 3.1). Peptides stock solutions were acetylated separately, one using D_0 -derivatization and the other D_3 -derivatization. Then the two samples were mixed in the desired ratios (1:10, 5:10, 1:1, 10:5, 10:2.5, 10:1.25, 10:1) and the resulting mixtures were combined with matrix solution (CCA-DMED or CCA-Py, 300 mM).

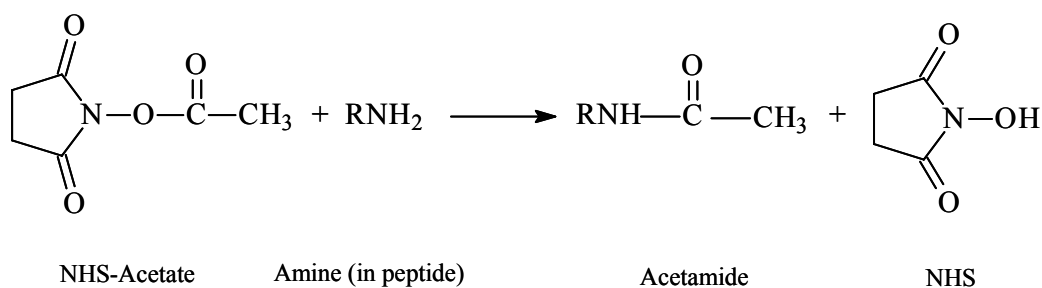


Figure 3.1: Reaction schemes for derivatization of substance P with NHS-acetate. R: the peptide chain.

3.2.3.6 *MALDI-TOF analysis*

Qualitative analysis of low molecular weight compounds was performed by operator driven analysis (manual measurement). For measurement of peak intensities, laser energies just above threshold of ion formation were applied and 100 shots were collected either in positive or negative mode.

For quantitative analysis, an automated data acquisition protocol AutoXecute™ (Bruker Daltonics, Leipzig, Germany) with fixed laser energy just above threshold was used. The AutoXecute™ protocol was set as following: the maximum allowed number of positions on each sample spot was selected to be 9. These 9 positions were arranged in a cross starting from the sample centre. In case of low molecular weight compounds, fuzzy control parameters of AutoXecute™ were as follows: the weight of fuzzy control was 1.5 in order to collect peaks with intensity above 200. Only signals with a mass resolution higher than 1300 (based on full width of half-maximum (FWHM)) and with a signal-to-noise ratio higher than 4 were collected. Noise range was 100. Maximum allowed shot number at one position of a spot was 25, and the maximum number of consecutively rejected trials was restricted to 50. On each sample spot, 100 shots were accumulated.

The fuzzy control parameters of AutoXecute™ for peptides were fixed as: Maximum allowed number of shots on one position was 30 and 150 shots were collected per spot. Only signals with a mass resolution higher than 1000 (based on full width of half-maximum (FWHM)) and with a signal-to-noise ratio higher than 5 were collected. For proteins, the maximum allowed number of positions on each sample spot was the same as in the measurement of the peptides. Maximum allowed shot number at one position of a spot was 50. On each sample spot, 300 shots were collected. Mass resolution of higher than 200 was selected for signals collection, because the signals of proteins were more broadened. The rest of the parameters were the same as in peptides analysis. The mass range of detection was fixed at ± 10 Da next to the analyte and internal standard (when present).

For the measurement of synthetic peptides in CCA-Py and SA-Py, 200 shots were collected per spot from 20 positions following a spiral on the sample spot, 10 shots per position. Five independent sample preparations per matrix were measured. For the measurement of the protein digests, external mass calibration was achieved using a mixture of standard peptides in CCA as matrix. The calibrants were placed on target positions close to analyte positions (near sample calibration). For each analysis 200 shots were collected in positive ion mode (20

measurement points lying on a spiral, 10 shots per point collected). The detection mass range was limited to m/z 750-3000. Masses were assigned using the SNAP-algorithm (settings: signal-to-noise threshold: 5, relative intensity threshold: 0%, quality factor threshold: 30, fragment peak width: 0.75 m/z) implemented in the FlexAnalysis software; spectra were neither baseline-corrected nor smoothed.

3.2.3.7 Database search

Database search was performed using the MASCOT search engine (Matrix Science, London, UK). Search was performed against the MSDB database (taxonomy: all entries). Peptide mass tolerance was 200 ppm, one missed cleavage site was allowed. Deamidation, cysteine-carbamidomethylation (only in case of protein excised from 2D-gels) and methionine oxidation were allowed as variable modifications.

3.2.4 Ionic Liquid (IL)

3.2.4.1 Sample preparation

Stock solutions (50 mM) of solid matrices (DHB, CCA, SA) were prepared in acetonitrile:water (2:1, v/v, 0.1% TFA). Stock solutions of ionic liquids were prepared by mixing 20 μL of IL with 980 μL acetonitrile:water (2:1, v/v, 0.1% TFA). Stock solutions of amino acids with concentration of 0.6 mM were prepared in acetonitrile:water (2:1, v/v, 0.1% TFA).

1 μL of an amino acid stock solution was mixed with 1 μL of an ionic liquid stock solution. The resulting mixture was mixed with 0.7 μL of matrix stock solution. Molar ratios of IL:analyte and of IL:matrix in the resulting mixtures are given in Table 3.1.

For quantification, stock solutions of 1 mM of alanine and 1- ^{13}C -alanine were prepared in acetonitrile:water (2:1, v/v, 0.1% TFA). 980 μL of stock solution of alanine was directly mixed with 20 μL of ionic liquid. From the resulting solutions various final molar ratios of alanine/1- ^{13}C -alanine (0.25-2) were prepared. The molar ratio of matrix (CCA) to the total amount of analytes (analyte plus internal standard) was kept at 50.

Aqueous stock solutions of peptides with concentrations of 0.4 mg/ml for angiotensin II, substance P, neurotensin and ACTH (18-39), 0.1 mg/ml for ACTH (1-17) and 1mg/ml for Leu-enkephalin and bradykinine were prepared. 1 μL of angiotensin II, substance P,

neurotensin, ACTH (18-39) and 2 μ L of ACTH (1-17) stock solutions were combined. This peptide mixture was mixed with 10 μ L of ionic liquid stock solution to a final molar ratio of ionic liquid to analyte of 5000. Bradykinine and Leu-enkephalin were measured separately at the same molar ionic liquid to analyte ratio. In all cases, the peptide/IL- mixtures were mixed with 10 μ L of CCA stock solution.

Molar ratios of IL:analyte and of IL:matrix in the resulting mixtures are given in Table 3.1.

Protein stock solutions were prepared with a concentration of 1mg/mL in water and were mixed with 10 μ L of IL stock solution. These mixtures were mixed with 10 μ L of SA stock solution. Molar ratios of IL:analyte and of IL:matrix in the resulting solutions are given in Table 3.1.

Table 3.1: Molar ratios of ionic liquid:analyte (IL/A) and ionic liquid:matrix (IL/M) applied for the analysis of amino acids, peptides and proteins using matrices DHB, CCA and SA.

Ionic liquid (IL)	Amino acids		Peptides		Proteins	
	IL/A	IL/M	IL/A	IL/M	IL/A	IL/M
[BMIM][OctSO ₄]	95	1.6	5000	1.1	50000	1.1
[BMIM][BF ₄]	176	3.0	5000	2.1	50000	2.1
[MMIM][(CH ₃) ₂ PO ₄]	195	3.3	5000	2.3	50000	2.3
[BMIM][PF ₆]	161	2.8	5000	1.9	50000	1.9
[BMIM][(CF ₃ SO ₂) ₂ N]	113	1.9	5000	1.3	50000	1.4

To investigate the availability of proton in ionic liquids different sets of hydrogen/deuterium (H/D) exchange experiments were performed by incubation of the ionic liquids with (i) D₂O, (ii) D₂O/NaOD (pH/D 8) at room temperature. Incubations were performed for 1 or 12 hours either in the dark or by irradiation with an UV-lamp ($\lambda = 254$ nm). Molar extinction coefficients of the ionic liquids in methanol were determined at 337 nm (ϵ_{337}) according to Lambert-Beers law using an UV-spectrometer (Unicam Helios Alpha, Spectronic Unicam, Cambridge, UK).

For determination of the substrate concentration of the enzymatic reaction D-amino acid oxidase (Chapter 3.2.4.2) by MALDI-MS, stock solution of phenylalanine was prepared at a concentration of 0.688g/25ml of Tris HCL buffer (50 mM, pH 8). A stock solution of the MALDI-matrix FA was prepared at a concentration of 50 mM in mixture of acetonitrile and water (2:1, V/V, 0.1%TFA). Calibration curve was measured using FA as matrix. Stock solutions of phenylalanine and 6-¹³C-phenylalanine (concentration of 1 mM) were prepared in Tris HCL buffer (10 mM, pH 8). From stock solutions, appropriate molar ratios of phenylalanine/6-¹³C-phenylalanine (0.25-2) were prepared. The molar ratio of matrices to the total amount of analytes (analyte plus internal standard) was kept at 50.

For the calibration curve in presence of IL, stock solutions of 1 mM of phenylalanine and 6-¹³C-phenylalanine were prepared in Tris HCL buffer (10 mM, pH 8). 98 µL of stock solution of phenylalanine was directly mixed with 2 µL of ionic liquid [BMIM][PF₆]. From the resulting solutions, appropriate final molar ratios of phenylalanine/6-¹³C-phenylalanine (0.25-2) were prepared. The molar ratios of matrix (FA) to the total amount of analytes (analyte plus internal standard) were kept at 50. 1 µL of mixture of matrix and analyte was placed on the target and dried at room temperature. For each sample, 5 spots were placed on the target.

3.2.4.2 *Monitoring of D-amino acid oxidase activity*

Aqueous stock solution of phenylalanine (substrate) was prepared at a concentration of 0.688 g/25 ml of Tris HCL buffer (50 mM, pH 8). Enzyme reaction was carried out with 40% IL in which 1.8 ml of substrate stock solution was added to 1.2 ml of water-immiscible IL ([BMIM][PF₆]) (final concentration of substrate=166 mM in the water phase). Reaction was initiated by adding 100 mg of immobilized-enzyme in mini-reactor, which was aerated by pure oxygen (6*100 Ncm³/min). 50 µL of samples were taken from enzyme reactions to quantify the substrate at different times. 2µL of diluted enzymatic reaction samples were mixed with 2µL of 6-¹³C-phenylalanine (concentration of 1 mM), followed by adding of 4 µL of matrix solution (FA in 70% acetonitrile, 0.1% TFA, concentration of 50 mM) for MALDI analysis.

3.2.4.3 *MALDI-ToF analysis*

External mass calibration was achieved using SA, DHB and CCA (analysis of low molecular weight compounds), standard peptides (analysis of peptides) and BSA (analysis of proteins)

in standard matrices. For qualitative analysis a manual analysis protocol was used. For each analysis 200 shots were collected in positive or negative ion mode. Limit of detection (LOD) was determined as described earlier (Tholey et al., 2002).

A manual analysis protocol was used for quantitative analysis. For each spot 200 shots were collected. Signals with a mass resolution higher than 1300 (based on full width of half-maximum (FWHM)) and a signal-to-noise ratio higher than 4 were accepted. Laser energies just above threshold were used. The detection mass range was ± 10 Da around analyte and internal standard.

4 Ionic Liquid Matrices (ILMs)

The selection of matrix is a key step for a successful analysis by MALDI-MS. Though there is no universal matrix compound applicable to all kinds of analytes, some common and essential features for a compound to be suitable as a matrix for MALDI is required.

The matrix must:

- 1) be able to absorb the light at the wavelength used
- 2) be able to transfer to or accept protons from analytes
- 3) be stable in the high vacuum applied in MALDI-MS
- 4) be chemically inert in terms of reactivity with analytes

The ILMs used in this study are a combination of an acid and a base in which the anion is the solid MALDI-matrix.

Most of the ILMs investigated here (Table 4.1) formed colourless to yellowish thin liquid layers on the target, after evaporation of the solvent, with the exception of CCA-Py and SA-Py which formed crystals. This is in contrast to the traditional solid matrices, which crystallize after solvent evaporation on the target. The crystal size depends on the matrix. For example, DHB crystals are big enough to be seen with the naked eyes, whereas CCA produces smaller crystals on the target (Figure 4.1). Although the two ILMs, CCA-Py and SA-Py, crystallized after evaporation on the target, their crystals size was smaller compared to corresponding solid matrices, CCA and SA. Armstrong and co-workers (Armstrong et al., 2001) reported a protocol for the synthesis of ILMs in which the solvent used for the synthesis is evaporated and the ionic liquid is then dissolved in the desired solvent prior to measurement. However, it was found in this study that this procedure is not necessary before measurement due to the fact that the solvent can be evaporated directly on the target at room temperature. Therefore the ionic liquid solutions could be directly mixed with the analyte solution and placed on the target.

4.1 Qualitative analysis and stability of ILMs

ILMs have been used as matrix for analysis of peptides and proteins and DNA oligomers (Armstrong et al., 2001; Carda-Broch et al., 2003), where the analyte signals are usually out of range of matrix signals. However, in the analysis of low molecular weight (LMW) compounds (below 500 Da), when the analyte signals are in the range of matrix signals and

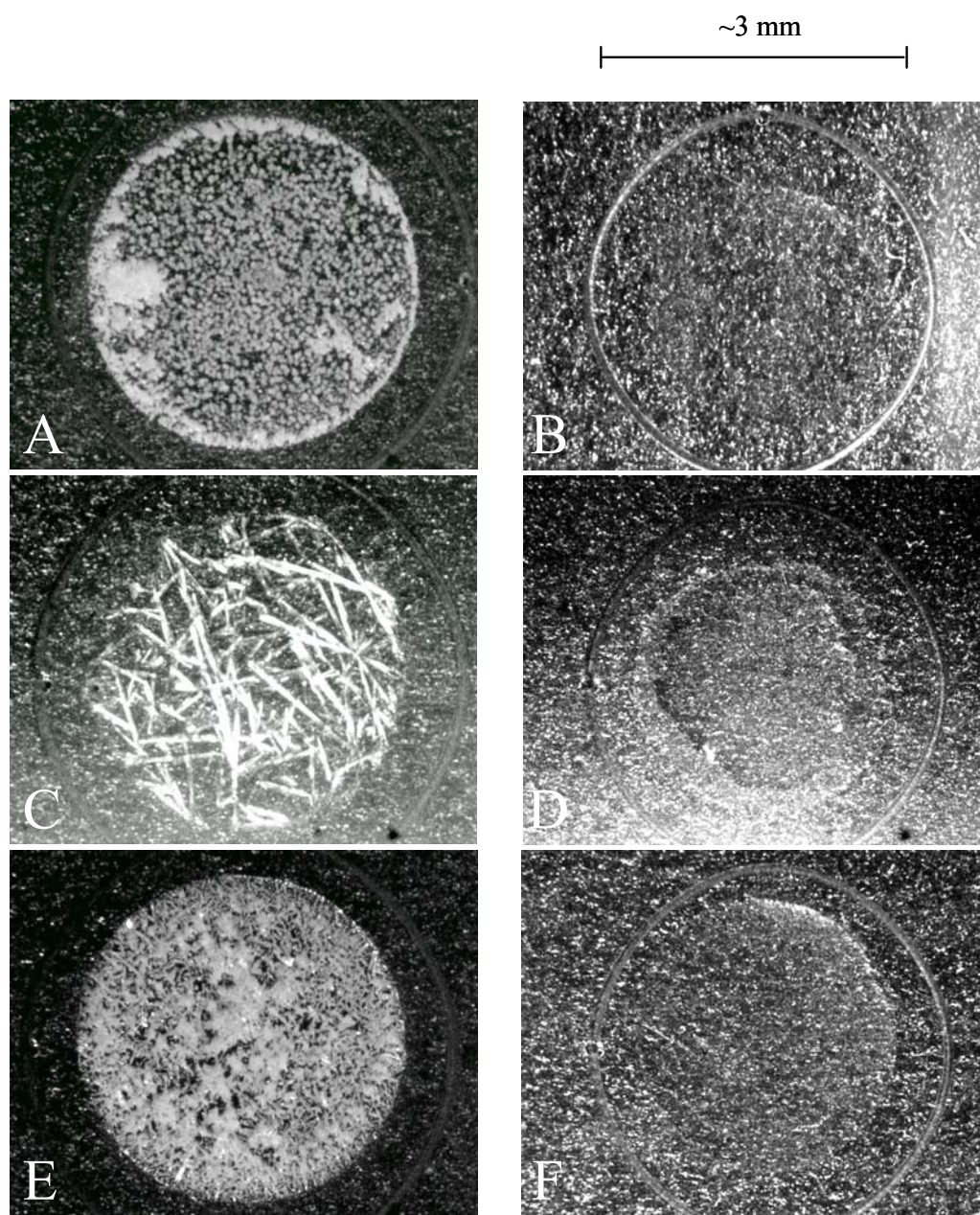


Figure 4.1: Microscopic photographs of solid matrices, A) CCA, C) DHB, E) SA, and their corresponding ILMs, B) CCA-MI, D) DHB-Py, F) SA-DMED. The solid matrices clearly show crystalline shadows. The needle-shaped crystals in case of DHB appear larger than crystals of CCA and SA. In contrast, the corresponding ILMs show a transparent and thin film on the target. The diameter of one spot on the target is ~ 3 mm.

can therefore overlap, a proper selection of matrix is necessary. Hence, the ILMs were first analyzed singularly in order to check the ions aroused from ILMs themselves in positive and negative ion modes (Table 4.1). It was found in all cases that pyridine formed only $[M+H]^+$ -ions. Tributylamine (TBA) in combination with DHB and CCA formed $[M+H]^+$ -signals

Table 4.1: Properties of solid matrices and ionic liquids matrices (ILM) in MALDI-MS. Signals of the matrices were measured in preparations without analytes.

ILM No.	Acid	Base	State of Aggregation	Positive Mode (acid)	Positive Mode (base)	Negative Mode (acid)
	DHB	-	solid	137 ^a , 154 ^b , 155 ^c , 177 ^d	-	153 ⁱ , 113 ^t , 307 ⁱ
1	DHB	Py	liquid	155 ^c , 177 ^d , 193 ^e , 369 [*] , 397 [*]	80 ^c	153 ⁱ , 113 ^t
2	DHB	MI	liquid	177 ^d , 193 ^e , 369 [*] , 397 [*]	83 ^c , 105 ^d , 121 ^e	153 ⁱ , 113 ^t
3	DHB	TBA	liquid	177 ^d , 193 ^e , 369 [*] , 397 [*]	186 ^c , 142 [*]	153 ⁱ , 113 ^t
4	DHB	TEA	liquid	155 ^c	100 [*] , 101 ^b , 102 ^c	153 ⁱ , 113 ^t
	CCA	-	solid	164 ^g , 172 ^a , 190 ^c , 212 ^d , 228 ^e , 379 ^h	-	144 ^f , 188 ⁱ , 113 ^t
5	CCA	Py	solid	190 ^c , 212 ^d , 228 ^e	80 ^c	144 ^f , 188 ⁱ , 113 ^t
6	CCA	MI	liquid	212 ^d , 228 ^e	83 ^c , 105 ^d , 121 ^e	144 ^f , 188 ⁱ , 113 ^t
7	CCA	TBA	liquid	212 ^d , 228 ^e	186 ^c , 142 [*]	144 ^f , 188 ⁱ , 113 ^t
8	CCA	TEA	liquid	172 ^a , 190 ^c	100 [*] , 102 ^c	144 ^f , 188 ⁱ , 113 ^t
	SA	-	solid	207 ^a , 224 ^b , 225 ^c , 247 ^d , 263 ^e	-	223 ⁱ , 447 ^k , 113 ^t
9	SA	Py	solid	207 ^a , 224 ^b , 225 ^c , 247 ^d , 263 ^e	80 ^c	223 ⁱ , 447 ^k , 113 ^t
10	SA	MI	liquid	207 ^a , 224 ^b , 225 ^c , 247 ^d , 263 ^e	83 ^c , 105 ^d , 121 ^e	223 ⁱ , 447 ^k , 113 ^t
11	SA	TBA	liquid	207 ^a , 224 ^b , 225 ^c , 247 ^d , 263 ^e	186 ^c , 208 ^d , 224 ^e , 142 [*]	223 ⁱ , 447 ^k , 113 ^t
12	SA	TEA	liquid	207 ^a , 224 ^b , 225 ^c , 247 ^d , 263 ^e	100 [*] , 101 ^b , 102 ^c	223 ⁱ , 447 ^k , 113 ^t

^a: [M-H₂O+H]⁺, ^b: [M]^{•+}, ^c: [M+H]⁺, ^d: [M+Na]⁺, ^e: [M+K]⁺, ^f: [M-CO₂H]⁻, ^g: [M-CN+H]⁺, ^h: [2M+H]⁺, ⁱ: [M-H]⁻, ^k: [2M-H]⁻, ^t: [TFA-H]⁻, *: not identified. No signals for the base compounds could be detected in the negative ion mode.

whereas [M+Na]⁺ and [M+K]⁺-ions were also observed in combination with sinapinic acid.

1-Methylimidazole (MI) formed in all cases [M+H]⁺-ions, [M+Na]⁺ and [M+K]⁺-adducts (Table 4.1). Triethylamine (TEA) formed [M+H]⁺-ions in all the combinations (Figure 4.2). Moreover, weak [M]^{•+} could be identified for TEA in combination with DHB and SA. The [M-H₂O+H]⁺ peak at m/z = 137 which commonly appears in solid matrix DHB could not be found in the case of DHB-based ILMs. Very weak [M+H]⁺ of DHB was only observed with pyridine and TEA as the counter ions. In the presence of the analytes this ion could no longer be observed. SA could be detected as [M]^{•+} and [M+H]⁺ in all cases, whereas CCA formed the protonized ion only with pyridine and TEA. DHB, CCA and SA showed signals for the [M-H]⁻-ion in negative ion mode in all cases.

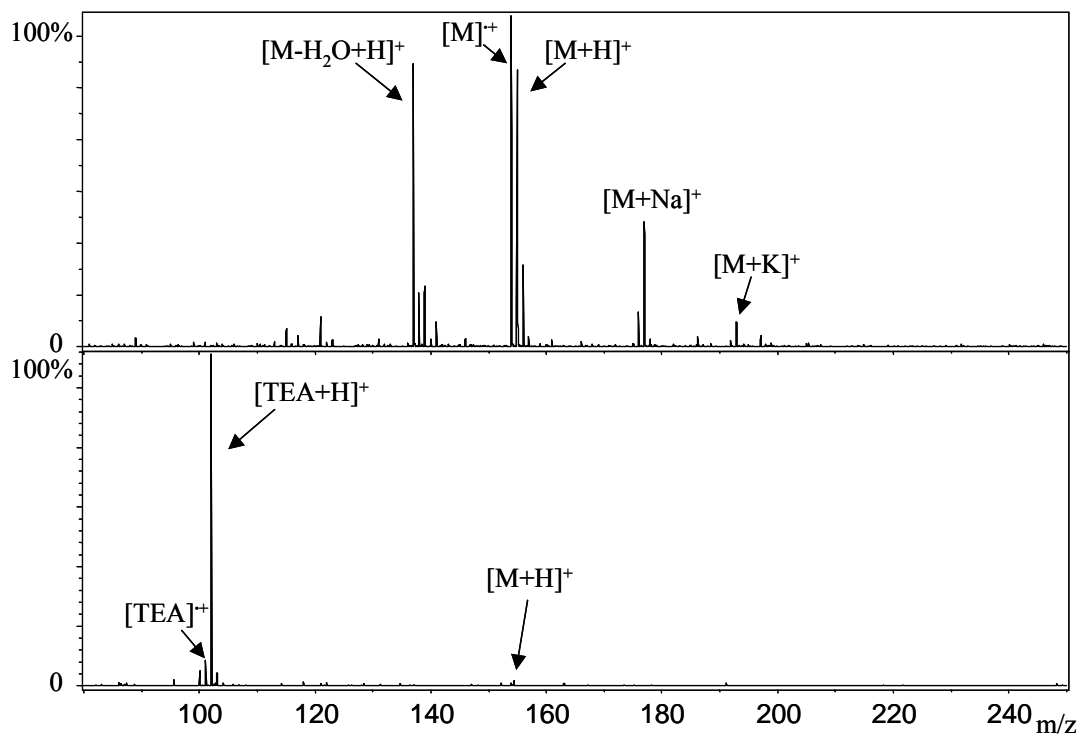


Figure 4.2: MALDI-spectra of DHB (top) and DHB-TEA (bottom) in positive ion mode. 200 shots were acquired for each spectrum. M: matrix molecule DHB.

Some additional non-identified peaks could be found in the ILMs. Possibly they are caused by impurities from the bases.

The analyses of ILMs by themselves described above showed that the spectra of ILMs differ in many cases from those of the solid matrices they are based on. The signals of the matrix were suppressed in many cases or even almost negligible. This reduced matrix signals background obtained by using ILMs resulted in a very clean spectrum suitable for measurement of LMW compounds. For example, as shown in Figure 4.2, the ILM of DHB-TEA presented a clean spectrum producing a nearly exclusive signal of the ion m/z 102 ($[TEA+H]^+$). In contrast, the spectrum of DHB consists of several intensive signals from matrix.

ILMs showed remarkable stability in high vacuum. The spectra quality was not changed even after storage of plate in the high vacuum for more than 12h. This is important when large numbers of samples have to be analyzed.

4.2 Sample homogeneity

The application of MALDI mass spectrometry for qualitative and quantitative analysis of small molecules, e.g. the substrates and products of enzyme catalyzed reactions (Bungert et al., 2004b; Hatisis et al., 2003; Ling et al., 1998), or peptides and proteins (Oda et al., 1999; Sechi, 2002) have been studied earlier. One of the main factors that hamper the application of MALDI for quantitative analysis is the inhomogeneity of samples in the crystallized matrices. This so-called hot spot formation causes a poor shot-to-shot and spot-to-spot reproducibility and is therefore a factor decreasing measurement accuracy and strongly increasing required measurement times. Hence, a number of studies has been published to present new sample preparation methods to promote sample homogeneity (Dai et al., 1999; Hensel et al., 1997; Nicola et al., 1995; Wittmann and Heinzle, 2001). This problem is more significant when large numbers of samples are analyzed in automated measurements. In this respect, the variations in laser power and increasing maximum allowed number of positions on each sample spot during the measurement have been shown to improve the quality of analysis (Kang et al., 2001). Nevertheless, this leads to remarkable prolongation of measurements time.

The main advantage of using ILMs was the significant enhancement of sample homogeneity (Armstrong et al., 2001; Mank et al., 2004). We observed this considerable improvement in sample homogeneity by moving the laser throughout the spot. Herein, the protonated or cationized (Na, K) signals of analyte were observed at each position irradiated by the laser. The variations of analyte peak intensity (protonated and Na/K-adducts) collected from each position on one spot were found to be less than 20%. For instance, arginine as tested analyte was measured in DHB-Py and DHB as ILM and corresponding solid matrix, respectively. The MALDI-spectra were randomly collected at nine different positions of spot. As can be seen in Table 4.2, the huge diversity of analyte signal intensity in DHB at each position of the spot produced a high percentage of relative standard deviation (RSD%) of 70%. This RSD% was reduced to 16% in the more homogeneous sample system DHB-Py. The deviation of 60% or more in peak intensity of peptides has also been reported earlier where common solid matrices were used for analysis (Armstrong et al., 2001). The random selection of points on a spot often delivers no signal in solid matrix systems. Hence, this leads to a higher RSD% in solid matrix compared to ILM. CCA preparations are generally more homogenous than those

of DHB and SA. However, when a mixture of peptides was analyzed using CCA-DMAPA and CCA as ILM and corresponding solid matrix, clear improvement in homogeneity could be seen in ILM (Table 4.2).

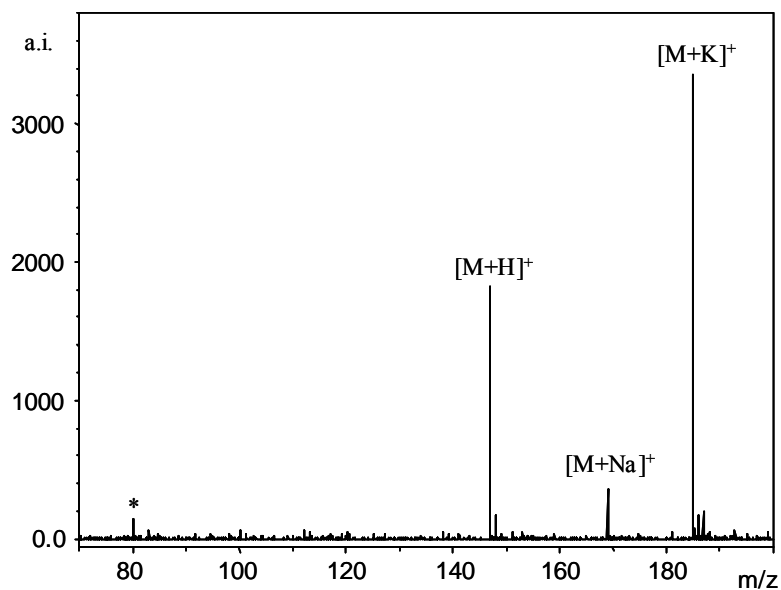
Table 4.2: Comparison of sample homogeneity in solid matrices and the corresponding ILM systems. The signals of analytes were collected randomly at nine different points of spot in the positive ion mode. Points having no signals were not considered for the analysis. 20 shots were collected at each point, totally 180 shots per spot were accumulated. Fixed laser energy just above the threshold was applied for each measurement.

Matrix	Analyte	Range of signal intensity	RSD%
DHB	Arginine	0-2303	70
DHB-Py	Arginine	1065-1867	16
CCA	Angiotensin II	779-2889	55
CCA-DMAPA	Angiotensin II	2962-3423	5
CCA	Substance P	1445-4026	39
CCA-DMAPA	Substance P	2343-3099	8.6
CCA	Neurotensin	1043-3110	33
CCA-DMAPA	Neurotensin	1433-1781	7.5
CCA	ACTH (18-39)	816-2989	41
CCA-DMAPA	ACTH (18-39)	945-1372	11.5

4.3 Analysis of low molecular weight compounds in ILMs

The ILMs were examined as MALDI-matrices for the qualitative analysis of all 20 naturally occurring amino acids. In addition, typical LMW compounds of biological interest such as sugars, vitamins, α -ketoacids, adenosine 5-triphosphate (ATP) and nicotinamide-adenosine dinucleotide (NAD⁺) were tested (Table 4.3). The ability of ILMs to ionize analytes depends both on the nature of the analyte as well as the ILM. Therefore, measurements were performed in both positive and negative ion mode (Figure 4.3). Signals of [M+H]⁺, [M+Na]⁺ and [M+K]⁺ could be identified for the analytes in the positive ion mode and [M-H]⁻-signals were the dominant peaks in negative ion mode analysis. Some analytes such as vitamin B1 (biotin) showed good peak intensities in positive ion mode whereas others as α -ketoglutarate,

a)



b)

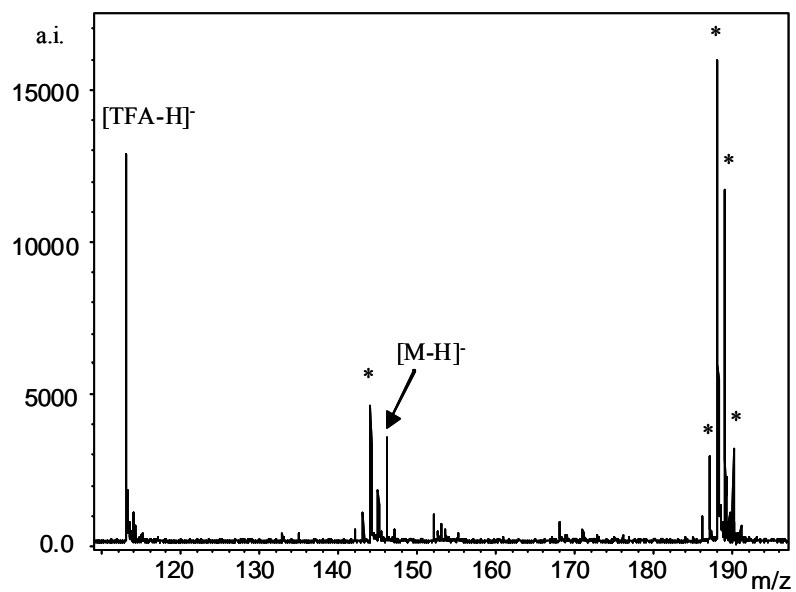


Figure 4.3: MALDI-MS spectra of (a) glutamine in DHB-Py in positive ion mode, and (b) glutamic acid in CCA-MI in negative ion mode. M is the corresponding analyte; * denotes peaks arising from the matrix systems.

ATP and NAD^+ could only be detected in the negative ion mode. Additionally, NAD^+ delivered only a signal for the $[\text{M-nicotinamide}]^-$ -fragment in the negative ion mode.

The mass resolution for the analytes was typically in the range between 3500-5000 and did not differ significantly between crystalline matrices and ILMs.

Typically, higher laser intensities were necessary for measurement in ILMs. Potentially, this higher energy is required to overcome ionic interactions between acid/base compounds of ILMs.

It was observed that not all amino acids could be measured in all matrix systems investigated here. There was no general correlation between the side chain properties of the amino acids (e.g. basic or acid side chains) and the matrix systems, which could be successfully applied for their measurement. Hence, for analysis of LMW compounds, preliminary experiments with a set of ILMs will be required to find out a ILM suited for the respective analyte, as it is necessary for solid matrices, too. Furthermore, potential overlap of matrix signals with the desired analyte has to be considered.

An optimal matrix-to-analyte ratio (M/A-ratio) of 10:1 to 100:1 (mol:mol) has been reported for the measurement of LMW compounds (Kang et al., 2000), whereas higher ratios of 1,000:1 to 100,000:1 (mol:mol) were found to be optimal for polymeric analytes (Karas and Hillenkamp, 1988). Using the ILM systems, the optimal ratios were between 1:1 to 10:1 (mol:mol). Acid-base combination of ILM and M/A-ratios were found to affect the formation of protonated signals as well as Na/K adducts. Besides the protonated ions, strong signals for sodium and potassium adducts could be observed in the positive ion mode. At higher M/A-ratios the intensities of $[\text{M+Na}]^+$ - and $[\text{M+K}]^+$ -signals were observed to be at least three times higher than those of the protonized ions. In some cases (e.g. for glycine and alanine), $[\text{M+H}]^+$ -signals could no longer be observed at ratios above 50:1, whereas for arginine and lysine the protonized ion-signal was still intensive.

Na/K-adduct formation was dependent on the compositions of ILMs. For example, in 1-methylimidazole containing ILM, Na/K-adducts were more intensive compared to pyridinium based ILMs. The effect of pyridinium based ILMs on adducts formation as well as analyte peak intensity will be discussed in more detail later (Chapter 4.7). The limits of detection for the analytes were determined as described before (Tholey et al., 2002). Amongst the amino acids, arginine (basic), glutamic acid (acidic) and alanine (uncharged) were chosen as analytes. Arabinose and biotin represented sugars and vitamins, respectively. ATP, NAD^+ and α -ketoglutarate were tested in negative mode. For all the cases DHB-Py was selected as ILM except for ATP and NAD^+ which were measured from CCA-Py. All other ILMs were

tested with arginine as a representing analyte. In all cases, LOD was found to be about 10^{-14} mol, which is comparable to the corresponding solid matrices. Note that spots usually had a diameter of ~ 3 mm (Figure 4.1).

Table 4.3: Analytes tested in ILMs. All analytes were measured at a molar matrix-to-analyte ratio of 1 with the exception of cysteine, lysine and arginine in matrix DHB-Py (ratio = 3).

Analyte	Positive Ion Mode	Negative Ion Mode	Ionic Liquid Matrix *
Alanine	a, b, c	d	1, 2, 3, 5, 6, 7, 9, 10, 11
Glycine	a, b, c	d	1
Leucine	a, b, c	d	1
Isoleucine	a, b, c	n.t.	1
Valine	a, b, c	n.t.	1
Proline	a, b, c	n.t.	1
Phenylalanine	a, b, c	n.t.	1
Tryptophan	a, b, c	n.t.	1
Tyrosine	a, b, c	n.t.	1
Serine	a, b, c	d	1, 5, 9
Threonine	a, b, c	n.t.	1
Methionine	a, b, c	n.t.	1
Cysteine	b, c	n.t.	1
Histidine	a, b, c	n.t.	1
Arginine	a, b, c	n.d.	1, 2, 3, 5, 6, 7, 9, 10, 11
Lysine	a, b, c	n.t.	1
Glutamic acid	a, b, c	d	1, 2, 3 ^{np} , 5 ^{np} , 6 ^{np} , 9, 10, 11
Glutamine	a, b, c	d	1
Aspartic acid	a, b, c	n.t.	1
Asparagine	a, b, c	n.t.	1
Fructose	b, c	[M-H] ⁻ (1)	1, 2, 5, 6, 7 ^{np} , 11 ^{np}
Arabinose	b, c	n.d.	1, 2, 5, 6, 7 ^{np} , 11 ^{np}
Thiamin	a	n.d.	1, 2, 5, 6, 7, 11
Biotin	a, b, c	n.d.	1, 2, 5, 6, 7, 11
Ascorbic Acid	b, c	d	1, 2, 5, 6, 7 ^{np} , 11
ATP	n.d.	d	1 ⁿⁿ , 2 ⁿⁿ , 5, 6, 7, 11
NAD ⁺	n.d.	[M-nicotinamide]	1 ⁿⁿ , 2 ⁿⁿ , 5, 6, 7, 11
α -ketoglutarate	n.d.	d, [M] ⁻ (1, 2)	1, 2, 5, 6, 7, 11

* Annotation of the matrix systems according to Table 4.1.

a : [M+H]⁺, b : [M+Na]⁺, c : [M+K]⁺, d : [M-H]⁻

values in brackets: signal has been observed only in this matrix system

n.d.: not detected

n.t.: not tested

^{np}: no peak in positive ion mode

ⁿⁿ: no peak in negative ion mode

4.3.1 Quantification of low molecular weight compounds applying internal standards

Low molecular weight compounds like amino acids, sugars and vitamins are substrates or products of many enzymatic reactions. Therefore, introduction of fast and reliable technical methods for quantification of these substrates and products are highly desired for screening of new biocatalysts. MALDI mass spectrometry is a robust technique for enzyme screening which is not dependant on fluorogenic/chromophoric substrates or products as it is a restriction factor for application of optical methods (Tholey and Heinzle, 2002). The method is fast and applicable for low concentrations (μM) and low volumes (μL) of samples. Additionally, measurements can be automated which is desirable for medium- or high-throughput enzyme screening process for a large number of analyses. Therefore, the optimization of automated analysis is one of the prerequisites.

The parameters for the automated measurements have been optimized for solid matrices (Kang et al., 2001). Due to very inhomogeneous samples (hot spot formation), the laser power was adjusted variably to avoid formation of saturated peak intensities that lead to false results.

Another problem using solid matrices was that a random selection of positions on one spot during the automated measurements often produced no signal. Hence, more number of positions on one spot sample is required. The quality of measurement improves by the accumulation of the more measurement points, but the measurement time will increase significantly.

Higher sample homogeneity in ILMs can help overcoming problems observed with solid matrices. The parameters for the automated measurement using the program package AutoXecute™ were optimized for the ILMs. The goal was to gain the highest possible mass resolution with maximal peak intensities and to avoid at the same time saturated peaks. The protocol was adapted to the measurement in ILM in order to compare the automated quantification in solid matrices and ILMs. A molar matrix to analyte ratio of 30:1 was chosen. The calibration curves were obtained with exactly the same measurement conditions in DHB as solid matrix and DHB-Py as ILM using glutamine and fully ^{13}C -labeled glutamine (U^{13}C -Gln) as analyte and internal standard, respectively. In both matrices linear correlations in relative signal intensities could be observed (Figure 4.4).

Glutamine showed higher intensities of sodium or potassium adducts compared to $[\text{M}+\text{H}]^+$

at this molar matrix to analyte ratio in ILMs. Due to stronger variations in the intensities for the cationized (Na/K)-adducts the less intense protonized ions were used for quantification.

The parameters for automated measurements were adjusted as follows: the number of positions on one sample spot was fixed to 9. 25 shots were collected per position and 100 shots per spot for each matrix system (DHB and DHB-Py). In case of the ILM, the acquisition of 100 shots per spot was usually already achieved with 4 out of the 9 allowed positions on one target spot, whereas in case of solid matrix more positions were necessary, depending on the distribution of hot spots. This leads to a higher number of values to be rejected as outliers, higher standard deviations and to a prolonged measurement time. The total number of sample spots in our example was 45.

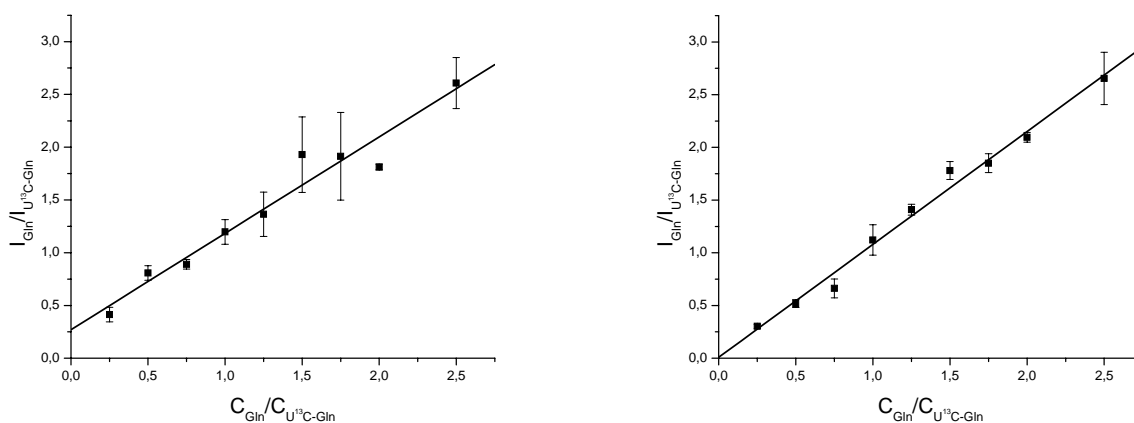


Figure 4.4: Relative quantitation of glutamine using $U^{13}C$ -glutamine as internal standard measured with the same automated measurement protocols in DHB (left) and DHB-Py (right). The molar matrix-to-analyte ratio was 30:1 in both cases. Error bars indicate the average of 5 independent measurements. 100 shots were collected for each spot. I: peak intensities of analyte/internal standard; C: concentrations of analyte/internal standard. Lines represent linear regression curves.

In case of solid matrix, the values of 4 measured spots (out of 45 measured spots) had to be rejected in the experiment shown here with one of them delivering no signals at all. For ILM, the number of rejected values was only 2 (Table 4.4). The total measurement time was 57 min for solid matrix and 46 minutes for ILM. This corresponds to a reduction of about 20%. In other studies, a reduction of measurement time up to 50% could be achieved for screening of sugar converting enzymes using ILMs (Bungert et al., 2004a). The coefficients of correlation were found to be $r^2 = 0.993$ in ILM and $r^2 = 0.974$ in solid DHB. It was mentioned earlier that hot spot formation leads frequently to the measurement of saturated signals which cannot be used for quantification. In order to avoid such signals it is often necessary to apply

dynamic laser intensities using fuzzy-logic algorithms (Jensen et al., 1997). In contrast to this, a constant laser power (or only small variations of it) can be applied in ILM systems due to the uniform signal intensities all over a sample spot. Thus the use of ILM allows a more accurate quantification in less time compared to solid matrices.

Table 4.4: Automated acquisition of quantitative data of glutamine in DHB and DHB-Py.

	DHB	DHB-Py
Molar matrix-to-analyte ratio*	30	30
Measured spots	45	45
Number of outliers	4 (8.8 %)	2 (4.4 %)
Measurement time per spot	76 sec	61 sec
Slope/ intercept of regression	0.91 / 0.26	1.07 / 0.007
r^2	0.974	0.993
Mean of standard deviation	13%	8%

* Amount of analyte sums analyte and internal standard.

4.4 Qualitative analysis of peptides and proteins in ILMs

MALDI is a soft ionization based technique which has proven to be one of prime ionization method for mass spectrometric analysis and investigation of macro-biomolecules, e.g. peptides and proteins (Karas et al., 1987; Tanaka et al., 1988). Not only does the method give information about the mass and sequence of these polymers, but it is also able to carry out analysis at high throughput and at high speed (few seconds per sample) in the field of proteomics (Cramer and Corless, 2005). However, inhomogeneity of sample with the use of solid matrices remains one of the major obstacles using MALDI in proteomics studies. The previous chapter described the use of ILMs for the analyses of LMW compounds. In this chapter, applications of ILMs for the measurement of peptides and proteins are discussed. For analysis of peptides, a mixture of five-peptides was used as analyte (Table 4.5).

Table 4.5: The mixture of five-peptides which was used as analyte in ILMs.

Peptides	Sequence	[M+H] ⁺
Angiotensin II	DRVYIHPF	1046.54
Substance P	RPKPQQFFGLM-NH ₂	1347.74
Neurotensin	pGlu-LYENKPRRPYIL	1672.92
ACTH (1-17)	SYSMEHFRWGKPVGKKR	2093.08
ACTH (18-39)	RPVKVYPNGAEDESAEAFPLGF	2465.2

The mixture of five-peptides was analyzed in different ILMs formed by the combination of CCA and InAA as acids with one of the two aliphatic amines, DMED and DMAPA, or the heteroaromatic pyridine as bases. Similar to the observation during analysis of LMW compounds, the signal intensities of Na/K-adducts were increased in ILMs compared to solid matrices (Figure 4.5). This increase of the alkali adducts signals was also reported earlier when ILMs were used as matrix (Mank et al., 2004). Besides the signals for Na/K-adducts, lower intensity signals of ions of the form $[M+2Na-H]^+$ and $[M+Na+K-H]^+$ could be observed. This enhancement of adduct formation was strongly influenced by the acid-base combination of ILM used for analysis. For example, CCA- DMAPA produced stronger Na/K- adducts compared CCA-Py.

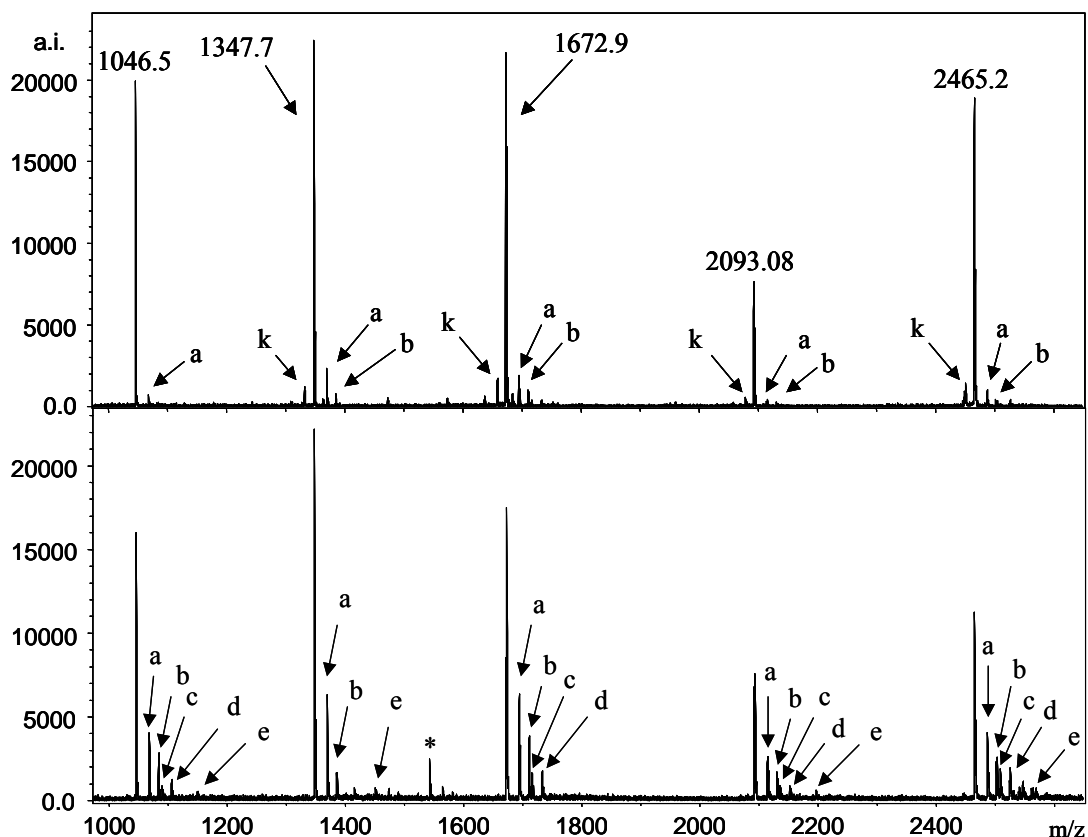


Figure 4.5: Mixture of the peptides angiotensin II ($m/z = 1046.5$), substance P ($m/z = 1347.7$), neurotensin ($m/z = 1672.9$), ACTH (1-17) ($m/z = 2093.08$) and ACTH (18-39) ($m/z = 2465.2$) measured in CCA (top) and CCA-DMAPA (bottom). a: $[M+Na]^+$, b: $[M+K]^+$, c: $[M+2Na-H]^+$, d: $[M+Na+K-H]^+$, e: DMAPA-adducts. k: $[M-14+H]^+$. Resolution of peptides peaks varied between ~ 7900 - 10200 (top) and ~ 4600 - 5900 (bottom). *: non-identified impurity.

Nevertheless, $[M+H]^+$ signals of peptides were in all cases more intensive than Na/K-adducts in all ILMs studied in this work. Peptides (substance P, neurotensin, ACTH (1-17), ACTH (18-39)) showed the signal $[M-14+H]^+$ in CCA as matrix. The identity of this signal is not clear up to now. The mass loss of 14 Da seems to be the mass of one methylene group (CH_2). It should be mentioned here that the mass loss of 14 Da (CH_2) of methylated aspartic acid or glutamic acid containing peptide could be observed in MALDI-MS/MS spectrum (Schmidt et al., 2006). The methylation of aspartic acid or glutamic acid can occur during the staining procedure of gels in acidic methanol (Haebel et al., 1998). However, in case of the standard peptides in which no methylation is expected, loss of such a group (CH_2) to produce the signal of $[M-14+H]^+$ is quite unlikely. Further investigation using MS/MS techniques could help to find out the reasons for potential changes in the peptides mass. However, this signal was not observed in ILM. The resolution of the signals did not differ significantly in ILMs

compared to the corresponding solid matrices. Similar to the observation in analysis of small molecules (Chapter 4.3), it was found that higher laser energies are also required to ionize the peptides in ILM compared to corresponding solid matrix (e.g. in CCA: 32% (arbitrary laser energy units), in ILM CCA-DMAPA: 40%).

In general, the peptides did not form any adducts with the components of ILM. An exception was the ILM of CCA-DMAPA in which weak adduct formation with the base could be observed (Figure 4.5). Further analyses using InAA-based ILM showed comparable results to those found in CCA-based ILMs.

The proteins insulin, lysozyme, carbonic anhydrase and BSA were measured in ILM SA-DMED. The mass range of proteins studied was between m/z 5700 to 66000 Da. In MALDI analysis using solid matrices, peaks of proteins are generally broadened when compared to peptides, resulting in lower resolution. This is mainly because of the use of linear rather than reflector mode for analysis. In case of the ILM, SA-DMED, the peaks of proteins were even more broadened in comparison to corresponding solid matrix SA (Figure 4.6). The broadening of signal was more pronounced with increasing protein mass.

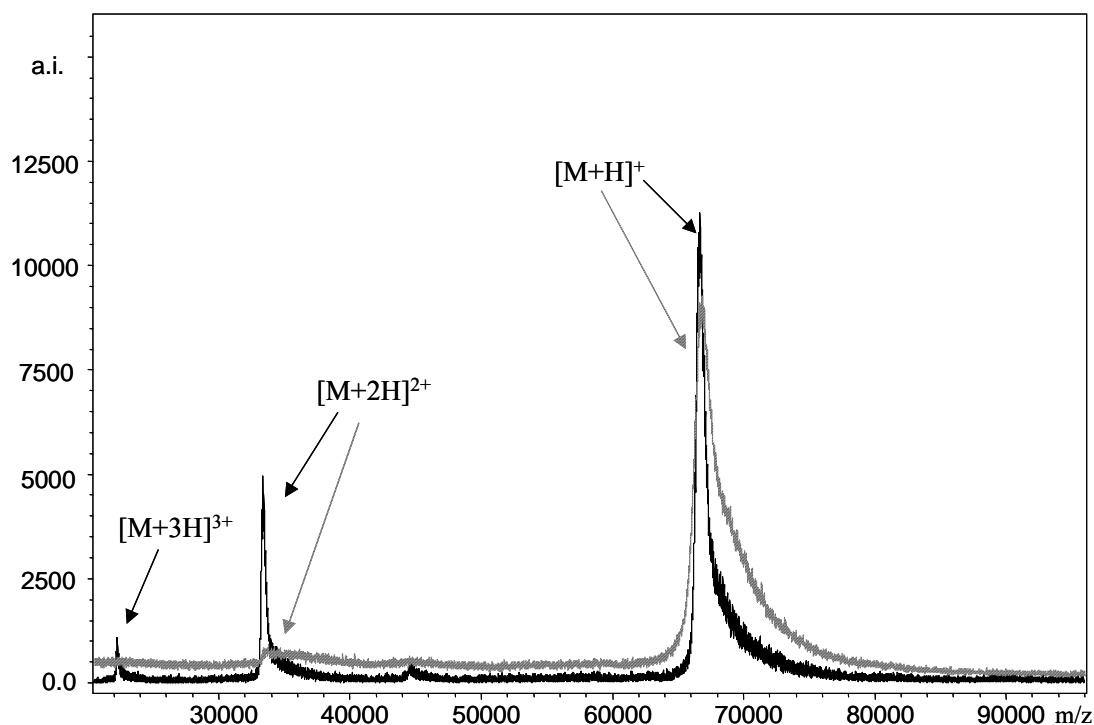


Figure 4.6: MALDI-spectrum of BSA ($m/z=66$ kDa) in SA (black line) as solid matrix and SA-DMED (dashed line) as ILM. 200 shots were collected for both cases.

Though difficult to pinpoint the actual factors which cause this more broadening in ILM, one of the possible reasons can be because of the use of higher laser energy for ILM to obtain a comparable result to the corresponding solid matrix. This elevated laser energy can cause more fragmentation in protein, and since these fragment peaks cannot be very well resolved, they can induce more peaks broadening. On the other hand, increased metal-adducts induced by using ILMs can be another explanations for broadening of the proteins peak.

Adduct formation with the base DMED could be clearly observed for the smallest protein studied here, insulin. For all other proteins tested no adduct formation was observed. The adduct peaks with bigger proteins could be hidden by the broad peaks of proteins in ILM which may not allow the detection of these adducts. The signals corresponding to the protein-SA adducts can be detected, especially with smaller proteins similar to the earlier observation (Galvani et al., 2001). These SA-adducts with proteins could not be identified for any tested proteins in SA-DMED. Together with the broadening of protein peaks in ILM and the operation of linear mode for protein analysis – resulting in lower resolution- the SA- adducts could not be probably resolved in the protein peaks. The double or triple intensive protonated signals that appear in analysis of proteins in SA were either very weak or not observed in ILM (Figure 4.6). It can be speculated that the presence of a base, which has a high proton affinity, in the composition of ILM can decrease the proton availability to produce doubly or triply protonized protein peak in ILM.

4.5 Quantification of peptides using isotopically labeled internal standard

The application of stable isotopes as internal standard (IS) in mass spectrometry has brought forwards a new era for quantitative proteomics. In recent years, a number of stable isotope labelling techniques have been introduced. Examples are isotope-coded affinity tag (ICAT) method (Gygi et al., 1999), ^{18}O labelling during enzymatic reaction (Bantscheff et al., 2004), isobaric multiplexing tagging (iTRAQ) reagents (Ross et al., 2004), isotope-coded protein label (ICPL) method (Schmidt et al., 2005). These methods employ the principle of tagging of the peptides and proteins to be quantified with chemical reagents. One of the samples is tagged with an isotopically heavier chemical reagent and the other with natural labelled chemical reagent. The quantification is achieved based on the ratio of heavy and light isotopes analyte in which the concentration of one of the isotopomers is known.

Herein, the model peptide, substance P, was labelled using NHS-acetate (D_3) and (D_0) as heavy and light isotope, respectively, as described in material and methods section. Two different ILMs (CCA-DMED and CCA-Py) were used for the quantification. The calibration curves were obtained in a molar D_3/D_0 range of 1-10. A mean standard deviation of 7% in CCA-DMED and 8.5% in CCA-Py with r^2 of 0.994 (for CCA-DMED) and of 0.997 (for CCA-Py) was achieved. It was demonstrated earlier (Chapter 4.3 and 4.4) that the use of solid matrices led to the higher standard deviation and increasing of measurement time in case of quantitative analysis by automated measurement. Therefore, further comparison of this experiment with corresponding solid matrix CCA was not carried out.

4.6 Influence of the molar matrix-to-analyte ratio on the ion response in ILM

The co-crystallizations of matrix and analyte cause the inhomogeneous sample preparation using solid matrices. Hence, little or no correlation between the peak intensity and amount of analyte on the target could be obtained, making the quantitative characterization by MALDI-MS a method depending on the application of IS. The use of isotopically labelled analogue of the analyte rather than structural analogue as IS has been proven to improve significantly the reliability of result (Horak et al., 2001; Kang et al., 2001). Potentially, the differences in the size, structure, crystallization behavior and ionization efficiency of structural analogue compared to the tested analyte are responsible for this phenomenon. Unfortunately, isotopically labeled standards are more difficult to be obtained for large biomolecules.

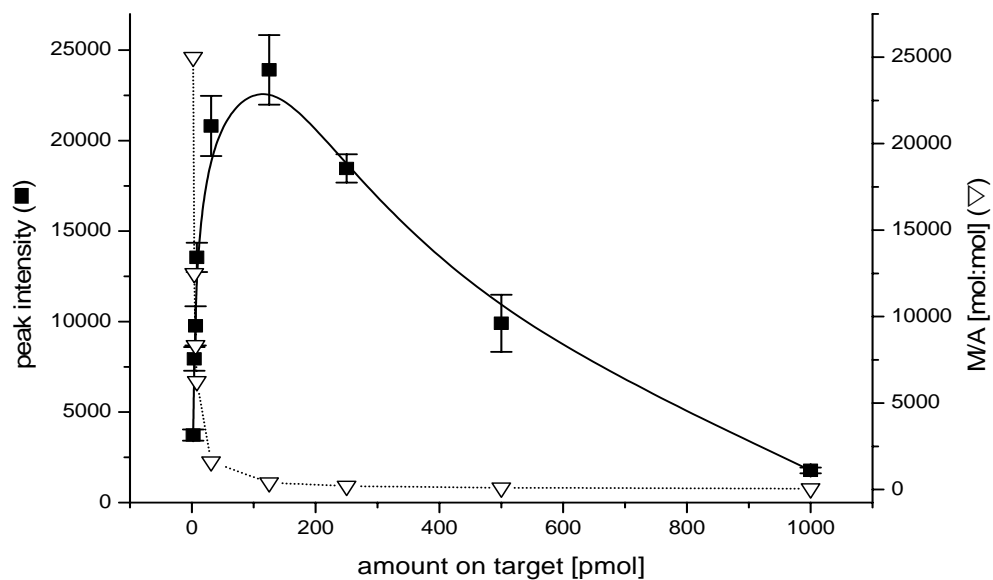
One obvious advantage of using ILMs for MALDI analysis is the significant improvement of sample homogeneity. ILMs were already shown to diminish the problems raised by inhomogeneity of the sample as well as hot spot-formation (Armstrong et al., 2001; Mank et al., 2004). The first attempt to evaluate the peptide quantification using ILMs was by Gross and co-workers (Li and Gross, 2004). They obtained good calibration curves with high linearity and reproducibility over a wide range of concentration. As revealed, the high sample homogeneity achieved using ILMs eliminated the need of isotopically labeled IS for quantitative analysis. Moreover, applicability of an IS with structure and molecular weight different from those of the analytes was shown for quantification of oligodeoxynucleotides (ODNs), peptides and small proteins (Li and Gross, 2004).

In this work, ILMs were examined for their potential for quantitative analysis of peptides without using IS. In other words, it was evaluated whether a direct correlation between peak intensity and the amount of analyte on the target can be observed. Neurotensin was used as analyte in ILM CCA-DMAPA. A dilution series of the peptide neurotensin in a constant amount of the ILM was prepared. Since the same amount of matrix was used for all the measurements, the M/A-ratios of the samples decreased by increasing the amount of analyte in the M/A-range of 25,000 (lowest amount of analyte) and 50 (highest amount of analyte) (Figure 4.7 (a)). The measurement was performed automatically and the laser energy was kept constant throughout the analysis. As shown in Figure 4.7 (a), the signal intensities increased nonlinearly with increasing analyte amounts up to about ~100 pmol. Above 100 pmol the intensities reached a maximum level, and further a decrease of the signal intensities was observed.

It is a well-known fact, that the molar matrix-to-analyte ratios has a strong influence on the detectability and intensity of analyte signals in MALDI-MS (Dreisewerd, 2003). Typically molar M/A-ratios between 10 and 100 were found to be optimal for LMW compounds (Kang et al., 2000). For peptides and proteins typically ratios in the order of 10^3 - 10^5 are applied (Karas and Hillenkamp, 1988). At higher sample amounts (corresponding to lower M/A-values) the amount of matrix may not be anymore sufficient for fulfilling its role in soft ionization and desorption of the analyte in MALDI-MS, leading to the decrease of signal intensities. The increase at low sample amounts with the corresponding higher M/A-ratios was nonlinear, but the deviation from linearity was not pronounced (Figure 4.7). Hence, this led to the working theory, that elevated M/A-ratios could favour a linear relation between intensity and sample amount.

Therefore, a second set of experiment was performed, in which the M/A-ratios were increased from 25,000 and 500,000. As shown in Figure 4.7 (b), under these conditions a linear relation ($r^2 = 0.995$, mean standard deviation = 8%) could be observed in the range between 500 fmol to 7 pmol. Above 7 pmol, the curve reached a plateau. This dynamic range is slightly lower than that found for relative quantifications (Li and Gross, 2004). The limitation of the dynamic range is mainly caused by three factors, which interfere with each other: (i) the laser energy applied, (ii) the amount of matrix which can be placed on the target, and (iii) the LOD and the ionization behaviour of the analyte. From practical reasons, for a quantification of an unknown sample, the laser energy has to be kept constant for the calibration curve as well as for the measurement itself. On the other hand, the laser energy has an influence on the detectability of low amounts of analytes and on the peak saturation at

(a)



(b)

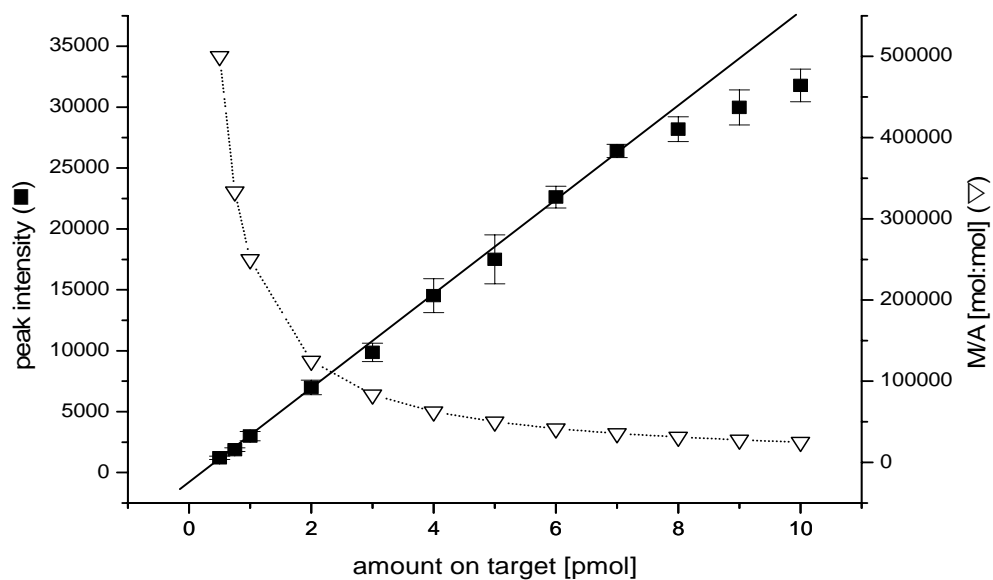


Figure 4.7: Peak intensities of neurotensin in dependence of the sample amount and the molar matrix-to-analyte (M/A) ratio applied. (a) M/A of 25,000 (2 pmol peptide) to 50 (1000 pmol peptide), matrix: CCA-DMAPA. (b) M/A between 500,000 (500 fmol peptide) to 35,700 (7 pmol peptide), $r^2 = 0.995$, mean standard deviation: 8%, matrix: CCA-DMAPA. All measurement points represent averages of 5 independent measurements; constant laser energy was applied throughout the measurement.

higher sample amounts. Therefore, laser energy has to be optimized and adapted to the analytical problem to be solved prior to the measurement of the calibration curve.

The use of different laser energies allows for a shift of the dynamic range either to higher or lower sample amounts, but this does not extend the dynamic range itself. In order to achieve the increased M/A-ratios resulting in the linear relation between sample amount and signal intensities, it is possible either to increase the matrix amount on the target or to decrease sample amount. The first factor is limited by practical reasons: it is not possible to increase the matrix amount unlimited on the target. In this study, typically 250 nmol of the ILM were spotted on the target. The second factor is limited by the LOD of the analyte. The LOD for peptides in ILM were reported earlier to be slightly increased compared to the corresponding crystalline matrices (Mank et al., 2004) but this effect depends strongly both on the nature of the analyte and the composition of the ILM.

The optimal M/A-ratios applied in ILMs were also examined in the pure crystallized matrix, CCA. Due to practical reasons regarding the solubility of CCA, the amount of analyte was reduced between 100-1000 fmol on the target to achieve same M/A-ratios applied in ILM. A roughly linear correlation ($r^2 = 0.65$, slope 16.32) could be observed between sample amount and signal intensity up to 700 fmol on target, however, the errors and deviations were remarkably increased (mean standard deviation=51%) compared to the results obtained using ILM (Figure 4.8). This is mainly caused by the inhomogeneous distribution of the analyte in the crystallized matrix.

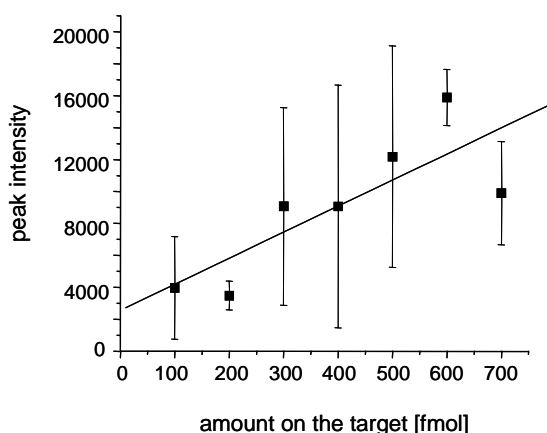


Figure 4.8: Calibration curve obtained for neurotensin using CCA as solid matrix. The same measurement condition applied for ILM shown in Figure 4.7 (b) was used. The M/A was varied between 500,000 (for 100 fmol analyte) to 71,400 (for 700 fmole analyte). Laser energy was constant just above the threshold level. $r^2 = 0.65$, mean standard deviation was 51%.

4.6.1 Quantification of a mixture of peptides without IS

The optimized M/A-ratio found for quantification of single peptide without IS was applied to quantify a mixture of peptides. The quantification of a mixture of angiotensin II, substance P, neurotensin and ACTH (1-17) was performed using matrix CCA-DMAPA. A linear correlation could be observed in the range of 250 fmol to 2.25 pmol between peak intensities of peptides and the amounts of peptides on target (Figure 4.9). In contrast to the situation observed for the single peptide, the obtained curves were not perfectly linear. The r^2 -values were 0.966 (ACTH (1-17)), 0.978 (neurotensin), 0.988 (angiotensin II), and 0.989 (substance P). One explanation for this non-ideal behaviour could be that the presence of one given peptide can influence the desorption/ionization response of another. This effect can be also observed in the slope of the calibration curve achieved for the isolated peptide neurotensin (9.46), which was altered to 8.49 in the mixture of peptides. Hence, due to this complex phenomenon, only single analyte can be quantified with high accuracy. However, the accuracy reached in this experiment is sufficient for the determination of relative enzyme activities in analyte mixtures as described later.

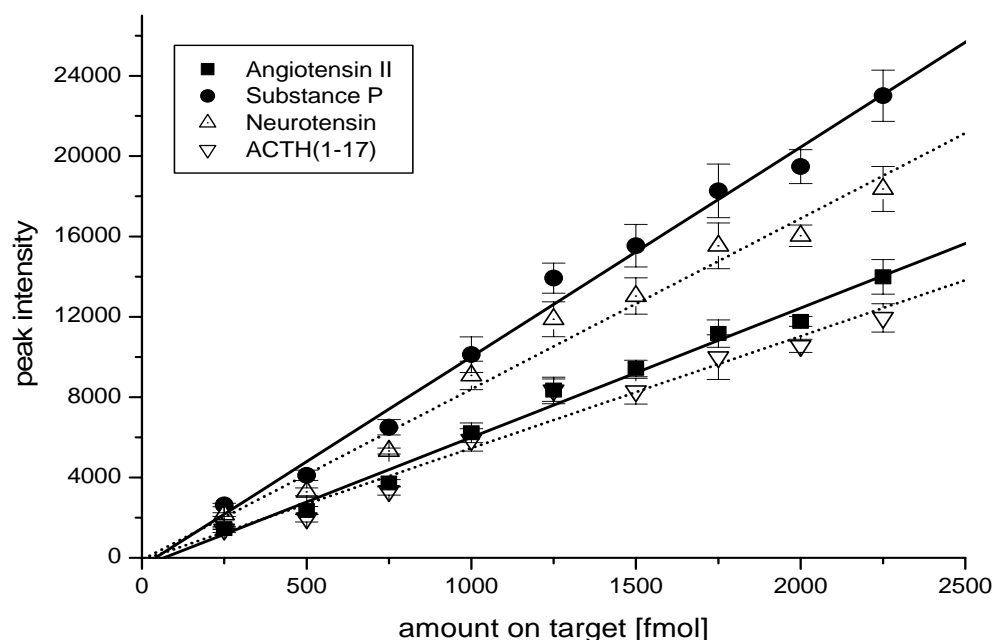


Figure 4.9: Calibration curves for a mixture of the peptides angiotensin II ($r^2=0.988$), substance P ($r^2=0.989$), neurotensin ($r^2=0.979$) and ACTH (1-17) ($r^2=0.966$) measured in CCA-DMAPA. Data points represent the average of 5 independent measurements. Fixed laser energy was applied.

Having different slopes of calibration curves for the four analytes (6.43 (angiotensin II), 10.43 (substance P), 8.49 (neurotensin), 5.57 (ACTH (1-17))) indicates that peptides have different efficiency concerning to their protonization in MALDI. It is known that peptide properties such as the amino acid sequence, hydrophobicity, and even size can influence their MALDI behaviour (Baumgart et al., 2004; Olumee et al., 1995; Wenschuh et al., 1998). However, no obvious correlation between peptide length, composition of the peptides and the corresponding slopes were found in the limited set of analytes investigated here, but a closer investigation of this could be a further potential application for the method presented.

4.6.2 Monitoring of enzyme catalyzed reactions without IS

Enzymes are known as highly specific catalysts, which are involved in all the metabolic pathways in biological systems. The determination enzyme kinetic is always necessary to gain more information about a new enzyme or new substrates/inhibitors for the given enzyme. MALDI-MS has been applied for enzyme screening when suitable IS was available (Bothner et al., 2000; Schluter et al., 2003). Herein, the feasibility of absolute quantification by MALDI-MS using ILMs for determination of enzyme activities was investigated in two sets of experiments: i) monitoring of the enzymatic conversion of a single peptide (enzyme screening) and determination of kinetic data, ii) observation of the enzymatic conversion of a peptide mixture (substrate/inhibitor screening).

4.6.2.1 Monitoring of the tryptic digest of single peptide

The tryptic digestion of the peptide neurotensin was investigated as a model reaction. Samples were taken after certain time intervals and mixed with the ILM InAA-DMED without any prepurification (e.g. desalting). It should be mentioned here that $[M+H]^+$ -signals have been used for all the analyses, since the protonated signals of peptides were quite stronger than Na/K-adducts signals. Digestion of neurotensin by trypsin created two products with m/z 661.4 and m/z 1030.5 corresponding to the peptides RPYIL and pGlu-LYENKPR, respectively. In addition to substrate signals, the signals of these two products could be also observed. According to the sequence of neurotensin given in Table 4.6, this peptide carries three potential cleavage sites for the trypsin-catalyzed reaction. Trypsin preferentially cleaves on the carboxyl side of arginine and lysine residues (Keil, 1992). Two arginine residues in the amino acid sequence of neurotensin are followed by proline residues, which are known to

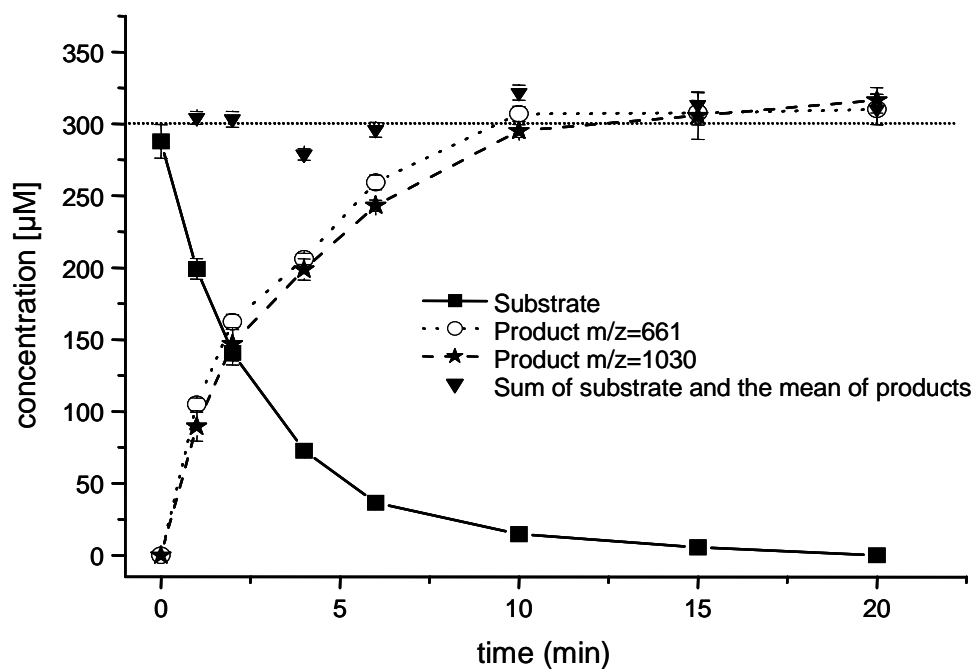
prevent a cleavage at these residues (Keil, 1992; Thiede et al., 2000). Figure 4.10 (a) shows the evolution of the concentrations of the substrate and the two products. Substrate concentrations were calculated using the calibration curve shown in Figure 4.10 (b), which was measured in the range of between 1 and 9 pmol on the target. The product concentrations could also be calculated using their calibration curves shown in Figure 4.10 (c).

The calibration curve of products was achieved based on their signal intensities which were obtained in enzyme reactions performed with three different initial substrate concentrations (see Chapter 4.6.2.1.1). It was assumed, that from each molecule of the substrate peptide two product peptides are formed in equimolar amounts. As can be seen in Figure 4.10 (c), a linear correlation could be found between signal intensities and the calculated amounts of the products.

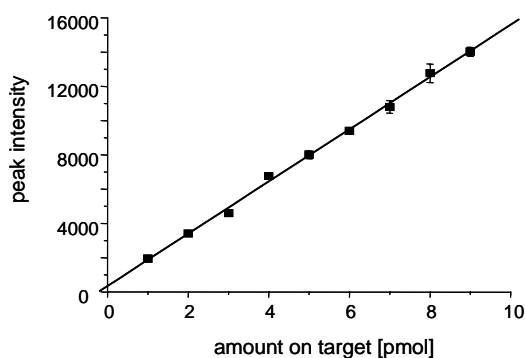
Small deviations could be observed between the two products concentrations (Figure 4.10 (a)). This can be mainly caused by the fact that the calibration curves consisted only three measurement points, which were generated by three product concentrations. As a further control, the calculated sum of substrates with the mean of the amounts of the products was constant over the complete reaction (Figure 4.10 (a)).

To compare the results of the substrate quantifications obtained without using IS, further control experiments were carried out by two established methods: (i) relative quantification by MALDI-MS in ILM using a homologous peptide (Trp¹¹-Neurotensin) as IS and (ii) quantification of the substrate by HPLC-UV-measurements with 214 nm detection (Figure 4.11). The average deviation between the three methods was 6%. The highest deviations were observed at the lowest concentrations (12%, 10 and 15 min.) whereas at high concentrations deviations were below 3%.

(a)



(b)



(c)

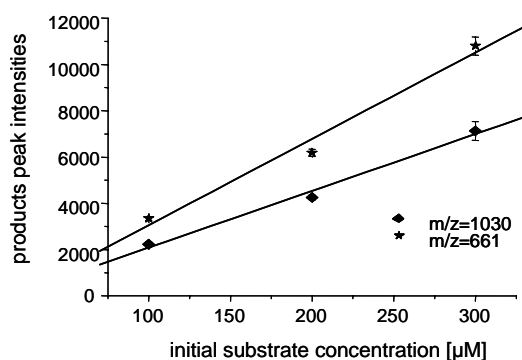


Figure 4.10: Tryptic digestion of neurotensin monitored in the matrix InAA-DMED. (a) Time dependent development of substrate and product concentrations, (b) Calibration curve for substrate measured in InAA-DMED, molar matrix-to-analyte ratios from 250,000 to 25,000, matrix amount: 250 nmol, each data point represents the average of 5 independent measurements, (c) Calibration curve obtained for two products (m/z 661 and m/z 1030). Substrate concentrations (a) were calculated using the calibration curve (b) and taking into account the dilution steps prior to sample preparation. Product concentrations (a) were calculated from calibration curves (c). Product amounts were calculated assuming equimolar product formation from the substrate. The dashed line (---▼---) in (a) represents the calculated sum of substrate and the mean of the two product concentrations.

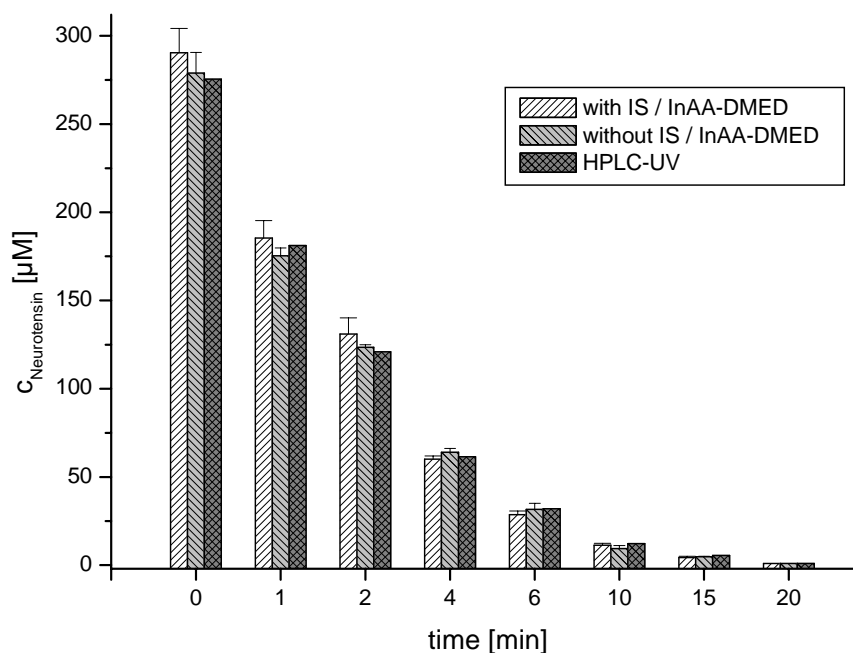


Figure 4.11: Comparison of substrate concentrations determined by quantitative MALDI-MS (five independent measurements) using the ILM (InAA-DMED) (i) with an internal standard (Trp¹¹-Neurotensin), or (ii) without internal standard and by HPLC-UV (214 nm, single measurement).

4.6.2.1.1 Enzyme kinetic study

In order to determine kinetic data, enzyme reactions were performed with three different initial concentrations of the substrate (Figure 4.12). The measurements were done in ILM InAA-DMED as described above. The substrate concentrations were obtained using the calibration curve presented in Figure 4.10 (b). The K_M value for the substrate neurotensin was calculated to be 520 μM using initial velocities of enzymatic reactions. This value lies in the range of comparable substrates found in the literature (Hill and Tomalin, 1982; Palm and Novotny, 2004). For more precise determination of kinetic parameters by Lineweaver-Burk-plot, more sampling points in the early phase of the reaction would be beneficial in order to cover a wider linear range.

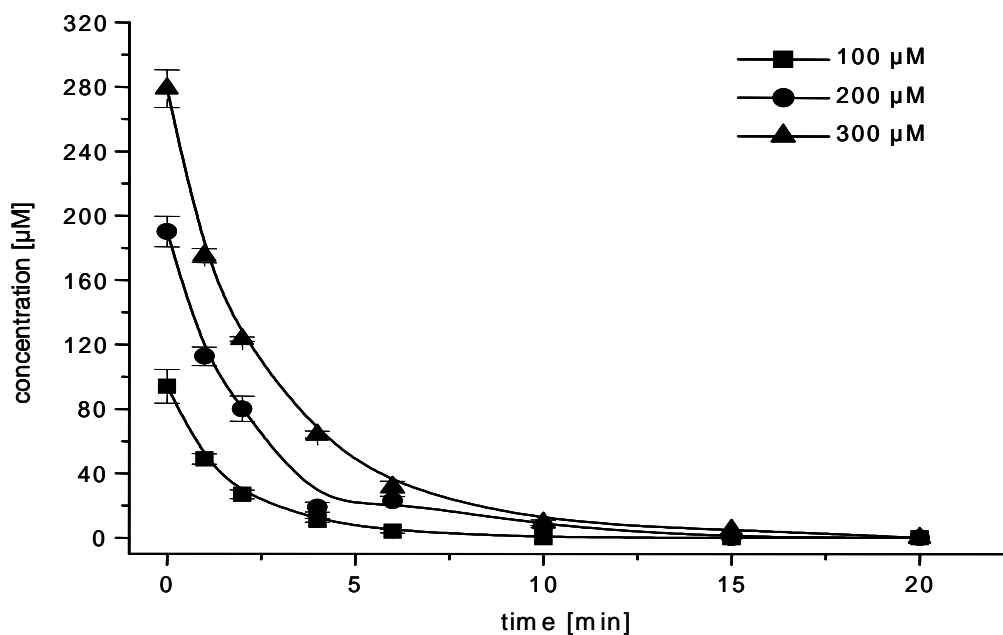


Figure 4.12: Substrate (neurotensin) consumption vs. time for three different initial substrate concentrations. Concentrations of substrate were calculated using the calibration curve shown in Figure 4.10 (b). Error bars indicate the average of 5 independent measurements. Applied matrix: InAA-DMED, amount of matrix on the target: 250 nmol.

4.6.2.2 *Semi-quantitative monitoring of multi-substrate conversions*

In a second set of experiments, tryptic digestion of five peptides mixture containing angiotensin II, substance P, neurotensin, ACTH (1-17) and ACTH (18-39)), by trypsin was monitored. The peptides responded differently in this enzymatic reaction. Figure 4.13 shows the signal intensities of the five peptides in their responses to tryptic digestion by trypsin. Though, all the peptides were combined in equimolar amount, ACTH (1-17) was the fastest digested amongst the peptides, followed by neurotensin. This order in digestion can be explained by the sequence of each individual peptide. Neurotensin has one, ACTH (1-17) three cleavage sites for trypsin (Table 4.6). The cleavage products described earlier for neurotensin as well as further product peptides originating from the cleavage of ACTH (1-17) could be identified in the spectra (Table 4.6).

A direct interpretation of the kinetic parameters of a peptide with more than one cleavage site is hampered by the fact that different cleavage sites may have different kinetic parameters. Additionally, the cleavage products may also be substrates for further cleavages. For example, in the case of the digestion of ACTH (1-17) which has three potential cleavage sites for trypsin, three products with m/z of 1055.6, 1056.5 and 1808.8 could be initially observed,

Table 4.6: Products of tryptic digestion of a five-peptide mixture measured in CCA-DMAPA.

analyte / sequence ^{a, b}	theoretical products of tryptic cleavage
	m/z / sequence / identification ^c
Angiotensin II DRVYI HPF	m/z = 290 / DR / (-) m/z = 775 / VYIHPFG / (-)
Neurotensin <i>p</i> Glu-LYEN <u>K</u> PR RP YIL	m/z = 661.4 / RP YIL / (+) m/z = 1030.5 / <i>p</i> Glu-LYEN KPR / (+)
Substance P <u>R</u> PK <u>P</u> Q QFFGL M-NH ₂	-
ACTH (1-17) SYSME HFRWG <u>K</u> PVGGK KR	m/z = 1056.5 / SYSMEHFR / (+) m/z = 1055.6 / WGKPVGGKKR / (+) m/z = 1808.8 / SYSMEHFRWGKPVGGK (+) m/z = 771.5 / WGKPVGGK / (+)
ACTH (18-39) <u>R</u> PV <u>K</u> VYPNGAEDESAAEAFPLEF	m/z = 499.3 / RPVK / (-) m/z = 1984.8 / VYPNGAEDESAAEAFPLEF / (+)

^a bold residues: cleavage site. ^b underlined residues: masked cleavage site. ^csignal detected: (+), not detected: (-)

followed by the disappearance of the two products peptides m/z 1055.6 and m/z 1808.8 (Figure 4.14). These two product peptides (m/z 1055.6 and m/z 1808.8 corresponding to the sequences WGKPVGGKKR and SYSMEHFRWGKPVGGK, respectively) also have cleavage sites for trypsin; hence they can be the further substrates for tryptic digest. The conversion of these two products resulted in the appearance of two more peptides with m/z of 1056.6 and m/z 771.5 corresponding to two fragments SYSMEHFR and WGKPVGGK, respectively (Table 4.6). Herein, only the cleavage product of the C-terminal arginine residue could not be detected in these sequential cleavages of ACTH (1-17).

It was shown earlier (Chapter 4.6.1) that peptides could influence the signal intensities of one another in the mixture, which is known to be the consequence of peak suppression event in MALDI. Possibly, the slight drop in signal intensity of the cleavage product peak of m/z 1056.5 shown in Figure 4.14 could be the result of such an event in MALDI.

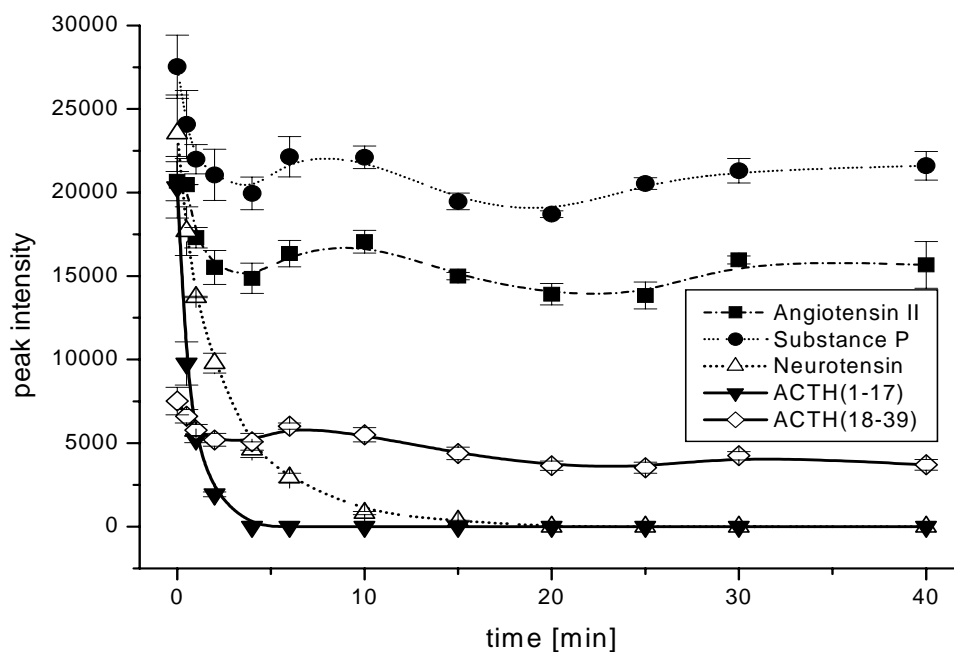


Figure 4.13: Tryptic digestion of a mixture of angiotensin II, substance P, neurotensin, ACTH (1-17) and ACTH (18-39) monitored in the matrix CCA-DMAPA. Initial on target-amount of each peptide was 2.5 pmol.

The signal intensities of the other three peptides in the mixture (angiotensin II, substance P and ACTH (18-39)) were also slightly reduced during the whole reaction time (Figure 4.13). The tryptic digestion of ACTH (18-39) was very slow compared to ACTH (1-17) and neurotensin, and its signal intensity was reduced by about 40% during the entire reaction. It consists of one possible cleavage site, forming a larger peptide fragment of m/z 1984.8 and a smaller one of m/z 499.3. The bigger cleavage product with m/z 1984.8 could be identified in the spectra; the second product with m/z 499.3 was not detected. The blank spectrum measured with the analyte free ILM did not show any signal at this m/z -value, thus signal overlap can be excluded as a reason for the non-detectability of the latter peptide. Potentially, the slower conversion of this peptide is caused by the neighboring sequence. The signal intensities of the peptides angiotensin II and substance P showed only a small loss of intensity of about 20% in the beginning of the reaction; afterwards, signal intensities were mainly constant. Substance P cannot be cleaved efficiently since both of the two tryptic cleavage sites of this peptide are neighbored by proline residues (Keil, 1992). No cleavage products were identified for this peptide. Although angiotensin II has one tryptic cleavage site, no cleavage products of this peptide could be detected in the spectrum.

To confirm results obtained from digestion of peptides in the mixture, tryptic digestion of

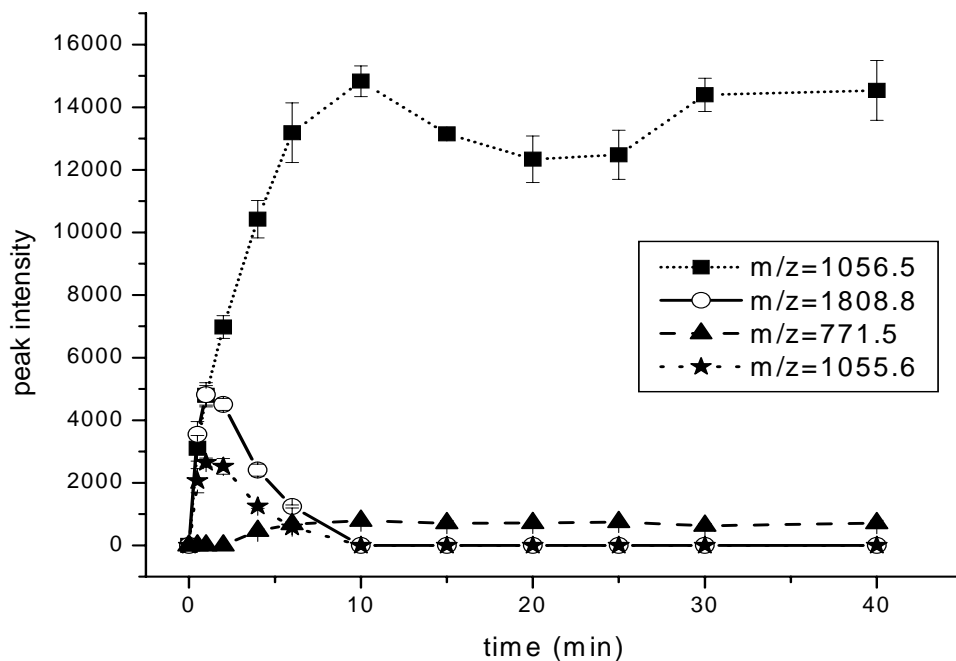


Figure 4.14: Time dependence of the production and disappearance of the peptides obtained from tryptic digestion of ACTH (1-17) in the mixture of peptides shown in Figure 4.13. Digestion was first begun with appearance of the peptide fragments formed by first-cleavage events, accompanied by the disappearance of the signals of these precursors. ILM: CCA-DMAPA.

these two peptides angiotensin II and substance P was performed individually. Similar behaviour as in digestion of peptide mixture could be observed for the digestion of single peptide in terms of reduction of peak intensity at the beginning of the reaction and to be nearly constant throughout the reaction (data not shown). Moreover, no product peaks could be identified in the digestion of the single peptide. The neighbouring amino acids of the cleavage site, an acidic N-terminal aspartic acid residue and a bulky hydrophobic C-terminal valine residue, could be a potential reason inhibiting the tryptic cleavage of angiotensin II (Table 4.6). Despite of non-detectability of any cleavage products of these two peptides, however, the reasons for the decrease of signal intensities at the beginning of the reaction still remain unexplainable.

To evaluate the validity of the experiment of multi-substrates digestion, parallel experiments using the established method using IS was performed. Using an IS with structure and molecular weight different from those of the analytes has been already shown for quantitative MALDI-analysis (Li and Gross, 2004). Therefore, Trp¹¹-Neurotensin was used as IS for all five-peptides to monitor the enzymatic conversion of the peptide mixture. The peptides

followed a similar time-dependent tryptic digest as reported above without IS (Figure 4.15). The two peptides, ACTH (1-17) and neurotensin, were first cleaved and further slow reduction of the signal intensity of the peptide ACTH (18-39) could be observed. The signal intensities of angiotensin II as well as substance P were fairly constant throughout the entire reaction, which indicates again that these two peptides were obviously not cleaved by trypsin. However, the initial drop in the signal intensities for two peptides could be also observed in this experiment. Moreover, the fluctuation of the signals of these two peptides was even more pronounced compared to the situation without IS which is probably caused by the presence of an additional analyte (IS) that induces even more peak suppression. Hence this also contributes to the advantages of IS-free quantification. The same behaviour was also observed for the cleavage product peaks described in the absence of IS.

As shown in Chapter 4.6.1, the slopes of the different peptides in the mixture depended on the molecular properties of the analytes and on the presence of other analytes. Further, caused by the formation of cleavage peptides as well as by different velocities of the reduction of the substrate amounts, the composition of the analyte mixture – and thus the problems related to peak suppression (Knochenmuss and Zenobi, 2003)- varies in an unpredictable way during enzymatic conversion. Therefore, for the monitoring of the enzymatic conversion of the peptide mixture, signal intensities rather than concentrations calculated from calibration curves are presented here. This hampers the determination of kinetic parameters, for example v_{\max} or K_M values, and therefore limits the method to semi-quantitative approach. Nevertheless, the differences in the evolution of the signal intensities are sufficient to identify good and bad substrates for an enzymatic conversion.

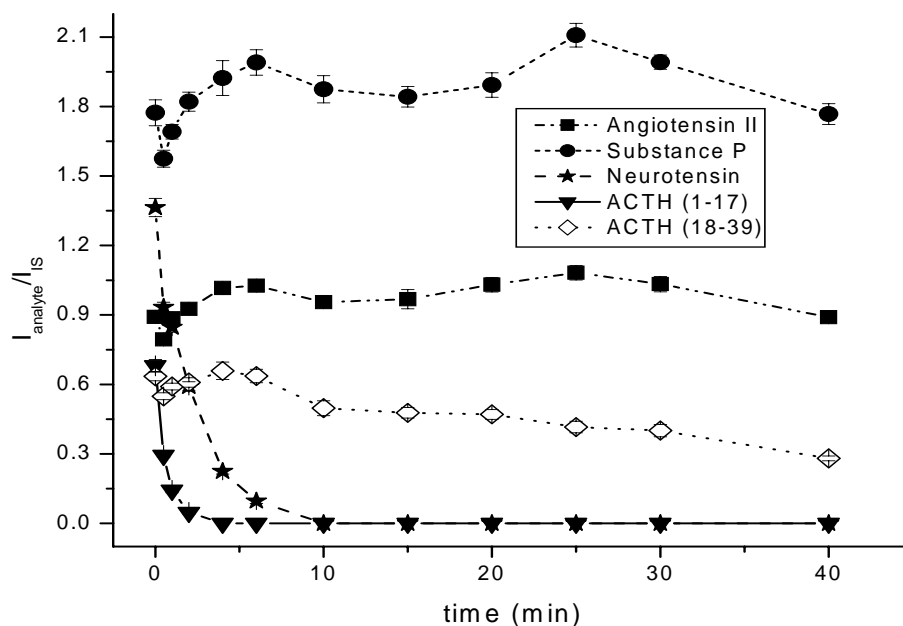


Figure 4.15: Monitoring of the tryptic digestion of five-peptides mixture using Trp¹¹-Neurotensin as IS in the matrix CCA-DMAPA.

4.6.3 Quantification of proteins without IS

Quantification of proteins is an important aspect in proteomics studies. Mass spectrometric approaches based both on MALDI as well as on ESI, have been successfully used for the analysis of proteins in the complex biological mixtures. The main focus was on the identification of proteins or the investigation of their structural modifications. In recent years, the combination of MS with stable isotope labelling as IS has enhanced remarkably the application of mass spectrometry for quantification of proteins. Labelling of proteins by stable isotopes can be achieved either by introduction of the labels to specific amino acid using chemical derivatization (Munchbach et al., 2000; Sechi, 2002), or by in-vivo labeling using ¹⁵N-isotope enrichment incorporated into the protein during cell growth (Wang et al., 2002). Therefore, to overcome the laborious job for labelling of the target protein, the capability of ILM for absolute quantification of proteins was examined at optimal M/A-ratios discussed earlier (Chapter 4.6). SA-DMED was applied as ILM for quantification of proteins. Individual calibration curves were obtained for four proteins, insulin (m/z 5720 Da), lysozyme (m/z 14300 Da), carbonic anhydrase (m/z 29000 Da) and BSA (m/z 66000 Da).

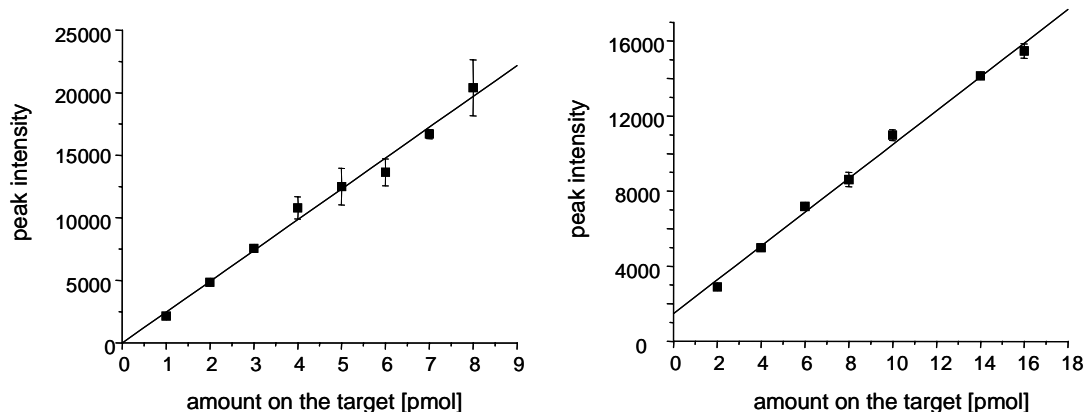


Figure 4.16: The calibration curves obtained for lysozyme (left, $r^2=0.987$) and BSA (right, $r^2=0.994$). 250000 pmol (on target) of matrix was applied with M/A-ratios of 250000-25000 for the measurement of lysozyme whereas the matrix amount was increased to 400000 (on target) for BSA measurement with M/A-ratios of 200000-25000. The error bars represent the average measurements of 5 independent sample spots. Applied matrix: SA-DMED.

As can be seen in Figure 4.16, a good linear correlation between the amount of the protein on the target and the peak intensity could be found at optimal M/A-ratio in ILM, indicated by r^2 -values in the range of 0.974 (for carbonic anhydrase) to 0.994 (for BSA) (Table 4.7). The linear range was similar as elucidated for peptides, spanning a range between 1-8 pmol on target. For larger proteins (carbonic anhydrase, BSA) this range of linearity could be extended more up to 16 pmol on target when matrix amount was increased (400000 pmol on target). Additionally, the mean value of standard deviation (%) obtained from measurement of each individual protein was very low (e.g. 2.5 % for BSA) which expressed again the high sample homogeneity achievable using ILM (Table 4.7).

Table 4.7: Detail features of calibration curves achieved for the four model proteins using SA-DMED as ILM.

Protein	R^2 value	Mean standard deviation (%)
Insulin	0.98723	6%
Lysozyme	0.98796	7%
Carbonic anhydrase	0.97466	3%
BSA	0.99473	2.5%

4.6.3.1 Monitoring of tryptic digest of BSA as model protein

Quantification of proteins without the need for IS could be a valuable tool for the monitoring of enzymatic reactions using proteins as substrates. In this respect, the digestion of BSA by trypsin as a model enzymatic reaction was performed. The reduction of BSA concentration could be monitored versus time using ILM, SA-DMED (Figure 4.17). The concentration of the protein was calculated using the calibration curve depicted in Figure 4.16. As can be seen in Figure 4.17, no more protein was detected after seven minutes. It should be mentioned that the longer time for digestion is necessary because the kinetic data of Figure 4.17 does only show the disappearance of the BSA but not complete digestion.

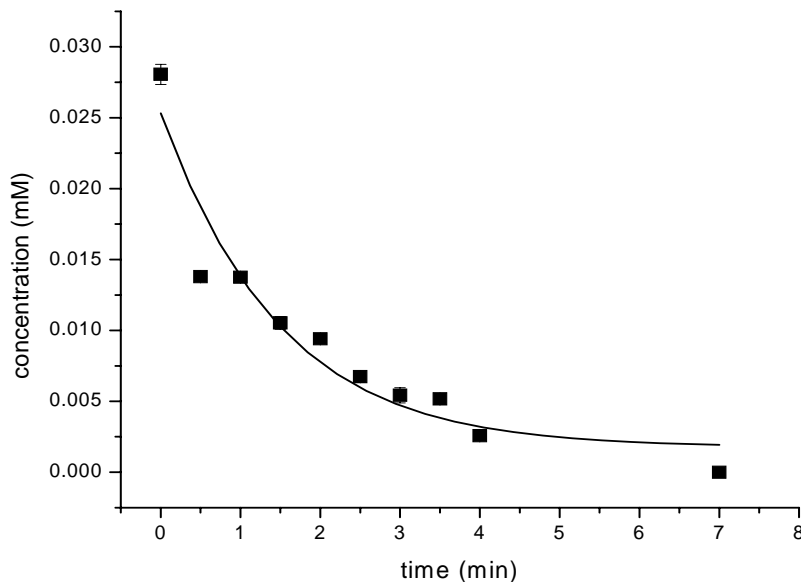


Figure 4.17: Tryptic digest of BSA (m/z 66000 Da) monitored versus time without using IS. The concentration of protein was calculated using the calibration curve shown in Figure 4.16. All measurement points represent averages of 5 independent measurements. Applied matrix: SA-DMED.

The method presented here, therefore, can be used for fast screening of new proteases, or investigations on effect of new inhibitors on different proteolytic enzymes. Additionally, it can be used as a fast method for selection of proper substrate amongst of the mixture of substrates for a new proteolytic enzyme. In this regard, the problem of peak suppressions mentioned earlier (Chapter 4.6.2.2) for the mixture of substrates should be considered.

4.7 Pyridinium-based ionic liquid matrices for proteome analysis

In recent years, MALDI-MS has drawn many attentions as a rapid analytical tool for the identification of proteins. Herein, a typical approach consists of tryptic digestion of protein and then measurements of peptide fragments (peptide mass fingerprint) obtained from digestion by MALDI-MS. Subsequently, the protein can be identified by comparing the observed mass fingerprint to the in-silico mass fingerprint of known proteins present in the databases. The key for successful protein identification is the improvement of measurement quality. The main criteria in this respect are high sensitivity and thus a low limit of detection, also expressed by high signal intensities or signal-to-noise ratios (S/N-ratios).

The enhancement in signal intensities of peptides could be achieved by structural modifications of the peptides to increase the protonization efficiency, e.g. guanidination of lysine containing peptides (Brancia et al., 2000); or by alkylation of cysteine residues (Sechi and Chait, 1998). Another factor that can improve the sensitivity is the reduction of formation of metal ion adducts and matrix clusters. These signals and impurities can also contribute to a loss of sensitivity both by dispersion of signal intensities to several peaks as well as by peak suppression effects. Additionally, the interpretation of the spectra in the presence of these adducts are more complicated. In this respect, the sample preparation methods and the matrix applied for the measurement have been proven to have a great impact on spectra quality and in sensitivity. The desalting methods such as desalting and reconcentration on reversed-phase microcolumns (Courchesne and Patterson, 1997; Gobom et al., 1999), on-target washing procedures (Smirnov et al., 2004; Vorm et al., 1994), addition of nitrocellulose (Landry et al., 2000) and macroporous polystyrene beads (Doucette et al., 2000) have been reported. The approaches based on addition of a co-matrix have been shown to be beneficial to the analysis of oligonucleotides, e.g. addition of sugars (Shahgholi et al., 2001), amines (Vandell and Limbach, 1999), and peptides, e.g. addition of monoammonium phosphate (Zhu and Papayannopoulos, 2003) or nitrocellulose (Kusmann et al., 1997).

The goal of this part of work is to test the ability of ILMs for the improved analysis of protein digests. As described earlier (Chapter 4.4 and 4.3), ILMs induce the formation of Na/K-adducts. However, ILM of pyridine (CCA-Py) showed comparable results to CCA concerning analyte signal intensity and adduct formation. Hence, in the present work measurement in the classical solid matrix CCA was compared with pyridinium based-CCA matrices.

4.7.1 Properties of the pyridinium-based ionic liquid matrices, analysis of model peptides and optimization of molar acid-base ratios

Here, we compared the spectra of peptides measured in the classical solid matrix CCA with those measured in the ILM CCA-pyridine (CCA-Py). Furthermore, non-stoichiometric mixtures of CCA with pyridine were tested. Pyridine was used as matrix additive, with molar ratios of CCA-Py of 5:1, 2.5:1, 1.6:1, 1.25:1. A mixture of 5 synthetic peptides covering a mass range of 1000 m/z to 2500 m/z was used as analyte for the comparison of these matrix systems. All matrices tested here, CCA-Py (ILM) and non-stoichiometric CCA-Py mixtures, were stable under high vacuum conditions applied in MALDI-MS shown by leaving a MALDI target in the vacuum chamber of the mass spectrometer for 12 h. No significant changes in spectral quality were found.

It was mentioned before (Chapter 4) that most of the ILMs formed a viscous layer on the target. An exception was the ionic liquid of pyridine, which tends to crystallize after evaporation of the solvent. This tendency in crystallization was observed in all non-stoichiometric of CCA-Py mixtures as well.

The mean standard deviations of 12%-21% obtained from signal intensities of the single peptides in an automated measurement of 5 independent sample spots indicated that the homogeneity of samples in pyridinium-based ILMs is not significantly improved in comparison to pure CCA. Nevertheless, the homogeneity of the samples was sufficient to allow a reliable comparison of S/N-ratios. The threshold laser energies necessary for the detection of the peptides did not vary significantly between pure CCA and the ILMs.

The combination of CCA and Py in different molar ratios showed a strong influence on the S/N-ratios of the five peptides tested here (Figure 4.18). At ratios CCA-Py-2.5:1 and 1.6:1, the S/N-ratios of four peptides were increased up to 1.9 fold for substance P, 1.25 fold for neurotensin, 2.5 fold for ACTH (1-17) and 1.7 fold for ACTH (18-39) compared to CCA. In contrast to other peptides, angiotensin II showed a reduction S/N-ratio of 30% at CCA-Py-1.6:1. At a ratio of CCA-Py-1:1 the S/N-ratios for the peptides angiotensin II, neurotensin and ACTH (18-39) were more decreased compared to CCA but were not significantly changed for substance P and ACTH (1-17). It should be mentioned that signal intensities of the peptides showed similar behaviour as shown for their S/N-ratios (Figure 4.18).

Another influence of the presence of pyridine was observed on the formation of alkali adducts. As described earlier (Chapter 4.4), more intensive Na/K-adducts were observed in

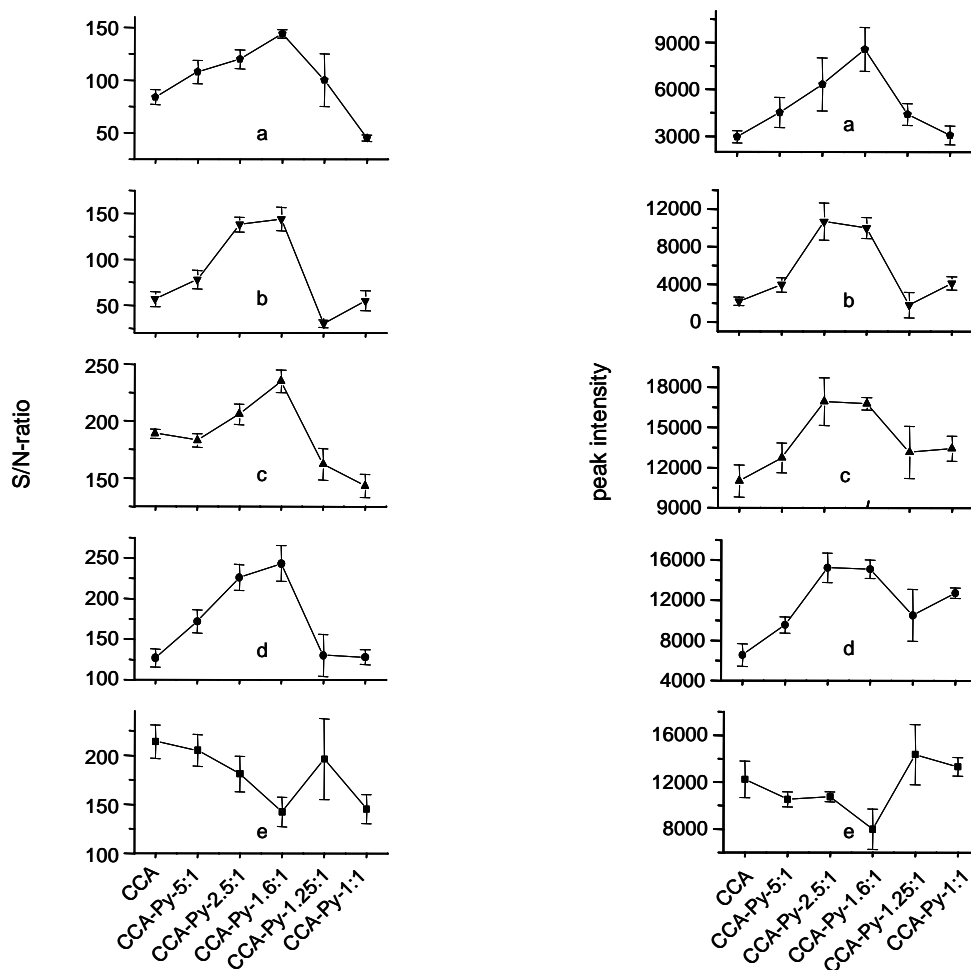


Figure 4.18: S/N-ratios (left) and signal intensities (right) of 5 synthetic peptides in dependence on the composition of the matrix. Molar ratios are given for the pyridinium-based matrices (CCA:Py). Each data point represents an average value of 5 independent measurements. Amount of peptides on the target: (a): ACTH(18-39) (0.7 pmol), (b) ACTH(1-17) (0.4 pmol), (c) neurotensin (1 pmol), (d) substance P (1.2 pmol), (e) angiotensin II (1.6 pmol).

ILMs compared to corresponding solid matrices. However, the intensities of adducts depend on the acid/base combination of ILMs (Chapter 4.4). The alkali adduct formation in CCA-Py-1:1 was not as strong as observed in other ILMs, yet it was more intense than in pure crystallized matrix CCA. Alkali-adduct formation was reduced or disappeared for all peptides at CCA-Py-2.5:1 and 1.6:1 ratios. Adducts between the peptides and components of the ILM, e.g. CCA or Py, could not be detected.

Improved sensitivity is important in achieving lower limits of detection. The presence of non-stoichiometric amount of pyridine not only could increase the S/N-ratios of peptides, but also reduce the level of chemical noise in the spectra compared to measurement in pure CCA (Figure 4.19). Therefore, the enhancement of signal intensity along with lower chemical

noise background and the reduction or absence of the alkali adducts signals obtained using non-stoichiometric of CCA-Py can clearly improve the sensitivity of analysis (Figure 4.19). As a result, LOD is reduced in the non-stoichiometric pyridinium-based ILM compared to pure CCA. Since the highest S/N-ratios for the model peptides was obtained in the stoichiometric range of CCA-Py-2.5:1 and 1.6:1, therefore, CCA-Py-2:1 was chosen for further experiments.

As shown in Figure 4.19, clear signals were identified for on-target amount of 2.5 fmol of substance P (S/N of 12) and for 1.4 fmol of ACTH (18-39) (S/N of 5) in the five peptide mixture using CCA-Py-2:1, whereas at this amount, no signal for these two peptides could be identified in CCA. These two peptides could be detected in CCA when 3.8 fmol and 2 fmol were applied for substance P and ACTH (18-39), respectively. Thus, a reduction of about 35% could be achieved in the LOD for these two peptides. The peptide ACTH (1-17) could not be detected in CCA, whereas a well-resolved peak with a S/N-ratio of 8 could be obtained at on-target amount of 1.2 fmol in CCA-Py-2:1. The other two peptides, angiotensin II and neurotensin, were found in both matrix systems, however, their S/N-ratios were increased in CCA-Py-2:1 compared to CCA (Figure 4.19).

For both matrices a gain in sensitivity by a factor of 2 was reached by the use of Anchor-chip-targets. Note that the limits of detection reported in this study are relatively high, which is potentially caused by a significant loss of detection power due to aging of the detector used in this study. Nevertheless, in comparison with the S/N-ratio values obtained in pure CCA a significant improvement in the LOD can clearly be assigned for the non-stoichiometric pyridinium-based ILMs.

All experiments performed at optimal CCA-Py-ratio of 2:1 were carried out in the positive ion mode where protonized ions could be detected. Further, the capability of this optimal matrix system (CCA-Py-2:1) was compared with CCA for the measurement of the five-peptide mixture in the negative ion mode. The results were similar to those presented in the analysis of positive ion mode. Compared to CCA, the S/N-ratios of four peptides were increased in CCA-Py-2:1 in the range of 1.1-fold (for ACTH (18-39)) to 6-fold (for ACTH (1-17)). For the peptide angiotensin II a reduction of 10% was observed.

Similar experiments as explained above for CCA were performed using SA, SA-Py (ILM) and non-stoichiometric amounts of pyridine with SA (pyridine as matrix additive, with molar ratios of SA-Py of 5:1, 2.5:1, 1.6:1, 1.25:1) for the analysis of the same five-peptides mixture as analyte. All matrix systems were stable in the high vacuum applied. The homogeneity of the samples was slightly reduced compared to CCA and did not differ much between the

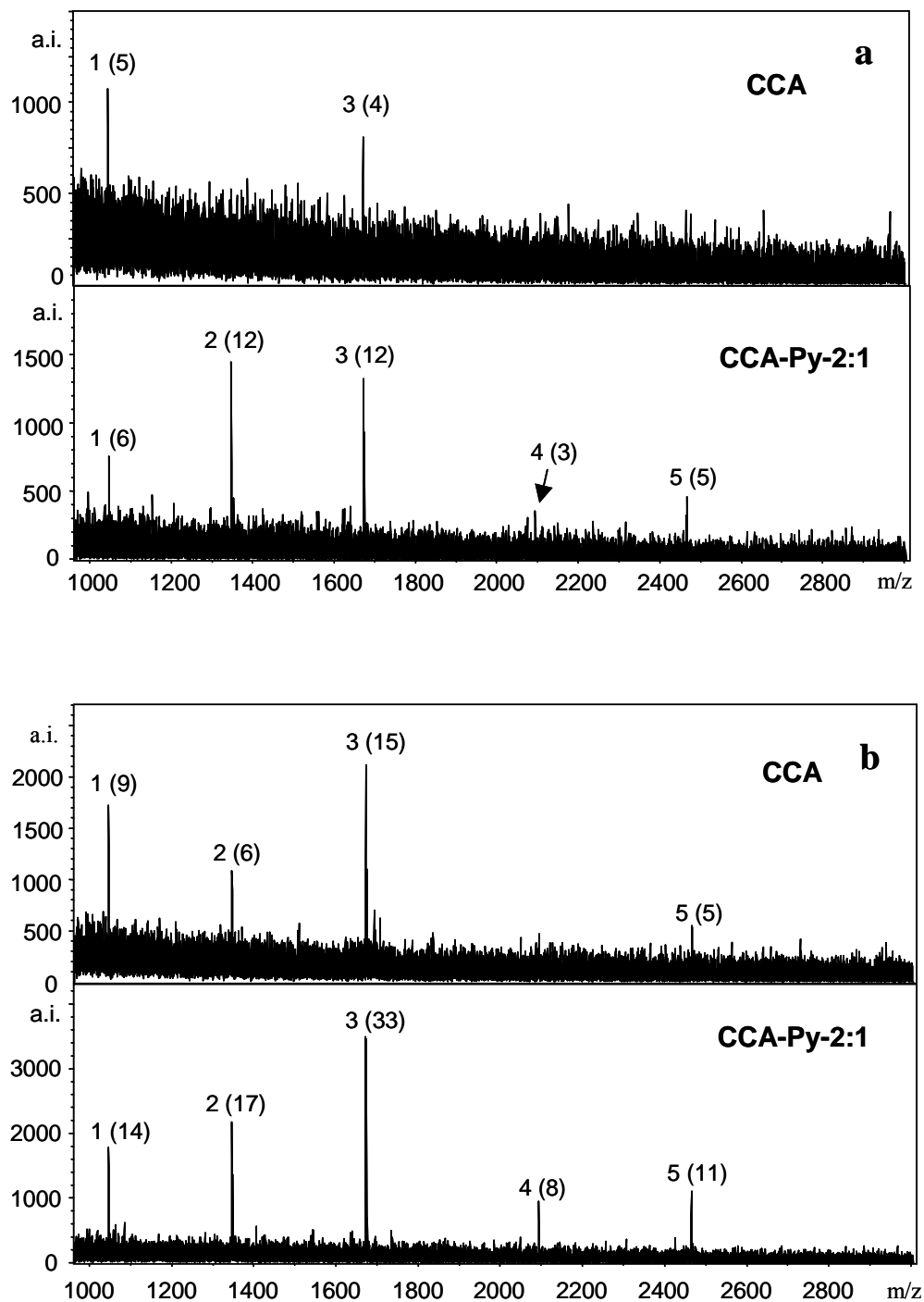


Figure 4.19: MALDI-ToF spectra of a mixture of 5 synthetic peptides measured in CCA and CCA-Py-2:1 (mol:mol).

(a) Sample amounts: angiotensin II (1): 3.2 fmol, substance P (2): 2.5 fmol, neurotensin (3): 2 fmol, ACTH(1-17) (4): 0.8 fmol, ACTH(18-39)(5): 1.4 fmol.

(b) Sample amounts: angiotensin II (1): 4.8 fmol, substance P (2): 3.8 fmol, neurotensin (3): 3 fmol, ACTH(1-17) (4): 1.2 fmol, ACTH(18-39)(5): 2 fmol.

200 shots measured in positive ion mode were accumulated. Numbers in brackets denote the S/N-ratios.

SA and SA-Py-mixtures. However, it was enough for comparison of S/N-ratios of the analytes in different matrix systems of SA.

When SA was used as matrix for the measurement, only ACTH (18-39) could be detected strongly followed by substance P. Other peptides in the mixture did not deliver considerable signal (Figure 4.20). However, all peptides showed significant enhancement in their S/N-ratios in the presence of pyridine. For example, the S/N-ratios were increased, 3-fold for angiotensin II, 4-fold for substance P, 4.8-fold for neurotensin, 8.7-fold for ACTH (1-17) and 1.9-fold for ACTH (18-39) in SA-Py-5:1 compared to SA.

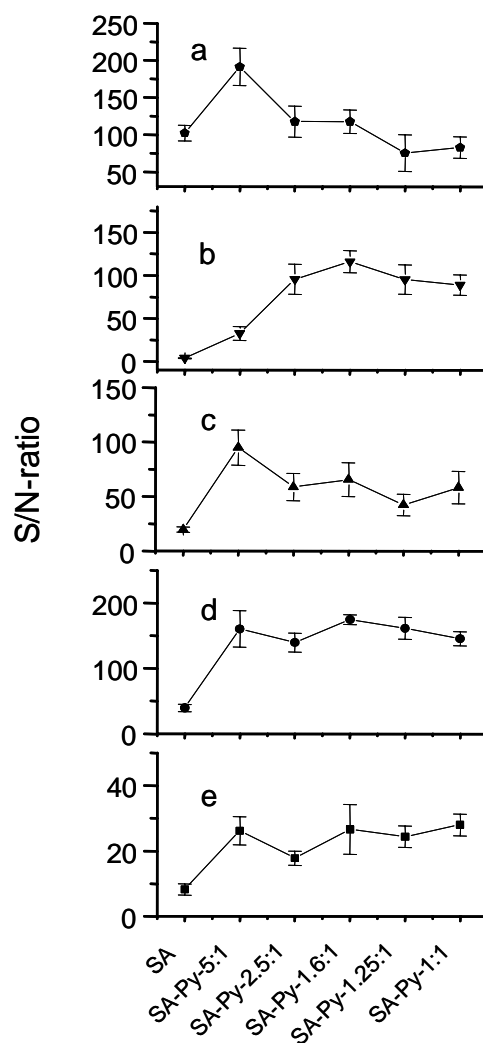


Figure 4.20: S/N-ratios of 5 synthetic peptides in dependence on molar ratio of SA:Py as matrix. Each data point represents an average value of 5 independent measurements. Amount of the peptides on the target: (a): ACTH(18-39) (0.7 pmol), (b): ACTH(1-17) (0.4 pmol), (c): neurotensin (1 pmol), (d): substance P (1.2 pmol), (e): angiotensin II (1.6 pmol).

The S/N-ratio of ACTH (1-17) was even increased up to 30-fold at SA-Py-1.6:1 compared to SA (Figure 4.20). Thus, in contrast to CCA, no optimal SA-Py-ratio was found. Note that SA was introduced as a suitable matrix for analysis of proteins (Beavis and Chait, 1989) but is not recommended for peptide analysis. Nevertheless, the combination of SA with Py in this experiment indicated the clear influence of pyridine as a matrix additive on S/N-ratios of peptides as well. Potential applications could be measurements of peptides in the presence of proteins, e.g. for monitoring of protein digestion both on the level of the substrate (protein) as well as on the peptidic products.

The reasons for the improved S/N-ratios and reduced alkali adduct formation in non-stoichiometric amounts of pyridine are not yet clear. Pyridine does not absorb in the wavelength applied for this study ($\lambda=337$ nm), therefore, the presence of pyridine can not directly influence the efficiency of light absorption of these matrix systems. However, as also explained for the analysis of oligonucleotides with ammonium salts (Nordhoff et al., 1992; Zhu et al., 1996), it can be speculated that the presence of a non-stoichiometric amount of the base may lead to substitution of Na^+/K^+ ion by proton transfer mediated by the base. Additionally, the reduction of noise clearly contributes to explanation for the increase in S/N-ratios of the peptides.

4.7.2 Analysis of tryptic protein digests in pyridinium-based ILM

The optimized molar CCA:Py-ratio of 2:1 found for the model peptides was applied for the analysis of the protein digests. Tryptic in-solution digests of 6 standard proteins in the range of 12 to 75 kDa were used (Table 4.8). Sample amounts of 30 or 100-fmol on-target were measured in two matrix systems, CCA as pure solid matrix and CCA-Py-2:1. The comparison of the measurement in these two matrix systems was performed in terms of identification of proteins in Mascot database-search, the number of peptides matched, the sequence coverage, the rank and the probability based MOWSE-score achieved (Padliya and Wood, 2004). Proteins were assigned as identified, if the MOWSE-score was above the significance level (75) provided by the MASCOT-search algorithm. For the analysis of data, monoisotopic peaks with S/N-ratios equal or higher than 5 were chosen. Note that the LOD was defined for the amount of analyte delivering signal with S/N-ratio higher than 3 (Tholey et al., 2002), but

it is common practice to take into account more intense signals especially in automated proteome analysis.

Figure 4.21 shows the MALDI spectra of a tryptic digest of 30 fmol BSA measured in both matrices. The measurement in CCA delivered five signals. Although all these five signals were imputed to the protein in database search with sequence coverage of 7% (Table 4.8), but the MOWSE-score was 57, which is below the significance level (75). Thus the protein was clearly not identified by this experiment. However, when CCA-Py-2:1 was used for the measurement, three additional signals (m/z 1193.68, 1305.80, 2045.19) were also identified, which could all be matched to the target protein in the database search. The sequence coverage was 15%, which is satisfactory for a protein of this size (66 kDa).

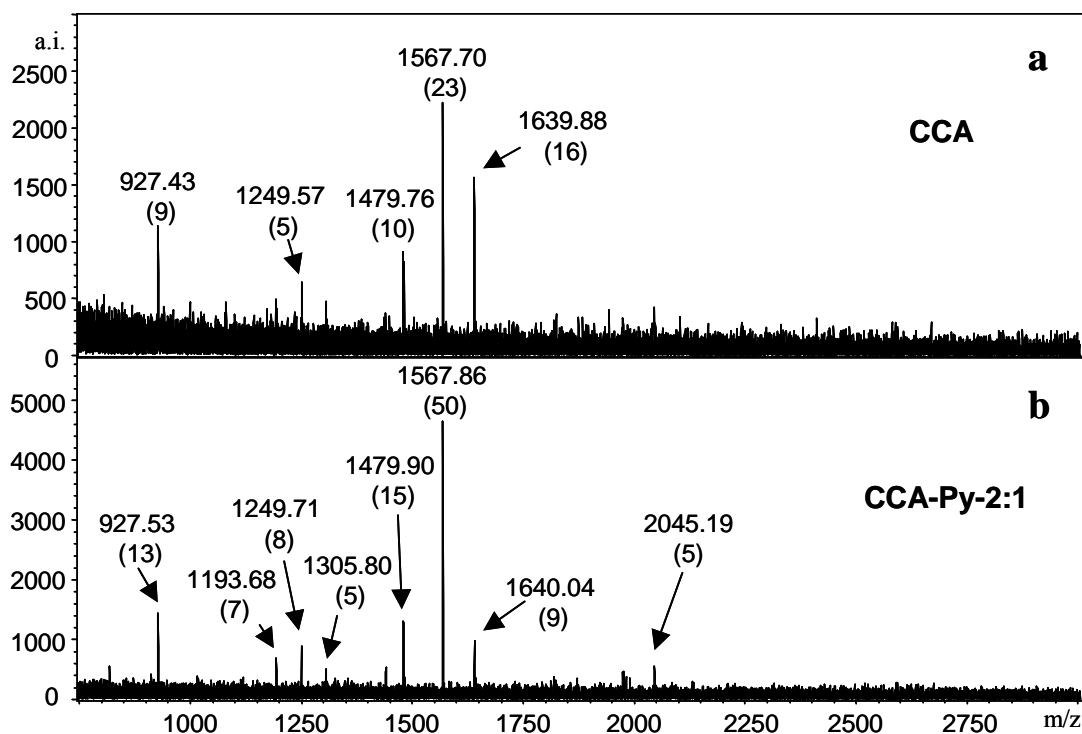


Figure 4.21: MALDI-ToF spectra of a tryptic digest of BSA (30 fmol) measured in (a) CCA, and (b) CCA-Py-2:1 (mol:mol). 200 shots measured in positive ion mode were accumulated. Only signals with S/N-ratios higher than 5 were assigned. Numbers in brackets denote the S/N-ratios.

The target protein was found on rank one with a MOWSE-score of 91, which is clearly above the threshold of confidence. As can be seen in Figure 4.21, the noise in the spectrum was significantly reduced in CCA-Py-2:1 compared to pure CCA which is consistent with the earlier observation for model peptides. The S/N-ratios of four of the peptides found in both

measurements (m/z 927.43, 1249.57, 1479.76, 1567.70) could be increased by factors of 1.4 to 2.2 in CCA-Py-2:1 compared to CCA. The fifth peptide (m/z 1640.00) was stronger in CCA (factor 1.8).

The differences in ionization properties of peptides in MALDI make a definition of LOD for a protein digest difficult. The measurement of 2.5 fmol of the tryptic BSA-digest delivered only 3 peptides (m/z 1479.72, 1567.65, 1639.86) in CCA, whereas 3 additional signals (m/z 1193.7, 1249.73, 1305.82) could be detected in CCA-Py-2:1. The protein could not be identified in database search at this amount in both matrices, but a MOWSE-score of 68 (first rank) and sequence coverage of 11% could be obtained in CCA-Py-2:1, whereas it was not

Table 4.8: Identification of tryptic protein digests by peptide mass fingerprint analysis in CCA and CCA-Py-2:1 (mol/mol). Samples: 30 fmol digest. Only signals with S/N-ratios higher than 5 were counted. Details for database search as given in the material and method section (chapter 3). The significance threshold for MASCOT search was 75 in all cases, proteins were denoted as identified (i.), when the MOWSE-score was bigger than the significance threshold and as not identified (n.i.) when the MOWSE-score was equal or below threshold.

	peptides matched / non-matched		rank / identified / MOWSE-score		sequence coverage (%)		mass accuracy matched peptides (RMS- error)(ppm)		no. unique matched peptides		no. unique non- matched signals	
	CCA	CCA- Py-2:1	CCA	CCA- Py- 2:1	CCA	CCA- Py-2:1	CCA	CCA- Py-2:1	CCA	CCA- Py- 2:1	CCA	CCA- Py- 2:1
Lysozyme	3/0	6/0	5/n.i./ 51	1/i./ 98	23	40	93	57	0	3	0	0
Carbonic Anhydrase	3/2	6/3	9/n.i./ 47	1/n.i./ 68	23	38	139	60	0	3	2	3
Lactate Dehydrogenase	8/0	7/1	2/i./ 110	1/i./ 87	22	19	16	44	2	1	0	1
Alcohol Dehydrogenase	4/0	6/0	2/n.i./ 54	1/i./ 81	17	25	114	74	0	2	0	0
BSA (30 fmol)	5/0	8/0	15/n.i./ 57	1/i./ 91	7	15	42	66	0	3	0	0
BSA (2.5 fmol)	3/0	6/0	- /n.i./ -	1/n.i./ 68	-	11	-	86	0	3	0	0
Glucose Oxidase	8/1	8/3	1/i./ 79	2/n.i./ 73	23	23	24	43	0	0	1	3

even observed in the list of MASCOT database search when CCA was used as matrix (Table 4.8).

The proteins lysozyme, alcohol dehydrogenase and carbonic anhydrase delivered similar results for which 3, 2 and 3, respectively, peptides were found uniquely in CCA-Py-2:1 (Table 4.8). Two proteins, lysozyme and alcohol dehydrogenase, could be unambiguously identified in database search when CCA-Py-2:1 was used, but not in CCA (MOWSE-score of 51 and 54, respectively). Carbonic anhydrase could not be identified in any of the matrices despite of having 3 unique peptides in CCA-Py-2:1, nevertheless, the sequence coverage was increased in CCA-Py-2:1 (38%) compared to CCA (23%). For glucose oxidase, the same number of peptides was found in both matrices; however, it could be identified in CCA and not in CCA-Py-2:1 because of a MOWSE-score just below the significance threshold. In the digest of lactate dehydrogenase, two unique peptides were found in CCA, but only one unique peptide in CCA-Py-2:1. Even so, the protein could be identified in both matrix systems. In the measurement of 30 fmol protein digests, 12 matching peptides were uniquely found in CCA-Py-2:1 whereas only 2 peptides could be uniquely found in CCA from analysis of all 6 proteins (Figure 4.22). Moreover, for the majority of the peptides found in both matrices, the S/N-ratios were increased in CCA-Py-2:1 (Figure 4.23).

In case of glucose oxidase, carbonic anhydrase and lactate dehydrogenase, additional peaks were observed in the matrix CCA-Py-2:1, which could not be assigned to the proteins. Some of these signals (m/z 1218.65 in glucose oxidase, m/z 1496.98 and 2218.41 in carbonic anhydrase) were found in both matrices. Other signals with S/N-ratios just above the S/N-threshold were found only in CCA-Py-2:1 (e.g. m/z 2112.19 in lactate dehydrogenase) but were also observable with smaller S/N-ratios in CCA. The appearance of such extra peaks can potentially cause wrong identification or non-identification of target protein in database search as can be seen here for the two proteins, carbonic anhydrase and glucose oxidase.

In second series of the experiments, 100 fmol (on target) of the proteins digests were measured in CCA and CCA-Py-2:1 (data not shown). The analysis of proteins digests in this amount delivered higher numbers of matched peptides compared to 30 fmol measurements, thus leading to increased MOWSE-scores and facilitated protein identification in database search. Although all proteins could be identified in database search for both matrix systems, higher percentage of sequence coverage with increased numbers of unique peptides could be achieved in CCA-Py-2:1 compared to CCA.

Figure 4.23 shows the comparison of the S/N-ratios of the peptides found in both matrices for both measurements of 30 as well as 100 fmol samples. In the measurement of 30 fmol

samples, two unique peptides found in CCA were in the lower mass range (m/z 929.58 and m/z 1118.6) and the unique peptides found in CCA-Py-2:1 were all at higher m/z values (Figure 4.22). However, no clear correlation could be found between m/z value and the tendency of the peptides to form stronger signals in CCA-Py-2:1. Further, the distribution of the peptides with higher S/N-ratios was uniformly distributed over the m/z range investigated (Figure 4.23). The S/N-ratios of 40% (in the measurement of 30 fmol protein) and 42 % (in the measurement of 100 fmol protein) of the peptides found in both matrices were increased up to 9-fold in the CCA-Py-2:1. For further 40 % of the peptides, the S/N-ratios were increased with factors up to 2, whereas about 20% of the peptides showed up to two fold higher S/N-ratios in CCA.

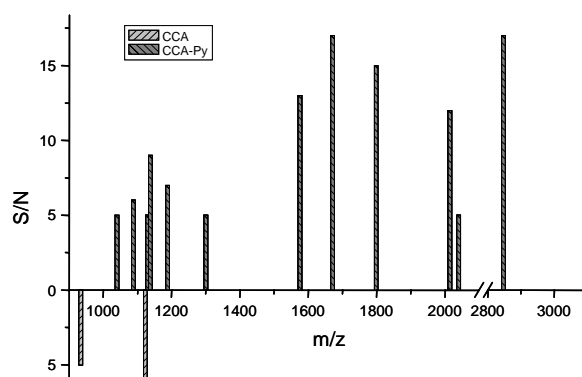


Figure 4.22: S/N-ratios in dependence of m/z -values of peptides assigned to the proteins found only in CCA (down bars) or CCA-Py-2:1 (mol:mol) (up bars) in tryptic digests (30 fmol) of 6 model proteins. Only signals with S/N-ratios higher than 5 were assigned. 200 shots measured in positive ion mode were accumulated.

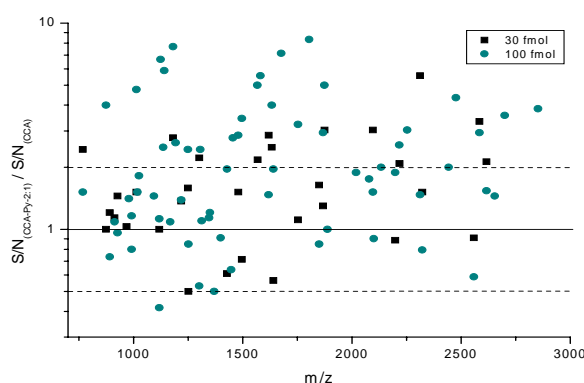


Figure 4.23: Ratios of S/N-ratios (logarithmic scale) of peptides in dependence of m/z -values measured in CCA-Py-2:1 (mol/mol) and CCA in tryptic digests of 6 proteins. Squares: 30 fmol, circles: 100 fmol digests. Total number of peptides: 97. Only signals with S/N-ratios higher than 5 were assigned. 200 shots measured in positive ion mode were accumulated. Dashed lines: ratios differed by a factor of 2.

Only one out of 97 peptides measured in both concentrations showed a 2.5-fold higher S/N-ratio in CCA compared to the measurement in the presence of pyridine.

Similar to the analysis of 30 fmol protein digests, the number of non-assigned signals was also increased in measurement of 100 fmol sample especially in the pyridinium-based ILMs. Some of these additional signals were observed in more than one digest (e.g. m/z 1066.22, 1084.77, 2093.16), others (e.g. m/z 1024.44, 1152.54, 1817.85, 1973.95, 2526.25) occurred only in single digest (here only the most intensive signals with S/N-ratios bigger than 10 were listed). It should be mentioned here that adducts between the analytes and compounds of the matrix (e.g. with pyridine) could not be observed. Therefore, the origin of these peaks is still unknown. However, one reason for the occurrence of these additional signals could be the presence of impurities or contaminations in the proteins. Furthermore, non-specific cleavage products (Konig et al., 2001) or transpeptidation products (Schaefer et al., 2005) can be also observed as by-products during tryptic cleavage of proteins. Potentially, small amounts of such impurities are detectable in CCA-Py-2:1 due to increased sensitivity of this matrix. For the elucidation of the origin of these additional signals, further experiments, e.g. MS/MS experiments, would be necessary.

The matrix clusters of CCA often appear in the MALDI spectra. The composition of these clusters consists of a certain number of CCA molecules with Na/K ions. It was described earlier, that washing of the MALDI samples with ammonium salts strongly reduces the formation of matrix clusters, which are mainly formed on the surface of the crystals (Smirnov et al., 2004). This procedure, however, did not significantly influence the formation of Na/K-adducts. By the addition of small amounts of ammonium salts to the matrix itself, a strong increase of S/N-ratios and thus of the spectrum quality could be reached (Smirnov et al., 2004). In our study, adducts with m/z values of 833.09 ($[4M+2K-H]^+$), 855.07 ($[4M+Na+2K-2H]^+$), 871.04 ($[4M+3K-2H]^+$) and 1060.09 ($[5M+3K-2H]^+$) have been observed especially in the measurement of the protein digests in CCA, whereas these matrix clusters were almost completely absent in CCA-Py-2:1. Therefore, the addition of non-stoichiometric amounts of pyridine leads to comparable effects without the need for additional washing steps. Nevertheless, the presence of the matrix additive cannot explain the reduction of matrix-cluster formation. Further experiments for the elucidation of the theoretical background will be necessary but are beyond the scope of this work. It should be mentioned here that a strong cluster formation was shown for measurements applying a laser with a wavelength of 355 nm (Smirnov et al., 2004). The reduction of cluster formation in pyridinium-based ILMs

observed here, contributes to the improved spectral quality and hence further facilitated identification of proteins.

The average errors of the m/z values of the matched peptides (expressed by the rms errors, Table 4.8) were influenced by the choice of the matrix. In three digests (lysozyme, carbonic anhydrase and alcohol dehydrogenase) this error was reduced by a factor up to 2 (Table 4.8). Thus, for the database search a mass tolerance of 100 ppm rather than the 200 ppm applied here for the comparison delivered the same results for protein identification in CCA-Py-2:1, whereas in CCA 4 of the 6 proteins could not be identified with this reduced mass tolerance. The errors in mass accuracy were particularly reduced for peptides with low S/N-ratios but were not significantly influenced for intensive signals. This is certainly caused by the fact that the peak shape of signals with low intensities frequently differs from the expected Gaussian-shape. Therefore the assignment of the (exact) mass of such peaks is more difficult than for ideally shaped peaks. Further, for small peaks the FWHM values determining the resolution of peaks were worse than for intensive peaks. On the other hand, the peak shapes, mass accuracy and resolution were not changed by the presence of pyridine, when higher concentrations of the analytes yielding intense signals were measured. As a consequence of the improved S/N-ratios and hence the more ideal peak forms in CCA-Py-2:1, the assignment of the masses and hence the mass accuracy and resolution achieved were improved, which clearly facilitates the analysis of spectra.

The results described above were accompanied with dilution of the digest samples prior to measurement. This dilution step not only dilutes the analytes but also potential impurities (e.g. salts, detergents). Therefore, to investigate the performance of the pyridinium-based ILM for non-diluted samples containing e.g. buffers and denaturing reagents which are necessary for the digestion of the protein, the digest of diluted BSA (final on-target amount: 30 fmol) was measured without any dilution or desalting steps. The results achieved were absolutely comparable to those obtained with the diluted samples. Only 6 peptides were observed in CCA, which did not allow the unambiguous identification of the protein (MOWSE-score 67). In CCA-Py-2:1, 7 peptides with a sequence coverage of 14% (MOWSE-score 79) were found. In accordance to the results described for the diluted samples, alkali-adducts signals, matrix clusters and chemical noise background were strongly reduced in the ILM.

A general strategy for the identification of the proteins obtained from a complex proteome samples is the separation of proteins mixture by one- or two-dimensional (1D or 2D) gel electrophoresis followed by digestion of the protein bands excided from the gel. The digests

are then subject of mass spectrometry based fingerprint analysis. Thus, to verify the capability of pyridinium-based ILM in this respect, the tryptic in-gel digestions of two model proteins (BSA and lysozyme) separated by 1D- gel electrophoresis was analysed in CCA and CCA-Py-2:1. The results obtained in this experiment did not differ from the earlier results described for the in-solution digestions of the proteins (data not shown). Moreover, the applicability of this matrix system was examined in a real-life proteomic experiment. Herein, the tryptic in-gel digestion of the protein (fructose-bisphosphate aldolase) excised from a coomassie-stained 2D-gel of the cytosolic proteome of *C. glutamicum* was performed. Figure 4.24 shows the corresponding MALDI-MS spectra measured in CCA and CCA-Py-2:1. Compared to measurement in CCA, the signal intensities and S/N-ratios of the peptides obtained from the tryptic cleavage were remarkably increased in CCA-Py-2:1 (e.g. S/N-ratio of the signal m/z 1607.76: 146 for CCA-Py-2:1, 50 for CCA). Sixteen signals could be identified in CCA, of which nine signals could be matched to the target protein with an average error of 148 ppm. Despite of gaining 44% sequence coverage in database search, the MOWSE-score (67) achieved was too low for unambiguous identification of the protein. In the measurement in CCA-Py-2:1, thirteen signals of the twenty five detected signals could be assigned to the target protein with an average rms error of 93 ppm. This led to a sequence coverage of 59% and a MOWSE-score of 89. Thus the protein could be identified unambiguously. In both measurements, a number of non-identified peaks could be also detected. All these signals (with the exception of a signal at m/z 1804.54 in CCA-Py-2:1) could be found in both matrices. Note that the four additionally non-identified peaks observed in CCA-Py-2:1 could be found in CCA, too, but were below the S/N-threshold of 5.

To check the compatibility of the pyridinium-based ILM with frequently used sample preparation methods, the measurement of the sample washed with 0.1% TFA solution was compared with the measurement in CCA-Py-2:1. The resulted measurement spectra did not change significantly between the two matrix systems (data not shown).

Moreover, solutions of ILMs in acetonitrile/water can be used for the elution of peptides from hydrophobic microcolumns used for desalting of the digest (Zip-Tip-preparation) and then directly applied for MALDI analysis.

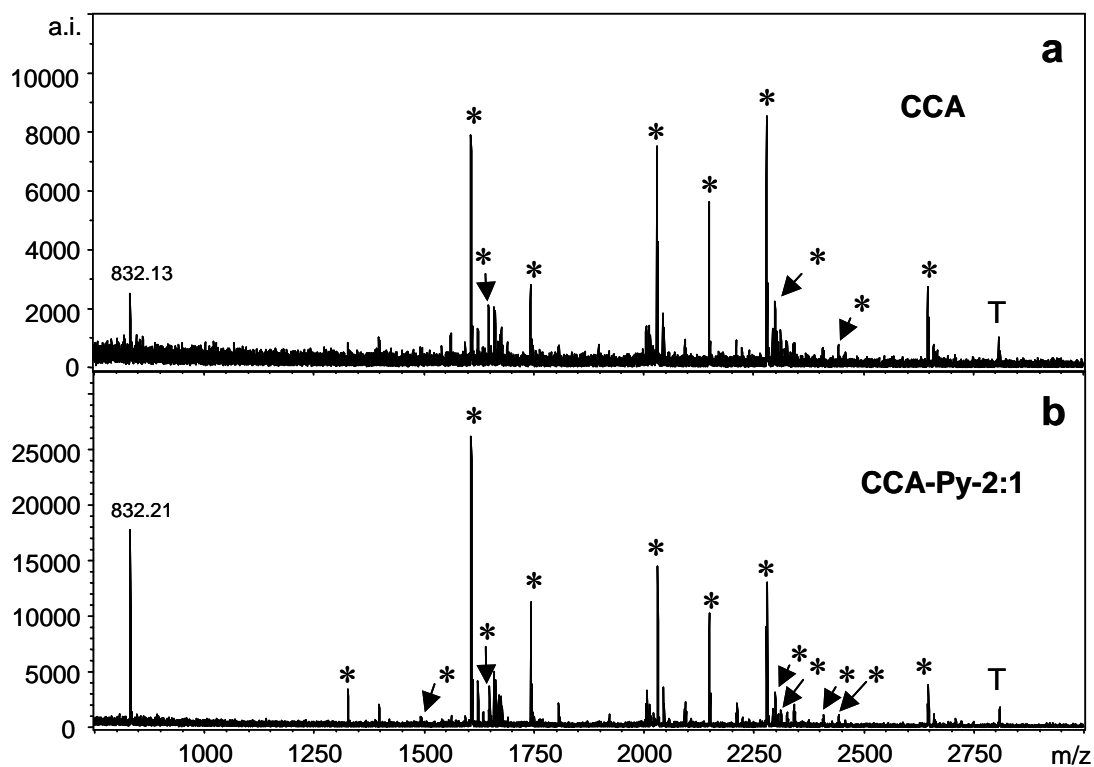


Figure 4.24: MALDI-TOF spectra of a tryptic in-gel digest of the protein fructose-bisphosphate aldolase excised from a coomassie-stained 2D-gel of the cytosolic proteome of the bacterium *C. glutamicum* measured in (a) CCA, and (b) CCA-Py-2:1 (mol:mol). *: peaks assigned to the target protein. T: peptide derived from trypsin autoproteolysis. Signal at m/z 821.13 (CCA) 832.21 (CCA-Py-2:1): potential deamidation product of the peptide IDGEVGNK. The signal was not used for protein identification in database search, because the mass deviation to the theoretical value was above 200 ppm in both spectra.

5 MALDI-MS for Analysis of Ionic Liquids (ILs) Containing Samples

Despite of wide applications of mass spectrometric methods for structural determination, it has not been very intensively used for characterization of ILs. Use of FAB (fast atom bombardment) mass spectrometry was the earliest attempt for characterization and identification of ILs (Abdul-Sada et al., 1992). Recently, electrospray ionization (ESI) mass spectrometry has also been used for identification of ILs as well as determination of their solubility in water (Alfassi et al., 2003).

In this report, the characterization of ILs was performed using MALDI-MS. The investigations were carried in two different modes i) laser desorption/ionization (LDI) mode to check whether diluted ILs can be analyzed directly and ii) MALDI mode after addition of solid matrices. However, simultaneous identification of both the cation $[\text{Cat}]^+$ and anion $[\text{An}]^-$ was difficult, because only monomeric ions were produced. Hence, separate experiments in positive ion mode for cations and in negative ion mode for anions were performed for both LDI as well as MALDI modes.

The analysis of LMW compounds (below 500 Da) is a prerequisite for the determination of enzyme activities or the analysis of chemical reactions in ILs. A number of methods are available for this purpose, but they suffer from several restrictions as described in the introduction (Chapter 2). Mass spectrometry may be an additional tool circumventing many of these problems. In this regard, application of MALDI-MS for the analysis LMW compounds dissolved in ILs is shown. Moreover, the analysis of peptides and proteins dissolved in ILs is discussed to investigate the possible chemical modifications of peptides and proteins in the presence of ILs.

5.1 Characterization of ILs

5.1.1 LDI-mode analysis

All the ILs selected for this study (Table 5.1) consists an imidazole ring (1-butyl-3-methyl-imidazolium (BMIM)). Therefore, they all show the same mass ions in the positive ion mode except 1,3-dimethyl-imidazolium (MMIM). In the positive ion mode, BMIM showed a strong signal at $m/z=139$ for $[\text{Cat}]^+$ (Table 5.1). Additionally, the signal at $m/z = 83$ caused by loss

of the butyl group was also observed (Figure 5.1). IL of MMIM gave only a strong peak signal at $m/z=97$ for $[\text{Cat}]^+$. Loss of methyl groups was not observed at both imidazolium cations. They did not show any $[\text{M}+\text{Na}]^+$ and $[\text{M}+\text{K}]^+$ -adducts. Due to having different anion $[\text{An}]^-$ groups in the ILs, different mass ions could be observed in the negative ion mode analysis. IL of $[\text{OctSO}_4]$ gave a strong $[\text{An}]^-$ -signal ($m/z=209$) and a weak fragment signal of $[\text{SO}_4]^-$ at $m/z=96$. The $[\text{An}]^-$ -peak of the $[(\text{CF}_3\text{SO}_2)_2\text{N}]$ IL was observed at $m/z=280$. Additionally, the fragments in the form of $[\text{M}-\text{CF}_3]^-$ at $m/z=211$ and $[\text{M}-\text{CF}_3\text{SO}_2]^-$ at $m/z=147$ were identified (Figure 5.1). IL of $[\text{PF}_6]$ showed the mass ion of $[\text{An}]^-$ at $m/z=145$ and $[\text{BF}_4]$ IL produced a $[\text{An}]^-$ -peak at $m/z=87$. The weak $[\text{An}]^-$ of $[(\text{CH}_3)_2\text{PO}_4]$ appeared at $m/z=125$ (Table 5.1). It was found that higher laser energy was necessary for the detection of ILs due to their comparably low absorption coefficient at the laser wavelength (337 nm) applied.

Table 5.1: Properties of the ILs and signals in laser desorption ionization (LDI)-MS.

Ionic Liquids	state of aggregation at 25°C	water miscibility	ϵ_{337} (methanol) [$\text{L}\cdot\text{mol}^{-1}\cdot\text{cm}^{-1}$]	positive ion mode	negative ion mode
[BMIM][OctSO₄]	liquid	miscible	0.71	83 ^a , 139 ^b	209 ^c , 96 ^d
[BMIM][BF₄]	liquid	miscible	0.15	83 ^a , 139 ^b	86/87 ^c , 280 [*]
[MMIM][(\text{CH}_3)_2\text{PO}_4]	liquid	miscible	0.224	97 ^b	125 ^c
[BMIM][PF₆]	liquid	immiscible	0.315	83 ^a , 139 ^b	145 ^c
[BMIM][(\text{CF}_3\text{SO}_2)_2\text{N}]	liquid	immiscible	0.5	83 ^a , 139 ^b	280 ^c , 211 ^e , 147 ^f

a = $[\text{Cat}-\text{Butyl}]^+$, b = $[\text{Cat}]^+$, c = $[\text{An}]^-$, d = $[\text{SO}_4]^-$, e = $[\text{An}-\text{CF}_3]^-$, f = $[\text{An}-\text{CF}_3\text{SO}_2]^-$, *: not identified. $[\text{BF}_4]^-$ shows two peaks for $[\text{An}]^-$, caused by the isotope distribution of boron. Cat: cation of IL, An: anion of the IL. Only signals with S/N-ratios higher than 5 were accepted. Bold: most intensive signals.

5.1.2 MALDI-mode analysis

Analysis of ILs with assistance of solid matrices, DHB, CCA and SA was performed in both positive and negative ion mode at a final molar IL:matrix ratio of 1:10 (Table 5.2). The obtained MALDI-spectra either in positive or negative ion mode contained same signals of ILs and their fragments found in LDI analysis. Moreover, some additional signals originated

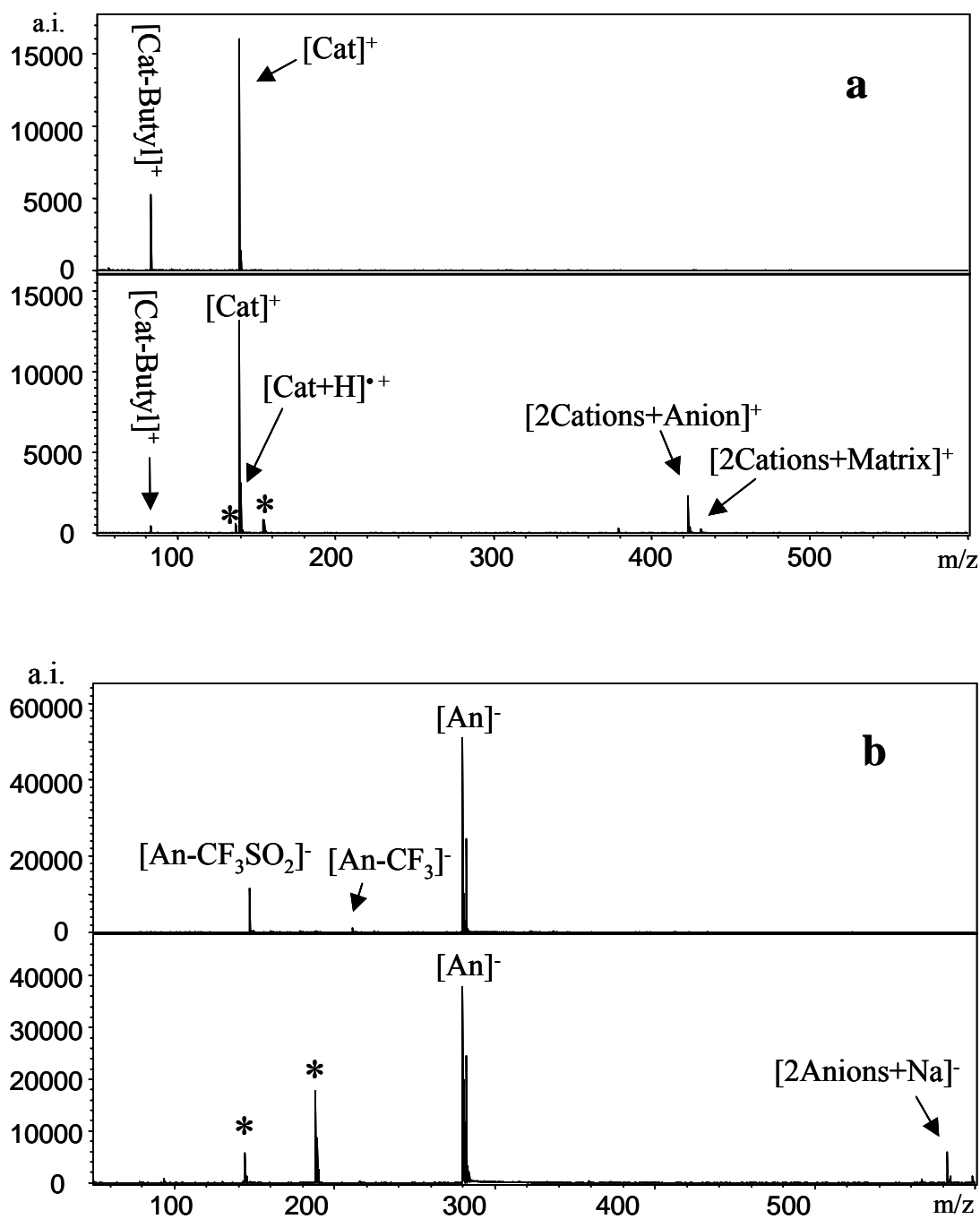


Figure 5.1: (a) [BMIM][PF₆] in positive ion mode measured by LDI- (top) and MALDI (bottom) using DHB as matrix. (b) [BMIM][(CF₃SO₂)₂N] in negative ion mode measured by LDI- (top) and MALDI (bottom) using CCA as matrix. [Cat]⁺: signal of IL cation. [An]⁻: signal of the IL anion. For all spectra, 200 shots were accumulated. A molar IL/matrix-ratio of 1:10 was applied in case of MALDI measurements. *: peaks from DHB and CCA, respectively.

from or induced by matrix substances were also observed as following:

Matrix molecules: The $[M+H]^+$ and $[M-H]^-$ signals of matrix molecules could be detected in the presence of ILs (Figure 5.1). However, the signal intensities were not very strong compared to the signals of the $[Cat]^+$ of IL in positive ion mode or the $[An]^-$ of IL in negative ion mode analyses, despite of 10-fold molar excess of matrix molecules to the ILs. Such suppression of matrix signals is typically observed at lower matrix-to-analyte ratios (Chan et al., 1992; Knochenmuss et al., 1996). Additionally, the Na/K-adducts typically found for pure matrix substances, disappeared in the presence of ILs in the positive ion mode (Table 5.2) (Figure 5.1).

IL molecules: In addition to the $[Cat]^+$ -signals of ILs found in LDI mode, $[Cat + H]^{2+}$ -signals were also observed in the positive ion mode of MALDI analysis. This signal was more intensive in CCA or DHB and weak in the case of SA.

Formation of aggregates: Another group of signals found only in MALDI-MS, were identified as aggregates between $[Cat]^+$ and $[An]^-$ of the ILs (Table 5.2). In the positive ion mode, the signals of these aggregates were more intense when DHB or CCA were used as matrices compared to the analysis in SA. For the ILs investigated here, aggregate ions of two IL-cations and one IL-anion, e.g. $[2BMIM+PF_6]^+$ were detected (Figure 5.1). No aggregate ion was detected for the IL $[BMIM][BF_4]$ in SA. Moreover, some weak signals obtained from aggregates between IL-cations and the MALDI-matrices CCA and DHB, e.g. $[2BMIM+CCA]^+$, could be observed, whereas no adducts were found between IL-cations and SA. In the negative ion mode, aggregate formation between two IL-anions and a single sodium ion were found, e.g. $[2PF_6+Na]^-$. In the case of the IL $[BMIM][PF_6]$, aggregates of two IL-anions and one IL-cation ($[2PF_6+BMIM]^-$) were observed either with high (DHB or CCA) or with low intensity (SA). The IL-anion $[BF_4]^-$ formed only weak aggregates in DHB and CCA, whereas none were observed in SA. In case of the IL $[MMIM][[(CH_3)_2PO_4]^-]$, no aggregate formation could be observed in negative ion mode.

5.2 Analysis of small molecules dissolved in ILs

ILs have been already tested for their applicability as MALDI-matrices for the analysis of peptides and proteins (Armstrong et al., 2001). It was found that ILs are not suitable to be used as matrix. However, since ILs could be analysed without assistance of matrix molecules (previous chapter), therefore, they were tested for their potential use as MALDI-matrices for

MALDI-MS for Analysis of Ionic Liquids (ILs) Containing samples

Table 5.2: Signals of ILs and MALDI-matrices in MALDI-MS: positive ion mode (top) and negative ion mode (bottom)

Ionic Liquid	CCA	DHB	SA
[BMIM][OctSO ₄]	83 ^a , 139^b , 140^c , 164 ^d , 172 ^e , 190 ^f , 379 ^g , 466 ⁱ , 487^h	83 ^a , 139^b , 140^c , 137 ^e , 154 ^j , 155 ^f , 431 ⁱ , 487^h	83 ^a , 139^b , 140 ^c , 207 ^e , 224 ^j , 225 ^f , 487 ^h
[BMIM][BF ₄]	83 ^a , 139^b , 140^c , 164 ^d , 172 ^e , 190 ^f , 379 ^g , 365^h , 466 ⁱ	83 ^a , 139^b , 140^c , 154 ^j , 155 ^f , 365^h , 431 ⁱ	83 ^a , 139^b , 140 ^c , 207 ^e , 224 ^j , 225 ^f
[MMIM][(CH ₃) ₂ PO ₄]	97^k , 98^l , 111 [*] , 164 ^d , 172 ^e , 190 ^f , 379 ^g , 319 ^h , 382 ⁱ	97^k , 98^l , 154 ^j , 155 ^f , 319^h , 347 ⁱ	97^k , 98 ^l , 207 ^e , 224 ^j , 225 ^f , 319 ^h
[BMIM][PF ₆]	83 ^a , 139^b , 140^c , 164 ^d , 172 ^e , 190 ^f , 379 ^g , 423^h , 466 ⁱ	83 ^a , 139^b , 140^c , 137 ^e , 154 ^j , 155 ^f , 423^h , 431 ⁱ	83 ^a , 139^b , 140 ^c , 207 ^e , 224 ^j , 225 ^f , 423 ^h
[BMIM][(CF ₃ SO ₂) ₂ N]	83 ^a , 139^b , 140^c , 164 ^d , 172 ^e , 190 ^f , 379 ^g , 466 ⁱ , 558 ^h	83 ^a , 139^b , 140^c , 137 ^e , 154 ^j , 155 ^f , 431 ⁱ , 558^h	83 ^a , 139^b , 140 ^c , 207 ^e , 224 ^j , 225 ^f , 558 ^h

Ionic Liquid	CCA	DHB	SA
[BMIM][OctSO ₄]	209^g , 144 ^b , 188 ^c , 189 ^d , 441^e	209^g , 153 ^c , 154 ^d , 307 ^f , 441 ^e	209^g , 223 ^c , 224 ^d , 447 ^f , 441 ^e
[BMIM][BF ₄]	86/ 87^h , 144 ^b , 188 ^c , 189 ^d , 197 ^e	86/ 87^h , 153 ^c , 154 ^d , 307 ^f , 197 ^e	86/ 87^h , 223 ^c , 224 ^d , 447 ^f
[MMIM][(CH ₃) ₂ PO ₄]	125 ^j , 144 ^b , 152 [*] , 188 ^c , 189 ^d	152 [*] , 153 ^c , 154 ^d , 307 ^f	125^j , 152 [*] , 223 ^c , 224 ^d , 447 ^f
[BMIM][PF ₆]	145^a , 144 ^b , 188 ^c , 189 ^d , 313^e , 429 ^k	145^a , 153 ^c , 154 ^d , 307 ^f , 313 ^e , 429 ^k	145^a , 223 ^c , 224 ^d , 313 ^e , 429 ^k , 447 ^f
[BMIM][(CF ₃ SO ₂) ₂ N]	280ⁱ , 144 ^b , 188 ^c , 189 ^d , 583^e	280ⁱ , 153 ^c , 154 ^d , 307 ^f , 583 ^e	280ⁱ , 223 ^c , 224 ^d , 447 ^f , 583 ^e

Table top: a = [BMIM-Butyl]⁺, b = [BMIM]⁺, c = [BMIM+H]⁺, d = [M-CN+H]⁺, e = [M-H₂O+H]⁺, f = [M+H]⁺, g = [2M+H]⁺, h = [2Cat+An]⁺, i = [2Cat+M]⁺, j = [M]⁺, k = [MMIM]⁺, l = [MMIM+H]⁺, * Not identified.

Table bottom: a = [PF₆]⁻, b = [M-COOH]⁻, c = [M-H]⁻, d = [M]⁻, e = [2An+Na]⁻, f = [2M-H]⁻, g = [OctSO₄]⁻, h = [BF₄]⁻, i = [(CF₃SO₂)₂N]⁻, j = [(CH₃)₂PO₄]⁻, k = [2An+Cat]⁻, * Not identified.

M denotes signals occurring from solid matrices. Cat: cation of IL, An: anion of IL. Only signals with S/N-ratios higher than 5 were accepted. Bold: most intensive signals of the ILs.

the analysis of amino acids. Similar to proteins and peptides, ILs were not able to ionize amino acids. Even aromatic amino acids such as tryptophan, which can be analyzed in LDI-MS (Karas et al., 1985), did not deliver signals in the presence of a molar excess of ILs (molar IL:tryptophan-ratio = 100). Weak $[M+H]^+$ ions of the amino acid could be detected in a mixture with an excess of analyte compared to IL (molar IL:tryptophan ratio = 0.1).

Since ILs were not suited to ionize amino acids, the analysis of amino acids in the presence of ILs was performed after addition of the solid matrices DHB, CCA and SA. Although amino acid signals could be observed in this condition, however, the appearance of the analyte signals depended on the nature of the ILs (Table 5.3). Amino acid signals could be observed only in the water-immiscible ILs [BMIM][PF₆] and [BMIM][(CF₃SO₂)₂N] and not in the presence of the water-miscible ILs [BMIM][OctSO₄], [BMIM][BF₄] and [MMIM][(CH₃)₂PO₄]. The matrix-to-analyte (M/A)-ratio is important for MALDI analysis (Wang et al., 1993). Despite of applying different molar IL:matrix:analyte ratios, amino acids remained undetectable in water-miscible IL. Even changes in amount of analyte on the target could not improve the measurement of amino acids in the presence of water-miscible ILs. For the measurement of LMW analytes, an optimal molar M/A-ratio in the range 10:1-100:1 was found (Kang et al., 2000). Optimal molar M/A-ratios for the analysis of amino acids in the presence of IL were found to be about 55:1-60:1, but analysis was possible in a range between 30:1 and 125:1. Peak widths (FWHM) of LMW analytes were not significantly changed compared to classical MALDI measurements.

ILs delivered a liquid film on the target when prepared for LDI analysis. Mixture of ILs with solid matrices followed the same crystallization behavior generally observed in pure solid matrixes on the target after evaporation of solvent. However, the crystal size of DHB was smaller in the mixture of IL-DHB compared to pure DHB. The presence of the ILs resulted in increased hot spot formation even when the otherwise relatively homogeneous matrix CCA was used and that is why more time and more number of shots was needed for analysis. The reasons for this behavior are not known.

Typically, higher laser energy was required for the detection of analyte in the presence of IL compared to pure solid matrices (~10% based on laser attenuation values). Despite of using higher laser energy the relative analyte ion intensities were lower than without IL. The high laser energy leads to a broadening of the signals of the components of the IL in some cases (Figure 5.2).

In accordance with the results observed for the matrix signals, Na/K-adducts were not observed for any of the LMW compounds tested here (Table 5.3) and they were only detected

as protonized ions. Hence, this hinders the analysis of sugars, since they are best detected as Na or K-adduct ions due to their low basicity. In fact, we could show that unmodified sugars cannot be analyzed under these conditions. In contrast, analysis of modified sugar derivatives like N-acetylglucosamine and D-gluconic acid, which can form protonated or deprotonated ions, was possible under the same conditions as applied for the amino acids (Table 5.3). The LOD for alanine in the system [BMIM][PF₆]/CCA was found to be 10⁻¹⁴ mol which is comparable to the values found earlier for the analysis in solid matrices (Tholey et al., 2002).

Table 5.3: Analysis of amino acids and sugars in ILs using solid matrices DHB, CCA and SA. Signal intensities (arbitrary units, measured at laser energies just above threshold) of [M+H]⁺ of the analytes after accumulation of 200 shots: + : below 2000; ++ : between 2000-5000; +++ : >5000; n.d.: not detected. *: measured in negative ion mode ([M-H]⁻).

	[BMIM] [OctSO ₄]	[BMIM] [BF ₄]	[MMIM] [(CH ₃) ₂ PO ₄]	[BMIM] [PF ₆]	[BMIM] [(CF ₃ SO ₂) ₂ N]	Matrix
Glutamic acid	n.d.	n.d.	n.d.	+++	++	CCA
Arginine	n.d.	n.d.	n.d.	+++	+++	CCA
Serine	n.d.	n.d.	n.d.	+++	++	CCA
Tyrosine	n.d.	n.d.	n.d.	+	+	CCA
Phenylalanine	n.d.	n.d.	n.d.	++	++	CCA
Alanine	n.d.	n.d.	n.d.	++	+++	CCA
Phenylglycine	n.d.	n.d.	n.d.	+	+	CCA
F-Phenylglycine	n.d.	n.d.	n.d.	+	+	CCA
Fructose	n.d.	n.d.	n.d.	n.d.	n.d.	CCA, DHB
N-Acetyl-D-glucoseamine	n.d.	n.d.	n.d.	+	+	DHB
D-Gluconic acid*	n.d.	n.d.	n.d.	+++	+++	SA

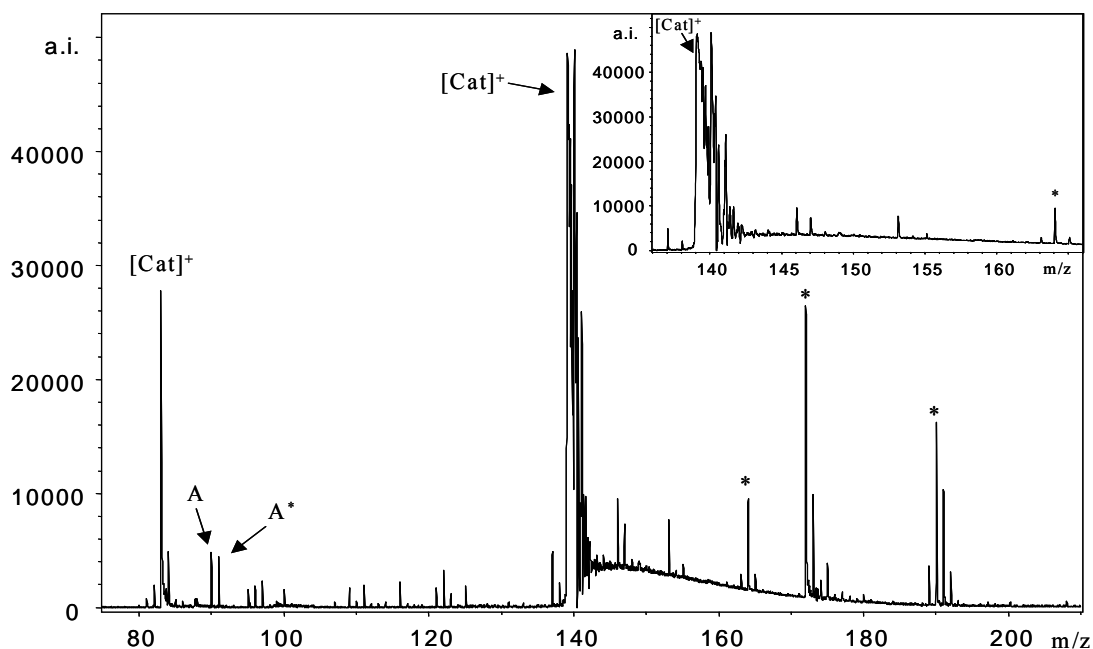


Figure 5.2: The positive ion mode MALDI-spectrum for a mixture of alanine, $1\text{-}^{13}\text{C}$ -alanine and IL [BMIM][PF₆] with CCA as matrix at molar IL:analyte ratio of 100:1 for quantification of alanine shown in figure 5.2. 200 shots were collected. The peak broadening of the IL signal (m/z 139) can be seen clearly (the insert shows a detailed view of the broadened signal of IL [Cat]⁺). [Cat]⁺: signals of IL cation, A: alanine, A*: $1\text{-}^{13}\text{C}$ -alanine, *: peaks from matrix CCA.

5.2.1 Quantification of low molecular weight compounds in IL

Homogeneity of samples is a major issue in quantitative analysis by MALDI-MS. As was discussed before (Chapter 4.3.1), the sample inhomogeneity could induce prolongation of analysis times and unsatisfactory standard deviations. However, despite of the inhomogeneity of the samples in the presence of ILs described above, quantitative analysis of alanine using $1\text{-}^{13}\text{C}$ -alanine as labeled internal standard could be performed in the system [BMIM][PF₆]/CCA. A linear calibration curve ($r^2=0.987$, mean standard deviation =11.5%) was obtained when a dilution series with different molar ratios of analyte to internal standard was applied (Figure 5.3). Due to inhomogeneous sample preparation in the presence of ILs quality of the calibration curve is not as good as that obtained using solid matrices (Kang et al., 2001). In contrast to an earlier report that automated analysis protocols could deliver most reliable results in the shortest time for quantitative MALDI analysis (Kang et al., 2001), it was not possible to use such a protocol for quantification in the presence of IL here. The reasons for this problem were peak broadening of the IL signals and increase of the baseline due to the need for elevated laser energy (Figure 5.2). This problem could not be overcome

by the data acquisition and analysis software used here. Therefore a manual analysis protocol was applied for the analysis. Despite of these limitations, quantitation of analytes dissolved in ILs can be performed relatively easy and fast if ISs are used. As will be shown later (Chapter 5.4), quantitative monitoring of the enzyme-catalyzed reaction performed in ILs will be possible using this manual protocol.

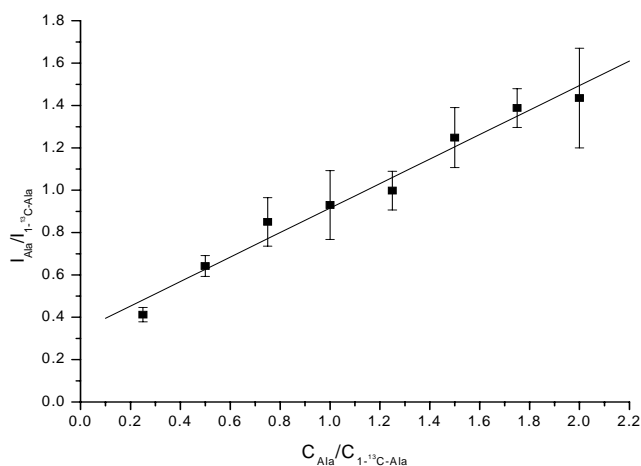


Figure 5.3: Relative quantitation of alanine using $1-^{13}C$ -alanine as IS in the system [BMIM][PF₆]/CCA at a molar IL:analyte (IL:A) ratio of 100:1. The molar M/(A+IS)-ratio was 50. Mean values of 5 spots per ratio were measured manually; 200 shots per spot were accumulated. I: peak intensities of analyte and internal standard; C: concentration of analyte and internal standard. r^2 : 0.987, mean standard deviation: 11.5%, intercept: 0.33.

5.3 Analysis of peptides and proteins in IL

The analysis of 5- to 22-mer peptides in the mass range between 556 and 2465 Da in the presence of ILs was tested after addition of CCA. The more intense signals of all peptides could be observed in the presence of water-immiscible ILs [BMIM][(CF₃SO₂)₂N] and [BMIM][PF₆] (Table 5.4). In the water-miscible ILs [BMIM][BF₄] and [MMIM][(CH₃)₂PO₄] only peaks with low intensities or even no signals (Leu-enkephalin) were observed. Peptides did not deliver any signals in the presence of [BMIM][OctSO₄]. Only [M+H]⁺ signals could be detected for all the peptides. Similar to the results observed for the analysis of amino acids, no Na/K-adducts could be found in the presence of ILs for the the peptides investigated here (Figure 5.4). Sample homogeneity was slightly reduced compared to classical MALDI preparations as described above for the amino acids. The LOD for peptides was about $9 \cdot 10^{-14}$ mol. Peak widths (FWHM) of the signals were again not changed

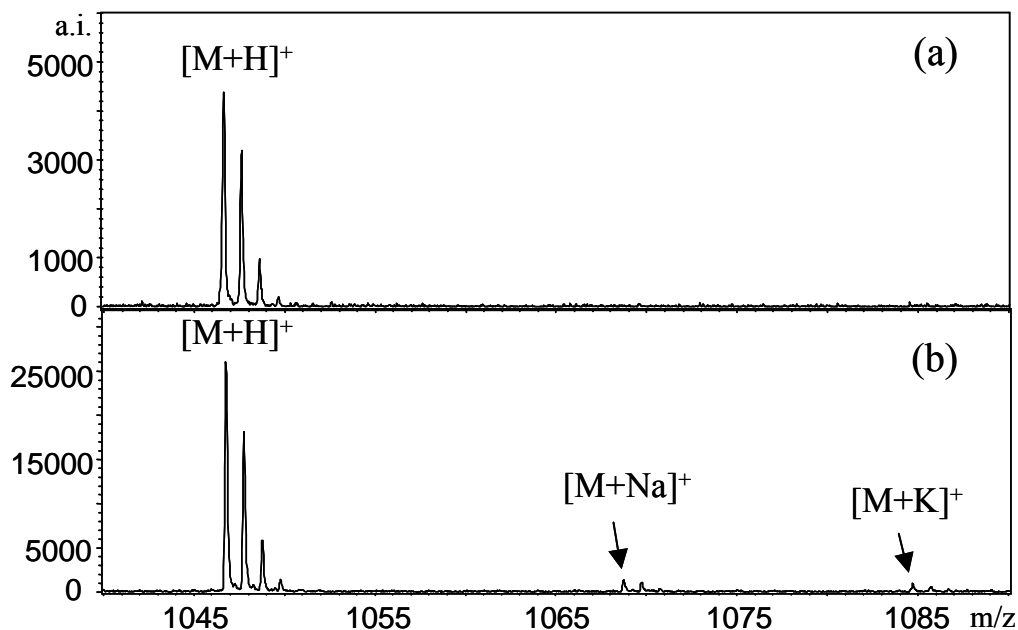


Figure 5.4: MALDI spectra of angiotensin II in CCA (a) in the presence of [BMIM][(CF₃SO₂)₂N] (FWHM: 0.15) and (b) without IL (FWHM: 0.13). 200 shots were accumulated in both cases.

significantly compared to measurement without ILs (Figure 5.4).

SA was used as matrix for the analysis of proteins dissolved in ILs. In contrast to amino acids and peptides, protein signals could be detected when dissolved both in water-miscible as well as water-immiscible ILs. However, their signals were more intensive in the water-miscible ILs. For all proteins, signals were observed in the water-miscible ILs [BMIM][BF₄] and in [MMIM][(CH₃)₂PO₄] (Table 5.4), whereas in [BMIM][OctSO₄] only signals for insulin and cytochrome C could be detected. Amongst the water-immiscible ILs, [BMIM][PF₆] gave signals for insulin and cytochrome C and a weak but still readily detectable signal for BSA, whereas in the presence of [BMIM][(CF₃SO₂)₂N] only insulin gave a signal. In addition to singly charged signals doubly charged signals could be also detected for proteins. In the presence of IL, the signals of the bigger proteins (BSA) were broader and less intense compared to analysis without IL. In case of [BMIM][BF₄], [BF₄]⁻ adducts could be observed for lysozyme (Figure 5.5). Anion-protein adducts have been observed before when anions of low basicity and high coordination affinity to protonated sites were present (Kruger and Karas, 2002; Salih and Zenobi, 1998). Adducts of cations or other anions of the ILs were not observed. The LOD for Cytochrome C in [BMIM][BF₄]/SA was found to be $8 \cdot 10^{-15}$ mol. The

Table 5.4: Analysis of peptides and proteins in ILs. Signal intensities (arbitrary units, measured at laser energies just above threshold) of $[M+H]^+$ of the analytes after accumulation of 200 shots: +: below 2000; ++: 2000 – 5000; +++: 5000 -10000; ++++: >10.000; n.d.: not detected.

	[BMIM] [OctSO ₄]	[BMIM] [BF ₄]	[MMIM] [(CH ₃) ₂ PO ₄]	[BMIM] [PF ₆]	[BMIM] [(CF ₃ SO ₂) ₂ N]	Matrix
Leu-enkephalin	n.d.	n.d.	n.d.	+	+	CCA
Bradykinin	n.d.	+	+	++	+++	CCA
Angiotensin II	n.d.	+	+	++	++	CCA
Substanz P	n.d.	+	+	++	+	CCA
Neurotensin	n.d.	+	+	+++	+++	CCA
ACTH(1-17)	n.d.	n.d.	+	+	+	CCA
ACTH(18-39)	n.d.	+	+	+	+	CCA
Insulin	+	++++	++++	++++	++	SA
Cytochrome C	+++	++++	++++	++	n.d.	SA
Lysozyme	n.d.	+++	+++	n.d.	n.d.	SA
BSA	n.d.	+	+	+	n.d.	SA

results acquired from the analysis of amino acids, peptides and proteins dissolved in ILs showed a likely correlation between the molecular weight of the analyte and their ionization behaviour in different ILs. As a rough rule, water-immiscible ILs seem to be more adequate for the detection of LMW analytes whereas biopolymers with higher masses can be analyzed more easily when dissolved in water-miscible ILs. It has to be mentioned, that water miscibility of an IL is not equivalent to its polarity, which is almost identical for the ILs investigated here (VanRantwijk et al., 2003). Although ILs can be classified according to their miscibility with water, water-immiscible ILs such as [BMIM][PF₆] can be dissolved in low amounts in water (up to 3%) (Anthony et al., 2001). This is also a prerequisite for dissolving analytes in these solvents as it was performed in the present work.

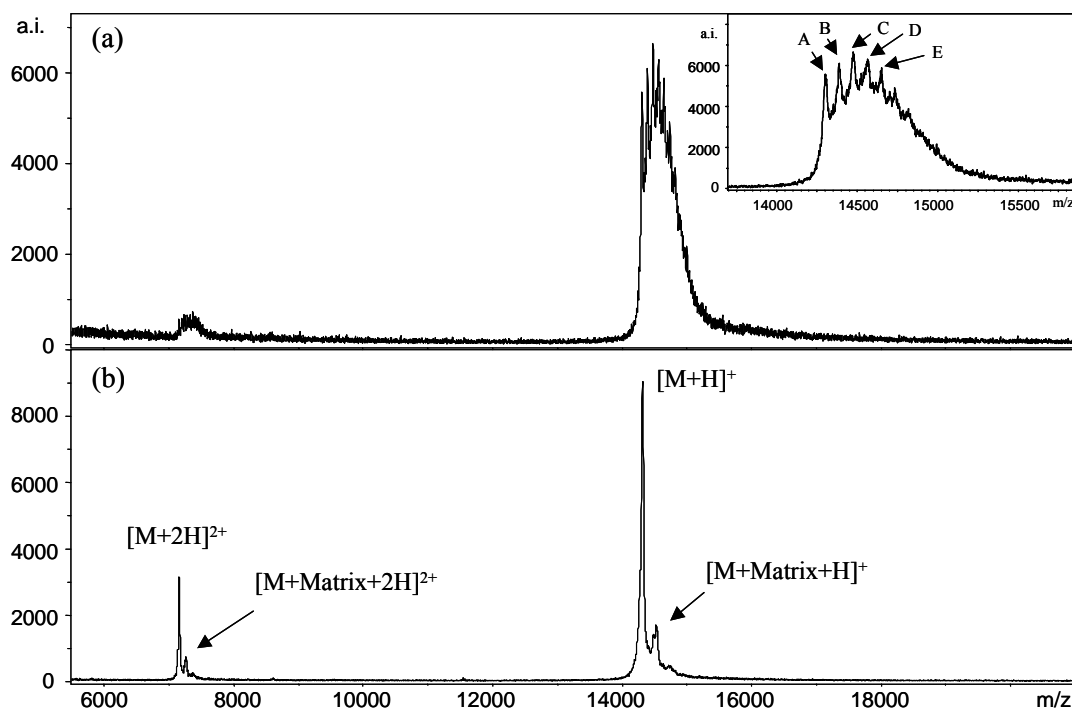


Figure 5.5: (a) MALDI mass spectrum of lysozyme (MW~14300) in [BMIM][BF₄] using SA as solid matrix (the insert shows a detailed view of the BF₄-adduct region: A: [M+H]⁺, B-E: adducts of 1-4 [BF₄]⁻ ions). A molar IL:matrix ratio of 50.000 and molar matrix to analyte ratio of 23000 was applied, 200 shots were accumulated. (b) MALDI-MS spectrum of lysozyme in SA without IL, a molar matrix to analyte ratio of 23000 was applied, 200 shots were accumulated.

5.4 Monitoring of the enzymatic reaction of D-amino acid oxidase in the presence of IL

The application of MALDI-MS for quantitative analysis of amino acids in the presence of ILs was described previously (Chapter 5.2.1). The applicability of the method was further examined for the monitoring of the enzymatic reaction of D-amino acid oxidase (DAAO) carried out in the presence of 40% IL, [BMIM][PF₆]. The enzyme catalyzes the oxidation of a variety of D-amino acids to their respective α -keto acids. Phenylalanine was used as a substrate for the reaction (Figure 5.6). To quantify the substrate, a calibration curve was established for phenylalanine. An important issue for the analysis of LMW analytes by MALDI-MS is the use of a matrix that (i) does not overlap with the analytes and (ii) does most effectively ionize the analytes. The selection of a proper matrix is more critical here because of the problems, which arise from the peak broadening of IL signals and increase of the baseline, which in turn are due to the need for elevated laser energies.

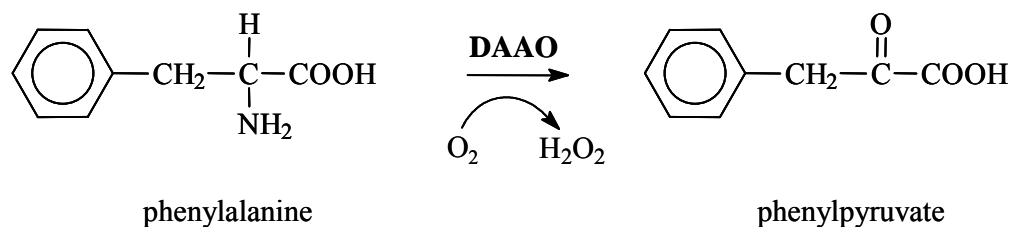


Figure 5.6: Scheme of conversion of phenylalanine to phenylpyruvate catalyzed by the enzyme D-amino acid oxidase (DAAO). Only the D-enantiomer of the substrate is converted by this enzyme.

For this study, the matrix ferulic acid (FA) was found to be better than CCA to achieve higher ionization efficiency of the analyte (phenylalanine) and avoiding overlap of matrix/IL/analyte signals. Additionally, $[\text{Cat}]^+$ -signal of IL was relatively less broadened in FA compared to measurement in CCA.

A satisfactory calibration curve could be achieved for phenylalanine using the isotopically labelled internal standard (6- ^{13}C -phenylalanine) (Figure 5.7 (a)). This calibration curve allowed the quantification of substrate during the enzymatic reaction. It was mentioned earlier that the presence of the ILs resulted in very inhomogeneous sample preparations. Therefore, this leads to a higher standard deviation and possibly of prolonged measurement time. The sample inhomogeneity was also pronounced here for the calibration curve of substrate measured in presence of $[\text{BMIM}][\text{PF}_6]$ with a mean standard deviation of 13%. Nevertheless, the quantitation of the substrate of the enzyme-catalyzed reaction in the presence of IL could be performed (Figure 5.7 (b)). To find out the reliability of the method, the results of the determination of substrate concentration in the enzymatic conversion shown in Figure 5.7 were compared with an established method, e.g. HPLC. The results obtained by MALDI-MS were in good agreement with those obtained by HPLC for the time-points investigated here (Figure 5.7 (b)).

Requirement of very short time of analysis using MALDI-MS compared to HPLC is considered as one of the advantages of using MALDI-MS (Bungert et al., 2004b). In this study, the measurement time was about 16 minutes per sample by HPLC, whereas the time was reduced to about 2 minutes per sample in the case of MALDI analysis. Note the measurement time using MALDI in the presence of IL is about 2-4 times longer than those achieved without ILs (Bungert et al., 2004a). This is mainly caused by the inhomogeneous sample preparation as mentioned before.

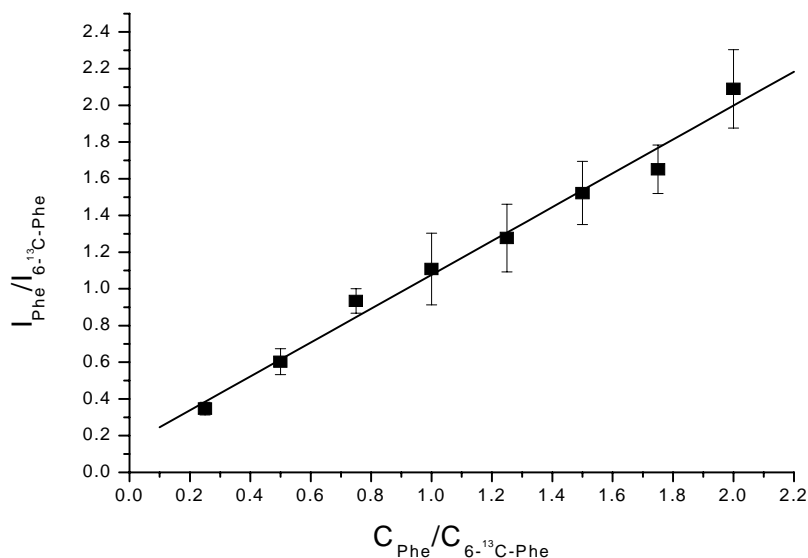


Figure 5.7: Calibration curve for quantification of phenylalanine in the presence of IL ([BMIM][PF₆]) using 6-¹³C-phenylalanine as IS. FA was used as matrix. The error bars indicate the average of 5 spots for each ratio. 200 shots were collected in the positive ion mode. The measurement was performed manually.

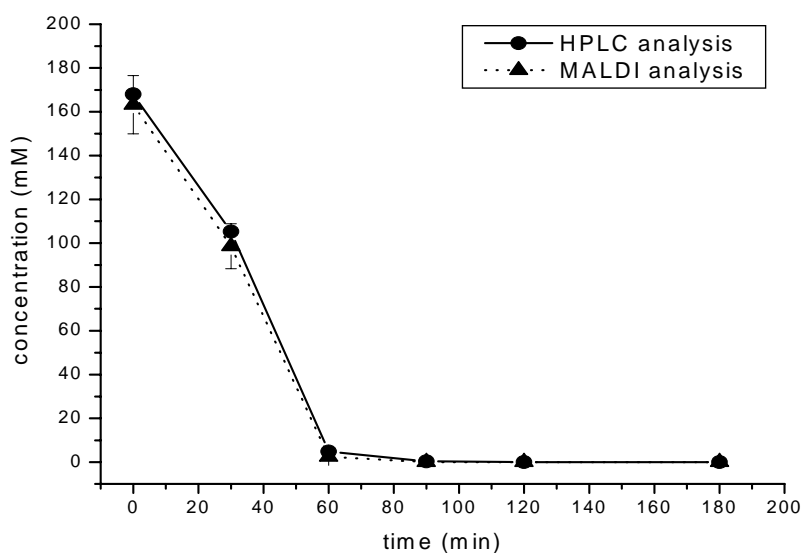


Figure 5.8: Monitoring of substrate consumption versus reaction time measured by MALDI and HPLC in enzyme-catalyzed reaction of DAAD in the presence of 40% IL ([BMIM][PF₆]). The error bars indicate the average of 5 spots for each ratio for MALDI measurement and two fold measurements for HPLC analysis. 200 shots were collected for MALDI measurement for each spot in the positive ion mode. The measurements were carried out manually for MALDI measurement. The HPLC results were kindly provided by Prof. Fischer's group, Institute for Food Technology, University of Hohenheim.

Nevertheless, in comparison with HPLC measurements the MALDI-based quantification clearly allows a noticeable increase in sample throughput.

6 Ion Formation in MALDI

Although MALDI mass spectrometry has been used for more than 10 years now, the mechanisms involved in ion generation and desorption are still not fully understood. All theories and models involve photoionization and chemical ionization which can be classified as primary and secondary ion formation processes, respectively (Karas and Kruger, 2003; Knochenmuss and Zenobi, 2003). According to these theories, primary ionization is related to generation of the first ions from neutral molecules in the sample by laser photons and can be correlated to the ionization potential (IP) of the molecules. These ions are often matrix-derived species. It was shown with pH-dependent dyes embedded in matrices that analytes were in the same charge state in matrix crystals as they have been in solution (Kruger et al., 2001). The primary process for these preformed ions is their desorption together with matrix clusters.

Secondary processes are those that lead to ions that are not directly generated by primary processes, in particular analyte ions. After desorption of an analyte from the matrix, protonization and cationization of analyte molecules will take place, which can be different from one analyte to another and from one matrix to another. The proton, H^+ , is generally supposed to be provided by matrix molecules. Proton affinity (PA) of the analyte and matrix molecules could probably describe proton transfer between matrix and analyte molecules (Zenobi and Knochenmuss, 1998). There is evidence that not only matrix serves as proton donor but also the solvent plays an active role in the cluster desorption process mentioned above. It was found that in matrix preparations a residual amount of the particular solvent, e.g. water and/or acetonitrile, could be found (Kruger et al., 2001). The residual solvent content (acetonitrile:water, 1:1/v:v) in matrix crystals was described to be between 0.3 to 3% in dried matrix preparations. It was also shown that in the best case a very weak $[M+H]^+$ signal can be observed when analyte and matrix are physically mixed and applied under solvent-free condition (Gluckmann et al., 2001). On the other hand, a solvent-free preparation method was presented allowing a successful ionization of neutral polymers and insulin (Trimpin et al., 2001). We did not investigate the solvent content in the ILMs presented here, but it has to be expected that there is still solvent and TFA (when used) present even after several hours under vacuum conditions in the mass spectrometer.

The sol-gel assisted laser desorption/ionization mass spectrometry with the matrix substance embedded in a sol-gel structure was introduced for the analysis of amino acids and peptides

(Lin and Chen, 2002b). The spectra measured from these systems are reported to be free of matrix signals. Further, the sodium and potassium adduct ions of the analytes commonly observed in conventional MALDI, were not observed in spectra generated from this matrix system. It was suggested that H_3O^+ and analyte may be simultaneously desorbed and the analyte molecules may be protonated in the gas phase via ion-molecule reactions, when the laser irradiated the sol-gel-derived DHB film. It can therefore be concluded that in ILMs as well as in solid matrices, both matrix and solvent molecules are involved in protonization mechanism thus affecting directly peak intensities.

Good peak intensities are a prerequisite for satisfying spectra quality and for qualitative and quantitative measurements. They can be reached by using higher laser energies, which on the other hand can cause fragmentation of analytes (and matrices). The comparison of peak intensities in different classical solid preparations is nearly impossible due to the lack of homogeneity. The use of ILMs minimizes this problem and may therefore be helpful for the direct comparison of different matrix systems. We performed basic experiments to explain the effect of both the components of the ionic liquids (acid and base) and the analytes on their ionization behaviour. Comparison of peak intensities of different analytes in one matrix system is possible because the same laser energy was used. On the other hand, for the comparison of intensities of one analyte in different matrices the additional effect of different laser energies has to be taken into account in some cases. Therefore, for determination of the peak intensities, laser energy was chosen just above the point at which the signal of analyte starts to occur (threshold level). The peak intensities varied strongly depending on the combination of acid-base-analyte (Table 6.1). The addition of TFA also had an influence on the peak intensities. In some cases, where no signal without addition of TFA could be detected, its addition allowed detection of the analyte.

Higher peak intensities compared to the solid matrix could be observed in some cases, in others suppression effects of one of the components could be found. Proton affinities as well as pK_a values of matrices (acid and base component) and analytes have to be taken into account for the explanation of these observations. It is also important to keep in mind the fact that all amino acids share similar pK_a -values for the α -amino- and the α -carboxylic groups, and the main differences are introduced by the side chains. The proton affinity of an amino acid is correlated to the whole molecule including both the α -amino- and α -carboxylic groups as well as the side chain function. In all experiments, proton affinities are thus more reliable for explanation of the ionization behaviour of the analyte compared to pK_a values.

Table 6.1: Peak intensities ($[M+H]^+$) of different analytes in solid or ILMs. The intensities were estimated at the optimal laser energy above threshold level. The values for bradykinin and human insulin were taken from reference (Armstrong et al., 2001), the values for the proton affinities (kJ/mol) from references (Hunter and Lias, 2003; Zenobi and Knochemuss, 1998), the pK_a -values of cation (base compound of the ILM) and analyte (side chain functionality) were provided by the chemical suppliers. PA_c : proton affinity of the cation, PA_a : proton affinity of analyte, M/A. molar matrix-to-analyte ratio, n.d.: not detected.

Matrix	Analyte	Peak Intensity	TFA	M/A	PA_c/PA_a (kJ/mol)	pK_a/pK_a cation/analyte
CCA	Arginine	8200	-	1	850.5 / 1051	3 / 12.5
CCA-TBA	Arginine	20000	-	1	998.5 / 1051	10.89 / 12.5
DHB	Arginine	5200	-	3	856 / 1051	2.97 / 12.5
DHB-Py	Arginine	n.d.	-	1		
DHB-TBA	Arginine	5000	-	1	998.5 / 1051	10.89 / 12.5
DHB-Py	Arginine	6500	-	3	930 / 1051	5.23 / 12.5
CCA	Glutamic acid	1000	-	1	850.5 / 913	3 / 4.25
CCA-TBA	Glutamic acid	n.d.	-	1	998.5 / 913	10.89 / 4.25
CCA	Alanine	4800	-	1	850.5 / 901.6	3 / -
CCA-TBA	Alanine	n.d.	-	1	998.5 / 901.6	10.89 / -
DHB	Alanine	5000	-	1	856 / 901.6	2.97 / -
DHB-TBA	Alanine	n.d.	-	1	998.5 / 901.6	10.89 / -
DHB	Glutamic acid	2200	-	1	856 / 913	2.97 / 4.25
DHB-TBA	Glutamic acid	n.d.	-	1	998.5 / 913	10.89 / 4.25
DHB-Py	Glutamic acid	n.d.	+	3	930 / 903.2	5.23 / 10.78
DHB-Py	Lysine	2200	+	3	930 / 996	5.23 / 10.53
CCA-TBA	Bradykinin	53000	+	50000	-	-
CCA	Bradykinin	40000	+	50000	-	-
SA-TBA	Bradykinin	50000	+	50000	-	-
SA	Bradykinin	12000	+	50000	-	-
CCA-TBA	Human insulin	11000	+	50000	-	-
CCA	Human insulin	24000	+	50000	-	-
SA-TBA	Human insulin	n.d.	+	50000	-	-
SA	Human insulin	43000	+	50000	-	-

For example, the $[M+H]^+$ -ion could be observed for lysine in DHB-PY, whereas that of cysteine could not be observed in this matrix. The pK_a -values of both amino acid side chains are very similar (Lys = 10.53, Cys = 10.78), but the proton affinity of lysine (996.0) is higher than that of cysteine (903.2) (Table 6.1).

Tributylamine in combination with DHB or CCA for example was found to have a positive effect on analytes like arginine, whereas neutral (in respect to the side chain) (alanine) and acidic analytes (glutamate) seemed to be suppressed. In contrast to arginine, for the second basic amino acid lysine the peak intensity for $[M+H]^+$ was not very high in DHB-TBA or CCA-TBA. This reflects again the influence of the proton affinity, because the difference in the proton affinities between lysine (996.0) and TBA (998.5) is very small, thus reducing protonization of the analyte.

The basic amino acids arginine and lysine did not show any peak in DHB-Py at a molar matrix-to-analyte ratio of one, in contrast to other amino acids. At a M/A of three, both amino acids could be detected in this matrix system. On the other hand, arginine showed a peak intensity of 5000 in DHB-TBA at a matrix-to-analyte ratio of one, which showed the complementary effect of TBA on a basic analyte (arginine) (Table 6.1). This may be caused by the fact that a strong base can facilitate the transfers of protons from the matrix to the analyte. On the other hand, the analyte must be able to accept protons from the matrix which corresponds to a higher proton affinity. CCA-TBA and SA-TBA were already used as matrix for the measurement of peptides and proteins (Armstrong et al., 2001). The nonapeptide Bradykinin showed higher peak intensities compared to both corresponding solid matrices. In contrast, insulin showed a lower peak intensity in CCA-TBA and no peak in SA-TBA. This could be referred to the reason mentioned above, because Bradykinine (Arg-Pro-Pro-Gly-Phe-Ser-Pro-Phe-Arg) has two arginine residues out of nine amino acids, whereas in insulin there is just one arginine out of fifty one amino acids. Additionally, amino acids sequence of insulin consists of many amino acids with low proton affinity such as Cysteine (Nicol and Smith, 1960).

6.1 Comparison of IL with ILM

The application of UV-MALDI is limited to the use of matrices which are able to absorb light in the wavelength applied (Karas et al., 1985). At present, most MALDI instruments are operating with lasers in the UV-range, either of 337 or 335 nm. The ILs tested here are

imidazolium salts (Figure 6.1), which do not significantly absorb at 337 nm applied in this study. Their main absorption band in solution (methanol) is between 260-300 nm. The molar absorption coefficients at 337 nm (ϵ_{337}) are below $1 \text{ L mol}^{-1} \text{ cm}^{-1}$ (Table 5.1). The absorption maximum of the highly viscous ILs without additional solvent is expected to be slightly red-shifted compared to the situation in solution, but is still expected to be very low compared to classical solid MALDI-matrices (the ϵ_{337} for 2,5-DHB in EtOH/H₂O 9:1 is about $3100 \text{ L} \cdot \text{mol}^{-1} \cdot \text{cm}^{-1}$ (Horneffer et al., 1999). In spite of having relatively low absorption at wavelength 337 nm, however, ILs could be analyzed without addition of solid matrices in LDI-MS as shown earlier (Chapter 5.1). This lack of capability to absorb efficiently the laser light at this wavelength (337 nm) could be one of the reasons that make ILs unsuitable as MALDI-matrices in contrast to ILMs. Because ILMs are formed by combination of solid MALDI-matrices with different bases and, thus, the presence of solid MALDI-matrices guarantee an efficient absorption (Figure 6.1).

Moreover, matrix molecules must provide protons to promote protonization of analyte (in positive ion mode analysis). It has been demonstrated earlier that ionic liquids having a cationic moiety with an acidic proton can produce the desired gas-phase ions. This led to the speculation that due to the lack of available protons in many ILs, the analyte cannot be protonized (Armstrong et al., 2001). In this context, the H/D-exchange experiment performed with ILs here (see Chapter 6.2.3) showed clear evidence for the exchange of a proton by deuterium. Therefore, the apparent lack of ability of ILs to protonize the analyte cannot be explained at this juncture.

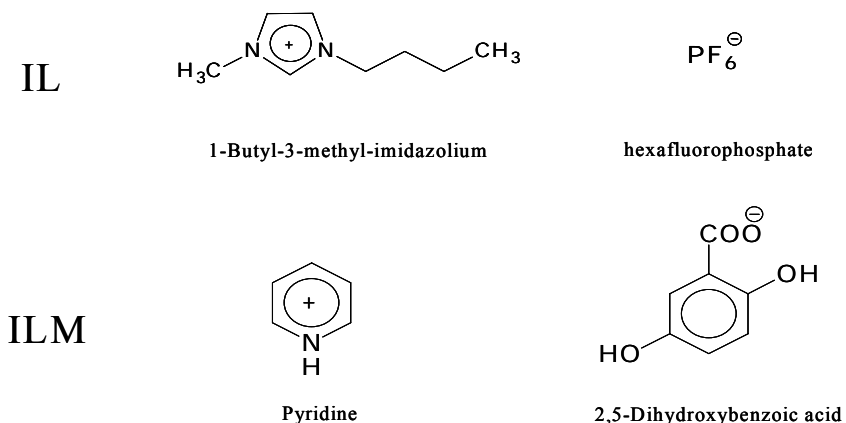


Figure 6.1: Typical structures of cation and anion of IL (top) and ILM (bottom).

6.2 Ion formation in LDI and MALDI analysis of ILs

In contrast to ILMs, ILs are not suited as MALDI-matrices. However, both the components of the IL as well as the analytes dissolved in IL can be analyzed when classical MALDI-matrices are added to the ILs. The presence of ILs in MALDI analysis leads to some characteristic observations with respect to ion formation and adduct formation, which deviate to a certain extent from standard MALDI analysis. These phenomena occur in dependence of the nature of the components of the ILs and only some general observations will be discussed here.

The most obvious features of MALDI in the presence of IL concern (i) the extensive adduct formation between IL-cations and IL-anions (in contrast to LDI), (ii) the nearly complete absence of metal ion adducts (Na^+ , K^+), (iii) the negligible adduct formation between analytes and IL-cations or IL-anions, respectively, (iv) the increased laser threshold resulting in peak broadening, which is most pronounced for IL signals, moderate for high-mass analytes (proteins), but absent in case of low-mass analytes, (v) the matrix-dependent detection of $[\text{Cat}+\text{H}]^{*+}$ ions of the IL cations and (vi) the influence of the water miscibility of the IL on analyte response.

6.2.1 Adduct formation between IL-cations and IL-anions

Like all salts, ILs exhibit ionic interactions in solution. These ionic interactions could be partially preserved upon mixing with a matrix or matrix solutions. Depending on the existence of loose or tight ion pairs in the condensed phase, either single ions or aggregates of different composition can be liberated upon laser irradiation. Although a close ionic contact must be assumed in pure IL, aggregates are only preserved with MALDI and not with LDI. Similar aggregates ($[\text{nCat}+(\text{n}-1)\text{An}]^+$) with $\text{n}=1-3$ were observed in electrospray ionization MS (Alfassi et al., 2003). Multi component clusters (n up to 22) as observed in FAB MS (Abdul-Sada et al., 1997) were not observed here. Liberation of adduct-free IL-cations from ionic adducts, e.g. of the form $[\text{2Cat}+\text{An}]^+$, can occur by proton transfer neutralization and subsequent desolvation of the neutralized anion, if the energy barrier of the respective proton transfer neutralization can be overcome. The fact that no adducts are observed in LDI may reflect the destruction of noncovalent ionic adducts when too much energy is transferred to them. On the other hand, the detection of IL-aggregates shows that tight ionic interactions are

at least partially preserved upon matrix admixture and that these aggregates can survive the considerably softer MALDI process.

6.2.2 Absence of metal ion adducts

In the presence of ILs no sodium- or potassium adducts were observed in MALDI analysis, neither for the matrix components nor for the analytes. The most straightforward explanation for this phenomenon is the displacement of metal cations by IL-cations and formation of ion-pairs where IL cations are attached to negatively charged groups. Vice versa, the displaced metal cations may form (tight) ion-pairs with IL-anions, which were indeed detected with MALDI. Cation exchange is a widely applied strategy to avoid metal ion adducts, particularly at acidic sites such as phosphate groups of oligonucleotides (Nordhoff et al., 1992; Zhu et al., 1996). Small cations with acidic protons like ammonia or pyridinium compounds are frequently used, since they can evaporate easily after neutralization reactions with anionic sites, which occur during or after laser excitation.

6.2.3 Absence of Adducts between IL-cations/anions and analytes

The imidazolium cations of the IL are alkylated at both nitrogen atoms and have therefore no acidic NH or OH group capable of proton transfer. Thus, imidazolium adducts should appear in MALDI spectra if close ion-pairs exist in the matrix crystal. This absence of IL-cationic adducts may be the consequence of long ionic distances in the matrix crystals. However, another way of adduct decomposition may also exist. N,N-substituted imidazolium ions are known as precursors of relatively stable carbenes, which have attracted some attention as ligands for organometallic complexes used as catalysts (Herrmann, 2002). These carbenes are formed upon proton abstraction at C2. NMR experiments including hydrogen-deuterium exchange studies showed, that the protons at C2 position of N,N-dialkylated imidazolium salts are slightly acidic having pKa-values in the range of 20-23 (Amyes et al., 2004).

We performed similar H/D-exchange experiments followed by MALDI mass spectrometry with the ILs [BMIM][BF₄] and [MMIM][(CH₃)₂PO₄]. The LDI spectra of both cations showed clear evidences for an exchange of a proton by deuterium after incubation of the IL with a basic D₂O solution. For the [MMIM]-salt, the [Cat]⁺ signal observed at m/z 97 shifted almost completely to m/z 98 upon 12 hours incubation with D₂O (Figure 6.2). For the [BMIM]-salt, additionally to the [Cat]⁺-signal at m/z = 139, further signals at m/z = 140

([Cat]⁺, one proton exchanged to deuterium) and $m/z = 141$ were detected. Interestingly, the formation of the ion at $m/z = 141$ was increased, when the H/D-exchange experiment was performed under UV-irradiation. The identity of the m/z 141 ion is still unknown. When a mixture of deuterium-exchanged [MMIM]-salt was mixed with DHB, the signals of DHB were not changed compared to the situation with non-exchanged [MMIM]-salt, thus reflecting, that the deuterium was not transferred to the matrix under these conditions.

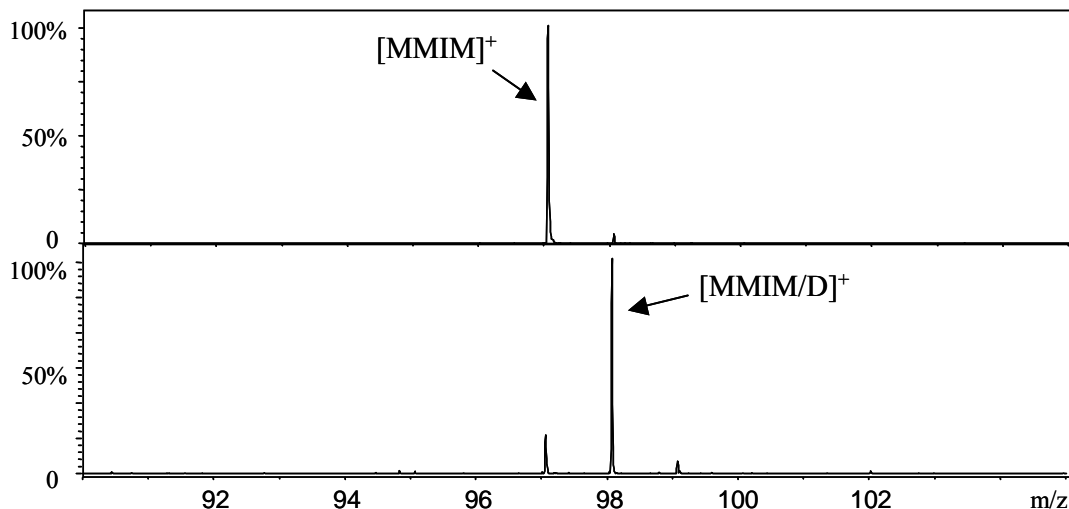


Figure 6.2: LDI mass spectra of [MMIM][(CH₃)₂PO₄] after incubation with water (top) and D₂O (bottom). 200 shots were accumulated for each spectrum.

6.2.4 Laser threshold and peak broadening in dependence of analyte size

The results of the H/D-exchange experiments together with the low abundance of cationic adducts suggest that metal cations at anionic sites are exchanged against imidazolium ions, which then are lost upon proton transfer-induced decomposition. This liberation of analytes from ionic-adduct precursors is only possible if sufficient energy is supplied to overcome the respective energy barrier, which may explain the relatively high laser intensity threshold. Such proton transfer neutralization should in principle occur not only in case of cationic adducts but also in case of anionic adducts. The preservation of anion adducts and their energy-dependent decomposition has been shown before (Kruger and Karas, 2002). Fragmentation of ionic adducts occurs both in the ion source and in the field-free drift region, and decomposition can result in peak broadening in case of high energy barriers, e.g. if

anions with low gas phase basicity are involved. The relatively broad MALDI signals of proteins in the presence of ILs may thus be the consequence of IL-adduct decomposition.

Matrix anions have considerably higher PA than IL-anions, because the latter are bases which correspond to strong acids. Consequently, proton transfer from an IL-cation to a matrix anion (ion-pair neutralization) should therefore have a much lower energy barrier than proton transfer neutralization between IL ion-pairs. Indeed, ionic adducts between IL-components are much more abundant than adducts between IL-cations and matrices. Moreover, the intensities of adducts between IL-cation and matrices correspond roughly to the PA of the corresponding matrix anion (Zenobi and Knochemuss, 1998), which may reflect an easier ion pair neutralization in case of DHB and CCA compared to SA. However, slightly different PA values were reported in the literature for the same matrix anion, and adduct generation may also reflect the tendency to form close-contact ion-pairs upon incorporation into the matrix crystal.

6.2.5 Matrix dependent formation of $[\text{Cat}+\text{H}]^{\bullet+}$ -ions

In LDI analysis, IL cations formed only $[\text{Cat}]^+$ -ions, whereas $[\text{Cat}+\text{H}]^{\bullet+}$ IL ions beside the $[\text{Cat}]^+$ were found after addition of solid MALDI-matrices. $[\text{Cat}+\text{H}]^{\bullet+}$ species could originate either from proton transfer followed by electron capture/transfer or directly via addition of hydrogen atoms. The existence of free H-radicals in the MALDI plume was verified by spectroscopic methods (Scott et al., 1994), and addition of hydrogen was observed before, e.g. at cytosine (Koomen and Russell, 2000) or azo-dyes (Kruger et al., 2001). Potentially, the not unambiguously identified signal at $m/z = 141$ in the H/D-exchange experiment mentioned above may be formed by such UV induced radical exchange reaction.

6.2.6 Influence of IL water miscibility on analyte response

The correlation of the water-miscibility of the IL with the response of amino acids, peptides and proteins in MALDI is quite remarkable. Whereas proteins give only minor MALDI signals in the presence of water-immiscible IL, small analytes like amino acids and peptides are easily detected. Vice versa, water-miscible ILs hinder the analysis of the latter. These observations suggest a mass-dependent influence of ILs on MALDI response. Alternatively, although there was no segregation observed during sample preparation, compound specific

enrichment in different zones of the samples or within crystals may nevertheless occur. Such segregation phenomena are common in MALDI (Chan et al., 1992; Dai et al., 1999), especially in case of hydrophobic analytes. Moreover, differences upon matrix crystallization and analyte incorporation can lead to similar discrimination effects (Cohen and Chait, 1996; Figueroa et al., 1998). An additional effect could be induced by the nature of the ILs, which are non- or only partly soluble in water. This may cause liquid phase separation and partitioning of analytes upon crystallization. However, this could not be observed during sample preparation.

7 Conclusions and Outlook

7.1 ILMs

ILMs showed a high potential to be applied as matrices, whereas ILs were not suited as matrices for MALDI-MS. The problems arising from the inhomogeneity of the sample preparation using solid matrices were significantly reduced by applying ILMs. ILMs allowed both qualitative and quantitative measurement of LMW molecules, peptides and proteins.

ILMs were successfully applied for the analyses of a variety of LMW compounds, such as amino acids, vitamins and sugars. However, as in the case of classical solid matrices, the prediction of the suitability of the ILMs for the measurement of a particular analyte is still not possible. Incorporating an isotopically labeled internal standard for quantification, the quality of a calibration curve with respect to standard deviation and linearity (r^2) improved in the case of amino acids when an ILM was used in comparison to the corresponding solid matrix. In this regard, the 20% reduction of measurement time could also contribute to the advantage of using ILM over solid matrices. Therefore, ILMs can be potentially used for screening of an enzyme-catalyzed reaction by MALDI-MS achieving better accuracy in analyses with shorter measurement time as compared to solid matrices.

The benefits of high sample homogeneity using ILMs together with increased M/A-ratios allowed a direct quantification of peptides and proteins by MALDI mass spectrometry without the use of internal standards. Herein, the obtained calibration curve for the model peptide showed a very good accuracy ($r^2 = 0.997$, mean standard deviation: 8%). The developed method was further applied for the screening of the protease activity. The reliability of the method for the quantitative analysis of protease screening was compared with two established methods, the relative quantification by MALDI-MS in ILM using a homologous peptide (Trp¹¹-Neurotensin) as internal standard and by HPLC-UV-measurements with 214 nm detection. An average deviation of 6% was obtained between these three methods.

Due to the problems related to peak suppression, semi-quantitative rather than absolute quantitative measurement was shown for monitoring of multi-substrate conversions. Nevertheless, the results were sufficient to clearly differentiate good and bad substrates for the enzymatic reaction presented here.

The importance of the M/A-ratio complicates the application of the method in cases where the concentration for the analytes is not known, e.g. for the quantification of peptides in a proteomics environment. For these applications a relative quantification rather than the absolute quantification presented here is recommended.

The application of pyridinium-based ILMs formed with α -cyano-4-hydroxycinnamic acid led to an improved spectral quality in terms of reduction of matrix clusters and chemical noise and the improvement of the signal-to-noise ratios of a number of peptides investigated in this study. Best results were obtained at a molar ratio of CCA:Py-2:1. The achievement of higher sequence coverage together with increased sensitivity thus allows a facilitated identification of proteins by peptide mass fingerprint analysis as well as an improved recognition of protein modifications. For a minority of the peptides investigated, the presence of pyridine led to a slight reduction of the S/N-ratios compared to CCA. Therefore, an optimal way for proteome analysis may be the use of both pure CCA as well as of the non-stoichiometric pyridinium-based ILM in parallel experiments.

The quantification method not using an IS is not restricted to proteolytic reactions. The method can principally be used for all kinds of enzymatic conversions, which go hand in hand with mass changes, e.g. transferase or oxidase/reductase catalyzed reactions as well as for non-enzymatic reactions. Therefore, IS-free quantitative MALDI-MS using ILMs is a suitable method for fast screening for new enzymes or for the search for substrates or inhibitors. This would have an ideal impact on the screening for new enzyme variants, either by obtaining quantitative data for a particular conversion or semi-quantitative data for the monitoring of the change of substrate or product amounts.

LMW compounds, e.g. amino acids, sugars and vitamins are the substrates and products of many biocatalytic reactions. MALDI quantitative analysis without use of an isotope labeled IS will be very applicable for these enzyme-screening processes. Similar to the absolute quantification of peptides and proteins, a set of experiments can be performed to find out the optimal M/A-ratio in which quantification for LMW compounds would be possible without need for an IS. In cases where absolute quantification of LMW compounds is not successful, ILMs can potentially facilitate the quantification with an IS not necessarily similar to the analyte. The application of the ILMs for quantification of peptides using non-analogous internal standard have delivered a satisfactory result (Li and Gross, 2004).

ILMs showed very good stability in the high vacuum applied in mass spectrometry. This could have a potential for the application of ILMs to stabilize otherwise volatile matrices like 4-nitroaniline or 3-aminoquinoline.

There are numerous combinations possible for a tailor-made synthesis of new ILMs. Depending on the combination of acid and base used, the physicochemical properties of the matrix, e.g. pH-values and UV-absorption spectra, can be changed. Therefore, these combinations can be tuned according to the desired analysis, for example for investigations of non-covalent interactions in proteins for which an optimal pH range is required to preserve their tertiary structure and thus retain non-covalent interactions. Additionally, the UV-absorption modification of the matrix may allow improving analyte signal intensity. Moreover, the different acid/base combinations modify the ionization behaviour in MALDI, which may improve the signal intensity of a tested analyte.

Although the use of ILMs has improved the sample homogeneity, it caused intensive Na/K-adducts compared to corresponding solid matrices depending on the acid/base combination used in ILMs. This could be a great benefit to the analysis of sugars, which can be detected best as metal-adducts. This can thus facilitate the screening of sugar converting enzyme reactions.

The preliminary experiments carried out in this study indicated that high sample homogeneity achieved using ILMs could make feasible the direct comparison of various analytes signal intensity in different matrices. Therefore, this may help to give new insight into the mechanisms related to the MALDI ionization, which is only partially understood. Additionally, the presence of both acidic and basic components in these matrix systems can contribute reaching this goal.

Further applications of ILMs can be in LC-MALDI coupling or in the analyses in the negative ion mode. Recently, ILMs were applied for the direct investigation of tissues by MALDI imaging (Lemaire et al., 2006). Thus, application of ILMs as a valuable tool for improved direct tissue analysis by MALDI imaging is expected in the future.

ILMs cannot replace classical known matrices, however, they do extend the field of MALDI-MS applications.

7.2 ILs

LDI and MALDI mass spectrometry are both methods, which allow investigation and characterization of ILs. The analysis is straightforward, and fragmentations can be used for a structural analysis of these solvents.

ILs were not suitable as MALDI-matrices, but the addition of classical MALDI-matrices enabled the analysis of amino acids, peptides and proteins dissolved in the ILs without the need for extraction procedures. Further, using a proper internal standard, a relative quantification was successfully performed in the presence of ILs. The developed quantification protocol was applied for the monitoring of oxidase-catalyzed reaction in the presence of ILs. The measured concentrations of substrate in the enzyme reaction by MALDI were comparable to those determined by HPLC. These features make screening of enzyme activities in the presence of ILs possible. Hence, the direct analysis of substrates and products of chemical and enzyme catalyzed reactions in ILs can be done without the need for pre-purification or separation steps. This allows in-process analysis of these reactions in ILs.

It is reasonable to expect that other LMW compounds, for example educts or products of chemical reactions, can be also analyzed by MALDI-MS in the presence of ILs. Like in classical MALDI analysis, a prediction of the best matrix system suited for a particular analyte has still to be found out by trial-and-error experiments.

Up to now it is still an unsolved question, whether proteins dissolved in ILs can undergo chemical modification. Direct investigation of proteins and tryptic peptides in ILs is a prerequisite to answer this question. In this regard, application of MALDI can reveal new insight for any potential modifications of proteins in the presence of ILs. These findings can improve designing of new ILs suitable for enzymes and thus, biocatalysis in ILs.

MALDI analysis in the presence of IL revealed a number of interesting observations, which are mainly related to ionic interactions, solubility and other effects which are relevant during sample preparation. A closer look on these special features in comparison to other sample preparation procedures in the absence of IL may be valuable, since their understanding could lead to sample preparation procedures with enhanced sensitivity.

8 References

- Abdul-Sada, A. K., Elaiwi, A. E., Greenway, A. M. and Seddon, K. R. (1997). Evidence for the clustering of substituted imidazolium salts via hydrogen bonding under the conditions of fast atom bombardment mass spectrometry. *Eur J Mass Spectrom* **3**, 245-7.
- Abdul-Sada, A. K., Greenway, A. M., Seddon, K. R. and Welton, T. (1992). Fast-Atom Bombardment mass Spectrometric evidence for the formation of tris[tetrachloroaluminate(III)]metallate(II) anions, $[M(AlCl_4)_3]^-$, in acidic ambient-temperature ionic liquids. *Org Mass Spectrom* **27**, 648-9.
- Alfassi, Z. B., Huie, R. E., Milman, B. L. and Neta, P. (2003). Electrospray ionization mass spectrometry of ionic liquids and determination of their solubility in water. *Anal Bioanal Chem* **377**, 159-64.
- Amyes, T. L., Diver, S. T., Richard, J. P., Rivas, F. M. and Toth, K. (2004). Formation and stability of N-heterocyclic carbenes in water: the carbon acid pKa of imidazolium cations in aqueous solution. *J Am Chem Soc* **126**, 4366-74.
- Anderson, J. L. and Armstrong, D. W. (2003). High-stability ionic liquids. A new class of stationary phases for gas chromatography. *Anal Chem* **75**, 4851-8.
- Anderson, J. L., Ding, J., Welton, T. and Armstrong, D. W. (2002). Characterizing ionic liquids on the basis of multiple solvation interactions. *J Am Chem Soc* **124**, 14247-54.
- Anthony, J. L., Maginn, E. J. and Brennecke, J. F. (2001). Solution thermodynamics of imidazolium-based ionic liquids and water. *J Phys Chem B* **105**, 10942-9.
- Armstrong, D. W., He, L. and Liu, Y. S. (1999). Examination of ionic liquids and their interaction with molecules, when used as stationary phases in gas chromatography. *Anal Chem* **71**, 3873-6.
- Armstrong, D. W., Zhang, L. K., He, L. and Gross, M. L. (2001). Ionic liquids as matrixes for matrix-assisted laser desorption/ionization mass spectrometry. *Anal Chem* **73**, 3679-86.
- Baker, G. A., Baker, S. N., Pandey, S. and Bright, F. V. (2005). An analytical view of ionic liquids. *Analyst* **130**, 800-8.
- Bantscheff, M., Dumpelfeld, B. and Kuster, B. (2004). Femtomol sensitivity post-digest (18)O labeling for relative quantification of differential protein complex composition. *Rapid Commun Mass Spectrom* **18**, 869-76.

- Baumgart, S., Lindner, Y., Kuhne, R., Oberemm, A., Wenschuh, H. and Krause, E. (2004). The contributions of specific amino acid side chains to signal intensities of peptides in matrix-assisted laser desorption/ionization mass spectrometry. *Rapid Commun Mass Spectrom* **18**, 863-8.
- Beavis, R. C. and Chait, B. T. (1989). Cinnamic acid derivatives as matrices for ultraviolet laser desorption mass spectrometry of proteins. *Rapid Commun Mass Spectrom* **3**, 432-5.
- Bonhote, P., Dias, A., Papageorgiou, N., Kalyanasundaram, K. and Grätzel, M. (1996). Hydrophobic, highly conductive ambient-temperature molten salts. *J Inorg Chem* **35**, 1168-78.
- Bothner, B., Chavez, R., Wei, J., Strupp, C., Phung, Q., Schneemann, A. and Siuzdak, G. (2000). Monitoring enzyme catalysis with mass spectrometry. *J Biol Chem* **275**, 13455-9.
- Brancia, F. L., Oliver, S. G. and Gaskell, S. J. (2000). Improved matrix-assisted laser desorption/ionization mass spectrometric analysis of tryptic hydrolysates of proteins following guanidination of lysine-containing peptides. *Rapid Commun Mass Spectrom* **14**, 2070-3.
- Bungert, D. (2004). Dissertation, *Technische Biochemie*, Saarland University.
- Bungert, D., Bastian, S., Heckmann-Pohl, D. M., Giffhorn, F., Heinzle, E. and Tholey, A. (2004a). Screening of sugar converting enzymes using quantitative MALDI-ToF mass spectrometry. *Biotechnol Letters* **26**, 1025-1030.
- Bungert, D., Heinzle, E. and Tholey, A. (2004b). Quantitative matrix-assisted laser desorption/ionization mass spectrometry for the determination of enzyme activities. *Anal Biochem* **326**, 167-75.
- Buzzeo, M. C., Evans, R. G. and Compton, R. G. (2004). Non-haloaluminate room-temperature ionic liquids in electrochemistry--a review. *Chemphyschem* **5**, 1106-20.
- Carda-Broch, S., Berthod, A. and Armstrong, D. W. (2003). Ionic matrices for matrix-assisted laser desorption/ionization time-of-flight detection of DNA oligomers. *Rapid Commun Mass Spectrom* **17**, 553-60.
- Chan, T. W. D., Colburn, A. W., Derrick, P. J., Gardiner, D. J. and Bowden, M. (1992). Suppression of matrix-ions in ultraviolet laser desorption: Scanning electron microscopy and Raman spectroscopy of the solid sample. *Org Mass Spectrom* **27**, 188-94.

- Chauvin, Y., Mussmann, L. and Olivier, H. (1996). A novel class of versatile solvents for two-phase catalysis: hydrogenation, isomerization, and hydroformylation of alkenes catalyzed by rhodium Complexes in liquid 1,3-dialkylimidazolium salts. *Angew Chem Int Ed Engl* **34**, 2698-700.
- Cohen, L. H. and Gusev, A. I. (2002). Small molecule analysis by MALDI mass spectrometry. *Anal Bioanal Chem* **373**, 571-86.
- Cohen, S. L. and Chait, B. T. (1996). Influence of matrix solution conditions on the MALDI-MS analysis of peptides and proteins. *Anal Chem* **68**, 31-7.
- Courchesne, P. L. and Patterson, S. D. (1997). Manual microcolumn chromatography for sample cleanup before mass spectrometry. *Biotechniques* **22**, 244-6, 248-50.
- Cramer, R. and Burlingame, A. L. (2000). Employing target modifications for the investigation of liquid infrared matrix-assisted laser desorption/ionization mass spectrometry. *Rapid Commun Mass Spectrom* **14**, 53-60.
- Cramer, R. and Corless, S. (2005). Liquid ultraviolet matrix-assisted laser desorption/ionization -- mass spectrometry for automated proteomic analysis. *Proteomics* **5**, 360-70.
- Cull, S. G., Holbrey, J. D., Vargas-Mora, V., Seddon, K. R. and Lye, G. J. (2000). Room-temperature ionic liquids as replacements for organic solvents in multiphase bioprocess operations. *Biotechnol Bioeng* **69**, 227-33.
- Dai, Y., Whittall, R. M. and Li, L. (1996). Confocal fluorescence microscopic imaging for investigating the analyte distribution in MALDI matrices. *Anal Chem* **68**, 2494-2500.
- Dai, Y., Whittall, R. M. and Li, L. (1999). Two-layer sample preparation: a method for MALDI-MS analysis of complex peptide and protein mixtures. *Anal Chem* **71**, 1087-91.
- Dally, J. E., Gorniak, J., Bowie, R. and Bentzley, C. M. (2003). Quantitation of underivatized free amino acids in mammalian cell culture media using matrix assisted laser desorption ionization time-of-flight mass spectrometry. *Anal. Chem* **75**, 5046-53.
- Deng, Y., Shi, F., Beng, J. and Qiao, K. (2001). Ionic liquid as a green catalytic reaction medium for esterifications. *J Mol Catal A: Chem* **165**, 33-6.
- Doucette, A., Craft, D. and Li, L. (2000). Protein concentration and enzyme digestion on microbeads for MALDI-TOF peptides mass mapping of proteins from dilute solutions. *Anal Chem* **72**, 3355-62.
- Dreisewerd, K. (2003). The desorption process in MALDI. *Chem Rev* **103**, 395-426.

- Duncan, M. W., Matanovic, G. and Cerpa-Poljak, A. (1993). Quantitative analysis of low molecular weight compounds of biological interest by matrix-assisted laser desorption ionization. *Rapid Commun Mass Spectrom* **7**, 1090-4.
- Durazo, A. and Abu-Omar, M. M. (2002). Deuterium NMR spectroscopy is a versatile and economical tool for monitoring reaction kinetics in ionic liquids. *Chem Commun*, 66-7.
- Earle, M. J., Seddon, K. R., Adams, C. J. and Roberts, G. (1998). Friedel–Crafts reactions in room temperature ionic liquids. *Chem Commun*, 2097-8.
- Erbeldinger, M., Mesiano, A. J. and Russell, A. J. (2000). Enzymatic catalysis of formation of Z-aspartame in ionic liquid - An alternative to enzymatic catalysis in organic solvents. *Biotechnol Prog* **16**, 1129-31.
- Fadeev, A. G. and Meagher, M. M. (2001). Opportunities for ionic liquids in recovery of biofuels. *Chem Commun*, 295-6.
- Fenn, J. B., Mann, M., Meng, C. K., Wong, S. F. and Whitehouse, C. M. (1989). Electrospray ionization for mass spectrometry of large biomolecules. *Science* **246**, 64-71.
- Figuroa, I. D., Torres, O. and Russell, D. H. (1998). Effects of the water content in the sample preparation for MALDI on the mass spectra. *Anal Chem* **70**, 4527-33.
- Fischer, T., Sethi, A., Welton, T. and Woolf, J. (1999). Diels-Alder reactions in room-temperature ionic liquids. *Tetrahedron Lett* **40**, 793-6.
- Freemantle, M. (1998). Designer Solvent, ionic liquids may boost clean technology development. *Chem Eng News* **76**, 32-4.
- Galvani, M., Hamdan, M., Righetti, P. G., Gelfi, C., Sebastiano, R. and Citterio, A. (2001). Investigating the reaction of a novel silica capillary coating compound with proteins/peptides by matrix-assisted laser desorption/ionisation time-of-flight mass spectrometry. *Rapid Commun Mass Spectrom* **15**, 210-6.
- Garden, R. W. and Sweedler, J. V. (2000). Heterogeneity within MALDI samples as revealed by mass spectrometric imaging. *Anal Chem* **72**, 30-6.
- Gluckmann, M., Pfenninger, A., Kruger, R., Thierolf, M., Karas, M., Horneffer, V., Hillenkamp, F. and Strupat, K. (2001). Mechanisms in MALDI analysis: surface interaction or incorporation of analytes? *Int J Mass Spectrom* **210-211**, 121-32.
- Gobom, J., Nordhoff, E., Mirgorodskaya, E., Ekman, R. and Roepstorff, P. (1999). Sample purification and preparation technique based on nano-scale reversed-phase columns for the sensitive analysis of complex peptide mixtures by matrix-assisted laser desorption/ionization mass spectrometry. *J Mass Spectrom* **34**, 105-16.

- Gusev, A. I., Wilkinson, W. R., Proctor, A. and Hercules, D. M. (1995). Improvement of signal reproducibility and matrix/comatrix effects in MALDI analysis. *Anal. Chem* **67**, 1034-1041.
- Gygi, S. P., Rist, B., Gerber, S. A., Turecek, F., Gelb, M. H. and Aebersold, R. (1999). Quantitative analysis of complex protein mixtures using isotope-coded affinity tags. *Nat Biotechnol* **17**, 994-9.
- Haebel, S., Albrecht, T., Sparbier, K., Walden, P., Korner, R. and Steup, M. (1998). Electrophoresis-related protein modification: alkylation of carboxy residues revealed by mass spectrometry. *Electrophoresis* **19**, 679-86.
- Hagiwara, R. and Ito, Y. (2000). Room temperature ionic liquids of alkylimidazolium cations and fluoroanions. *J Fluorine Chem* **105**, 221-7.
- Hatsis, P., Brombacher, S., Corr, J., Kovarik, P. and Volmer, D. A. (2003). Quantitative analysis of small pharmaceutical drugs using a high repetition rate laser matrix-assisted laser/desorption ionization source. *Rapid Commun Mass Spectrom* **17**, 2303-9.
- Helmke, S. M., Yen, C. Y., Cios, K. J., Nunley, K., Bristow, M. R., Duncan, M. W. and Perryman, M. B. (2004). Simultaneous quantification of human cardiac alpha- and beta-myosin heavy chain proteins by MALDI-TOF mass spectrometry. *Anal Chem* **76**, 1683-9.
- Hensel, R. R., King, R. C. and Owens, K. G. (1997). Electrospray sample preparation for improved quantitation in matrix-assisted laser desorption/ionization time-of-flight mass spectrometry. *Rapid Commun Mass Spectrom* **11**, 1785-93.
- Herrmann, W. A. (2002). N-Heterocyclic carbenes: A new concept in organometallic catalysis. *Angew Chem Int Ed* **41**, 1290-309.
- Hill, C. R. and Tomalin, G. (1982). A conductometric method for the assay of amidase and peptidase activities. *Anal Biochem* **120**, 165-75.
- Hillenkamp, F., Karas, M., Beavis, R. C. and Chait, B. T. (1991). Matrix-assisted laser desorption/ionization mass spectrometry of biopolymers. *Anal Chem* **63**, 1193A-1203A.
- Holbrey, J. D. and Rogers, R. D. (2003). Physicochemical properties of ionic liquids in Wasserscheid, P. and Welton, T. (Eds), *Ionic liquids in synthesis*, WILEY-VCH.
- Horak, J., Werther, W. and Schmid, E. R. (2001). Optimisation of the quantitative determination of chlormequat by matrix-assisted laser desorption/ionisation mass spectrometry. *Rapid Commun Mass Spectrom* **15**, 241-8.

- Horneffer, V., Dreisewerd, K., Ludemann, H. C., Hillenkamp, F., Lage, M. and Strupat, K. (1999). Is the incorporation of analytes into matrix crystals a prerequisite for matrix-assisted laser desorption/ionization mass spectrometry? A study of five positional isomers of dihydroxybenzoic acid. *Int J Mass Spectrom* **187**, 859-70.
- Horneffer, V., Forsmann, A., Strupat, K., Hillenkamp, F. and Kubitscheck, U. (2001). Localization of analyte molecules in MALDI preparations by confocal laser scanning microscopy. *Anal Chem* **73**, 1016-22.
- Huddleston, J. G. and Rogers, R. D. (1998). Room temperature ionic liquids as novel media for clean liquid-liquid extraction. *Chem Commun*, 1765-66.
- Hunter, E. P. and Lias, S. G. (2003). Proton Affinity Evaluation" in NIST Chemistry WebBook, *NIST Standard Reference Database Number 69*, Eds. P.J. Linstrom and W.G. Mallard, National Institute of Standards and Technology.
- Jain, N., Kumar, A., Chauhan, S. and Chauhan, S. M. S. (2005). Chemical and biochemical transformations in ionic liquids. *Tetrahedron* **61**, 1015-60.
- Jensen, O. N., Mortensen, P., Vorm, O. and Mann, M. (1997). Automation of matrix-assisted laser desorption/ionization mass spectrometry using fuzzy logic feedback control. *Anal Chem* **69**, 1706-14.
- Jiang, T., Gu, Y., Liang, B., Li, J., Shi, Y. and Qu, Q. (2003). Dynamically coating the capillary with 1-alkyl-3-methylimidazolium-based ionic liquids for separation of basic proteins by capillary electrophoresis. *Anal Chim Acta* **479**, 249-54.
- Jones, J. J., Batoy, S. M., Wilkins, C. L., Liyanage, R. and Lay, J. O., Jr. (2005). Ionic liquid matrix-induced metastable decay of peptides and oligonucleotides and stabilization of phospholipids in MALDI FTMS analyses. *J Am Soc Mass Spectrom* **16**, 2000-8.
- Kaftzik, N., Wasserscheid, P. and Kragl, U. (2002). Use of ionic liquids to increase the yield and enzyme stability in the -galactosidase catalysed synthesis of N-acetyllactosamine. *Org Proc Res Dev* **6**, 558-61.
- Kang, M. J., Tholey, A. and Heinzle, E. (2000). Quantitation of low molecular mass substrates and products of enzyme catalyzed reactions using matrix-assisted laser desorption/ionization time-of-flight mass spectrometry. *Rapid Commun Mass Spectrom* **14**, 1972-8.
- Kang, M. J., Tholey, A. and Heinzle, E. (2001). Application of automated matrix-assisted laser desorption/ionization time-of-flight mass spectrometry for the measurement of enzyme activities. *Rapid Commun Mass Spectrom* **15**, 1327-33.

- Karas, M., Bachman, D., Bahr, U. and Hillenkamp, F. (1987). Matrix-assisted ultraviolet laser desorption of non-volatile compounds. *Int J Mass Spectrom Ion Proc* **78**, 53-68.
- Karas, M., Bachmann, D. and Hillenkamp, F. (1985). Influence of the wavelength in high-irradiance ultraviolet laser desorption mass spectrometry of organic molecules. *Anal Chem* **57**, 2935-9.
- Karas, M. and Hillenkamp, F. (1988). Laser desorption ionization of proteins with molecular masses exceeding 10,000 daltons. *Anal Chem* **60**, 2299-301.
- Karas, M. and Kruger, R. (2003). Ion formation in MALDI: the cluster ionization mechanism. *Chem Rev* **103**, 427-40.
- Kaufmann, D. E., Nouroozian, M. and Henze, H. (1996). Molten salts as an efficient medium for palladium catalyzed C-C coupling reactions. *Synlett*, 1091-2.
- Keil, B. (1992). Specificity of proteolysis. *Springer-Verlag Berlin-Heidelberg-NewYork*, 355.
- Kim, K. W., Song, B., M.Y., C. and Kim, M. J. (2001). Biocatalysis in ionic liquids: Markedly enhanced enantioselectivity of lipase. *Org Lett* **3**, 1507-9.
- Knochenmuss, R., Dubois, F., Dale, M. J. and Zenobi, R. (1996). The matrix suppression effect and ionization mechanisms in matrix-assisted laser desorption/ionization. *Rapid Commun Mass Spectrom* **10**, 871-7.
- Knochenmuss, R. and Zenobi, R. (2003). MALDI ionization: the role of in-plume processes. *Chem Rev* **103**, 441-52.
- Konig, S., Zeller, M., Peter-Katalinic, J., Roth, J., Sorg, C. and Vogl, T. (2001). Use of nonspecific cleavage products for protein sequence analysis as shown on calcein isolated from human granulocytes. *J Am Soc Mass Spectrom* **12**, 1180-5.
- Koomen, J. M. and Russell, D. H. (2000). Ultraviolet/matrix-assisted laser desorption/ionization mass spectrometric characterization of 2,5-dihydroxybenzoic acid-induced reductive hydrogenation of oligonucleotides on cytosine residues. *J Mass Spectrom* **35**, 1025-34.
- Kragl, U., Eckstein, M. and Kaftzik, N. (2002). Enzyme catalysis in ionic liquids. *Curr Opin Biotechnol* **13**, 565-71.
- Kruger, R. and Karas, M. (2002). Formation and fate of ion pairs during MALDI analysis: anion adduct generation as an indicative tool to determine ionization processes. *J Am Soc Mass Spectrom* **13**, 1218-26.
- Kruger, R., Pfenninger, A., Fournier, I., Gluckmann, M. and Karas, M. (2001). Analyte incorporation and ionization in matrix-assisted laser desorption/ionization visualized by pH indicator molecular probes. *Anal Chem* **73**, 5812-21.

- Kussmann, M., Lassing, U., Sturmer, C. A., Przybylski, M. and Roepstorff, P. (1997). Matrix-assisted laser desorption/ionization mass spectrometric peptide mapping of the neural cell adhesion protein neurolin purified by sodium dodecyl sulfate polyacrylamide gel electrophoresis or acidic precipitation. *J Mass Spectrom* **32**, 483-93.
- Landry, F., Lombardo, C. R. and Smith, J. W. (2000). A method for application of samples to matrix-assisted laser desorption ionization time-of-flight targets that enhances peptide detection. *Anal Biochem* **279**, 1-8.
- Laszlo, J. A. and Compton, D. L. (2001). Alpha-chymotrypsin catalysis in imidazolium-based ionic liquids. *Biotechnol Bioeng* **75**, 181-6.
- Lemaire, R., Tabet, J. C., Ducoroy, P., Hendra, J. B., Salzet, M. and Fournier, I. (2006). Solid ionic matrixes for direct tissue analysis and MALDI imaging. *Anal Chem* **78**, 809-19.
- Li, Y. L. and Gross, M. L. (2004). Ionic-liquid matrixes for quantitative analysis by MALDI-TOF mass spectrometry. *J Am Soc Mass Spectrom* **15**, 1833-7.
- Li, Y. L., Gross, M. L. and Hsu, F. F. (2005). Ionic-liquid matrixes for improved analysis of phospholipids by MALDI-TOF mass spectrometry. *J Am Soc Mass Spectrom* **16**, 679-82.
- Lin, Y. S. and Chen, Y. C. (2002a). Laser desorption/ionization time-of-flight mass spectrometry on sol-gel-derived 2,5-dihydroxybenzoic acid film. *Anal Chem* **74**, 5793-8.
- Lin, Y. S. and Chen, Y. C. (2002b). Laser desorption/ionization time-of-flight mass spectrometry on sol-gel-derived 2,5-dihydroxybenzoic acid film. *Anal Chem* **74**, 5793-8.
- Ling, Y. C., Lin, L. and Chen, Y. T. (1998). Quantitative analysis of antibiotics by matrix-assisted laser desorption/ionization time-of-flight mass spectrometry. *Rapid Commun Mass Spectrom* **12**, 317-27.
- Madeira Lau, R., Van Rintwijk, F., K.R., S. and R.A., S. (2000). Lipase-catalyzed reactions in ionic liquids. *Organ Lett* **2**, 4189-91.
- Mank, M., Stahl, B. and Boehm, G. (2004). 2,5-Dihydroxybenzoic acid butylamine and other ionic liquid matrixes for enhanced MALDI-MS analysis of biomolecules. *Anal Chem* **76**, 2938-50.
- Massart, D. L., Vandeginste, B. G. M., Buydens, L. M. C., De Jong, S., Lewi, P. J. and Smeyers-Verbeke, J. (1997). Handbook of Chemometrics and Qualimetrics: Part A. *Elsevier Science*.

- McEwen, A. B., Ngo, H. L., LeCompte, K. and Goldman, J. L. (1999). Electrochemical properties of imidazolium salt electrolytes for electrochemical capacitor applications. *J Electrochem Soc* **146**, 1687-95.
- Miliotis, T., Kjellstrom, S., Nilsson, J., Laurell, T., Edholm, L. E. and Marko-Varga, G. (2002). Ready-made matrix-assisted laser desorption/ionization target plates coated with thin matrix layer for automated sample deposition in high-density array format. *Rapid Commun Mass Spectrom* **16**, 117-26.
- Muddiman, D. C., Gusev, A. I., Proctor, A., Hercules, D. M., Venkataramanan, R. and Diven, W. (1994). Quantitative measurement of cyclosporin A in blood by time-of-flight mass spectrometry. *Anal Chem* **66**, 2362-8.
- Munchbach, M., Quadroni, M., Miotto, G. and James, P. (2000). Quantitation and facilitated de novo sequencing of proteins by isotopic N-terminal labeling of peptides with a fragmentation-directing moiety. *Anal Chem* **72**, 4047-57.
- Nelson, R. W., McLean, M. A. and Hutchens, T. W. (1994). Quantitative determination of proteins by matrix-assisted laser desorption/ionization time-of-flight mass spectrometry. *Anal Chem* **66**, 1408-15.
- Nicol, D. S. and Smith, L. F. (1960). Amino-acid sequence of human insulin. *Nature* **187**, 483-5.
- Nicola, A. J., Gusev, A. I., Proctor, A., Jackson, E. K. and Hercules, D. M. (1995). Application of the fast-evaporation sample preparation method for improving quantification of angiotensin II by matrix-assisted laser desorption/ionization. *Rapid Commun Mass Spectrom* **9**, 1164-71.
- Niwayama, S., Kurono, S. and Matsumoto, H. (2003). Synthesis of ¹³C-labeled iodoacetanilide and application to quantitative peptide analysis by isotope differential mass spectrometry. *Bioorg Med Chem Lett* **13**, 2913-6.
- Nordhoff, E., Ingendoh, A., Cramer, R., Overberg, A., Stahl, B., Karas, M., Hillenkamp, F. and Crain, P. F. (1992). Matrix-assisted laser desorption/ionization mass spectrometry of nucleic acids with wavelengths in the ultraviolet and infrared. *Rapid Commun Mass Spectrom* **6**, 771-6.
- Oda, Y., Huang, K., Cross, F. R., Cowburn, D. and Chait, B. T. (1999). Accurate quantitation of protein expression and site-specific phosphorylation. *Proc Natl Acad Sci U S A* **96**, 6591-6.

- Okrasa, K., Guibe-Jampel, E. and Therisod, M. (2003). Ionic liquids as a new reaction medium for oxidase–peroxidase-catalyzed sulfoxidation. *Tetrahedron: Asymmetry* **14**, 2487-90.
- Olumee, Z., Sadeghi, M., Tang, X. D. and Vertes, A. (1995). Amino acid-composition and wavelength effects in matrix-assisted laser-desorption/ionization. *Rapid Commun Mass Spectrom* **9**, 744-52.
- Onnerfjord, P., Ekstrom, S., Bergquist, J., Nilsson, J., Laurell, T. and Marko-Varga, G. (1999). Homogeneous sample preparation for automated high throughput analysis with matrix-assisted laser desorption/ionisation time-of-flight mass spectrometry. *Rapid Commun Mass Spectrom* **13**, 315-22.
- Oxley, J. D., Prozorov, T. and Suslick, K. S. (2003). Sonochemistry and sonoluminescence of room-temperature ionic liquids. *J Am Chem Soc* **125**, 11138-9.
- Padliya, N. D. and Wood, T. D. (2004). A strategy to improve peptide mass fingerprinting matches through the optimization of matrix-assisted laser desorption/ionization matrix selection and formulation. *Proteomics* **4**, 466-73.
- Palm, A. K. and Novotny, M. V. (2004). Analytical characterization of a facile porous polymer monolithic trypsin microreactor enabling peptide mass mapping using mass spectrometry. *Rapid Commun Mass Spectrom* **18**, 1374-82.
- Park, S. and Kazlauskas, R. J. (2001). Improved preparation and use of room-temperature ionic liquids in lipase-catalyzed enantio- and regioselective acylations. *J Organ Chem* **66**, 8395-401.
- Pfründer, H., Amidjojo, M., Kragl, U. and Weuster-Botz, D. (2004). Efficient whole-Cell biotransformation in a biphasic ionic liquid/water system. *Angew Chem Int Ed Engl* **43**, 4529-31.
- Ross, P. L., Huang, Y. N., Marchese, J. N., Williamson, B., Parker, K., Hattan, S., Khainovski, N., Pillai, S., Dey, S., Daniels, S., Purkayastha, S., Juhasz, P., Martin, S., Bartlet-Jones, M., He, F., Jacobson, A. and Pappin, D. J. (2004). Multiplexed protein quantitation in *Saccharomyces cerevisiae* using amine-reactive isobaric tagging reagents. *Mol Cell Proteomics* **3**, 1154-69.
- Salih, B. and Zenobi, R. (1998). MALDI mass spectrometry of dye-peptide and dye-protein complexes. *Anal Chem* **70**, 1536-43.
- Schaefer, H., Chamrad, D. C., Marcus, K., Reidegeld, K. A., Bluggel, M. and Meyer, H. E. (2005). Tryptic transpeptidation products observed in proteome analysis by liquid chromatography-tandem mass spectrometry. *Proteomics* **5**, 846-52.

- Schluter, H., Jankowski, J., Rykl, J., Thiemann, J., Belgardt, S., Zidek, W., Wittmann, B. and Pohl, T. (2003). Detection of protease activities with the mass-spectrometry-assisted enzyme-screening (MES) system. *Anal Bioanal Chem* **377**, 1102-7.
- Schmidt, A., Kellermann, J. and Lottspeich, F. (2005). A novel strategy for quantitative proteomics using isotope-coded protein labels. *Proteomics* **5**, 4-15.
- Schmidt, F., Krah, A., Schmid, M., Jungblut, P. R. and Thiede, B. (2006). Distinctive mass losses of tryptic peptides generated by matrix-assisted laser desorption/ionization time-of-flight/time-of-flight. *Rapid Commun Mass Spectrom* **20**, 933-6.
- Schöfer, S. H., Kaftzik, N., Kragl, U. and Wasserscheid, P. (2001). Enzyme catalysis in ionic liquids: lipase catalysed kinetic resolution of 1-phenylethanol with improved enantioselectivity. *Chem Commun*, 425-6.
- Schürenberg, M., Dreisewerd, K. and Hillenkamp, F. (1999). Laser desorption/ionization mass spectrometry of peptides and proteins with particle suspension matrixes. *Anal Chem* **71**, 221-9.
- Scott, C. T. J., Kosmidis, C., Jia, W. J., Ledingham, K. W. D. and Singhal, R. P. (1994). Formation of atomic hydrogen in matrix assisted laser desorption/ionization. *Rapid Commun Mass Spectrom* **8**, 829-32.
- Sechi, S. (2002). A method to identify and simultaneously determine the relative quantities of proteins isolated by gel electrophoresis. *Rapid Commun Mass Spectrom* **16**, 1416-24.
- Sechi, S. and Chait, B. T. (1998). Modification of cysteine residues by alkylation. A tool in peptide mapping and protein identification. *Anal Chem* **70**, 5150-8.
- Shahgholi, M., Garcia, B. A., Chiu, N. H., Heaney, P. J. and Tang, K. (2001). Sugar additives for MALDI matrices improve signal allowing the smallest nucleotide change (A:T) in a DNA sequence to be resolved. *Nucleic Acids Res* **29**, E91.
- Smirnov, I. P., Zhu, X., Taylor, T., Huang, Y., Ross, P., Papayanopoulos, I. A., Martin, S. A. and Pappin, D. J. (2004). Suppression of alpha-cyano-4-hydroxycinnamic acid matrix clusters and reduction of chemical noise in MALDI-TOF mass spectrometry. *Anal Chem* **76**, 2958-65.
- Song, C. E. and Roh, E. J. (2000). Practical method to recycle a chiral (salen)Mn epoxidation catalyst by using an ionic liquid. *Chem Commun*, 837-8.
- Stepnowski, P., Muller, A., Behrend, P., Ranke, J., Hoffmann, J. and Jastorff, B. (2003). Reversed-phase liquid chromatographic method for the determination of selected room-temperature ionic liquid cations. *J Chromatogr A* **993**, 173-8.

- Surette, J. K. D., Green, L. and Singer, R. D. (1996). 1-Ethyl-3-methylimidazolium halogenoaluminate melts as reaction media for the Friedel–Crafts acylation of ferrocene. *Chem Commun*, 2753-4.
- Sze, E. T., Chan, T. W. and Wang, G. (1998). Formulation of matrix solutions for use in matrix-assisted laser desorption/ionization of biomolecules. *J Am Soc Mass Spectrom* **9**, 166-74.
- Tanaka, K., Waki, H., Ido, Y., Akita, S., Yoshida, Y. and Yoshida, T. (1988). Protein and polymer analyses up to m/z 100 000 by laser ionization time-of-flight mass spectrometry. *Rapid Commun Mass Spectrom* **2**, 151-153.
- Tang, X., Sadeghi, M., Olumee, Z., Vertes, A., Braatz, J. A., McIlwain, L. K. and Dreifuss, P. A. (1996). Detection and quantitation of beta-2-microglobulin glycosylated end products in human serum by matrix-assisted laser desorption/ionization mass spectrometry. *Anal Chem* **68**, 3740-5.
- Thiede, B., Lamer, S., Mattow, J., Siejak, F., Dimmler, C., Rudel, T. and Jungblut, P. R. (2000). Analysis of missed cleavage sites, tryptophan oxidation and N-terminal pyroglutamylation after in-gel tryptic digestion. *Rapid Commun Mass Spectrom* **14**, 496-502.
- Tholey, A. and Heinzle, E. (2002). Methods for biocatalyst screening. *Adv Biochem Eng Biotechnol* **74**, 1-19.
- Tholey, A., Wittmann, C., Kang, M. J., Bungert, D., Hollemeyer, K. and Heinzle, E. (2002). Derivatization of small biomolecules for optimized matrix-assisted laser desorption/ionization mass spectrometry. *J Mass Spectrom* **37**, 963-73.
- Trimpin, S., Rouhanipour, A., Az, R., Rader, H. J. and Mullen, K. (2001). New aspects in matrix-assisted laser desorption/ionization time-of-flight mass spectrometry: a universal solvent-free sample preparation. *Rapid Commun Mass Spectrom* **15**, 1364-73.
- Turney, K. and Harrison, W. W. (2004). Liquid supports for ultraviolet atmospheric pressure matrix-assisted laser desorption/ionization. *Rapid Commun Mass Spectrom* **18**, 629-35.
- Vandell, V. E. and Limbach, P. A. (1999). Polyamine co-matrices for matrix-assisted laser desorption/ionization mass spectrometry of oligonucleotides. *Rapid Commun Mass Spectrom* **13**, 2014-21.
- VanRantwijk, F., Madeira Lau, R. and Sheldon, R. A. (2003). Biocatalytic transformations in ionic liquids. *Trends in Biotechnol* **21**, 131-8.

- Visser, A. E., Swatloski, R. P., Reichert, W. M., Griffin, S. T. and Rogers, R. D. (2000). Traditional extractants in nontraditional solvents: Groups 1 and 2 extraction by crown ethers in room-temperature ionic liquids. *Ind Eng Chem Res* **39**, 3596-604.
- Vorm, O., Roepstorff, P. and Mann, M. (1994). Improved resolution and very high sensitivity in MALDI TOF of matrix surfaces made by fast evaporation. *Anal Chem* **66**, 3281-7.
- Wang, B. H., Dreisewerd, K., Bahr, U., Karas, M. and Hillenkamp, F. (1993). Gas-phase cationization and protonation of neutrals generated by matrix-assisted laser desorption. *J Am Soc Mass Spectrom* **4**, 393-8.
- Wang, Q., Jakubowski, J. A., Sweedler, J. V. and Bohn, P. W. (2004). Quantitative submonolayer spatial mapping of Arg-Gly-Asp-containing peptide organomercaptan gradients on gold with matrix-assisted laser desorption/ionization mass spectrometry. *Anal Chem* **76**, 1-8.
- Wang, Y. K., Ma, Z., Quinn, D. F. and Fu, E. W. (2002). Inverse ¹⁵N-metabolic labeling/mass spectrometry for comparative proteomics and rapid identification of protein markers/targets. *Rapid Commun Mass Spectrom* **16**, 1389-97.
- Wasserscheid, P. and Keim, W. (2000). Ionic Liquids-New "Solutions" for transition metal catalysis. *Angew Chem Int Ed Engl* **39**, 3772-89.
- Wenschuh, H., Halada, P., Lamer, S., Jungblut, P. and Krause, E. (1998). The ease of peptide detection by matrix-assisted laser desorption/ionization mass spectrometry: the effect of secondary structure on signal intensity. *Rapid Commun Mass Spectrom* **12**, 115-9.
- Wittmann, C. and Heinzle, E. (2001). Application of MALDI-TOF MS to lysine-producing *Corynebacterium glutamicum*: a novel approach for metabolic flux analysis. *Eur J Biochem* **268**, 2441-55.
- Xiang, F. and Beavis, R. C. (1994). A method to increase contaminant tolerance in protein matrix assisted laser desorption/ionization by the fabrication of thin protein-doped polycrystalline films. *Rapid Commun Mass Spectrom* **8**, 199-204.
- Xiaohua, X., Liang, Z., Xia, L. and Jiang, S. (2004). Ionic liquids as additives in high performance liquid chromatography: Analysis of amines and the interaction mechanism of ionic liquids. *Anal Chim Acta* **519**, 207-11.
- Yan, W., Gardella, J. A., Jr. and Wood, T. D. (2002). Quantitative analysis of technical polymer mixtures by matrix assisted laser desorption/ionization time of flight mass spectrometry. *J Am Soc Mass Spectrom* **13**, 914-20.

- Yanes, E. G., Gratz, S. R., Baldwin, M. J., Robison, S. E. and Stalcup, A. M. (2001). Capillary electrophoretic application of 1-alkyl-3-methylimidazolium-based ionic liquids. *Anal Chem* **73**, 3838-44.
- Zenobi, R. and Knochemuss, R. (1998). Ion formation in Maldi Mass Spectrometry. *Mass Spectrometry Reviews* **17**, 337-366.
- Zhang, W., He, L., Gu, Y., Liu, X. and Jiang, S. (2003). Effect of ionic Liquids as mobile phase additives on retention of catecholamines in reversed-phase high-performance liquid chromatography. *Anal Lett* **36**, 827-38.
- Zhao, H. and Malhotra, S. V. (2002). Enzymatic resolution of amino acid esters using ionic liquid N-ethyl pyridinium trifluoroacetate. *Biotechnol Letters* **24**, 1257-60.
- Zhu, X. and Papayannopoulos, I. A. (2003). Improvement in the detection of low concentration protein digests on a MALDI TOF/TOF workstation by reducing -cyano-4-hydroxycinnamic acid adduct ions. *J Biomol Tech* **14**, 298-307.
- Zhu, Y. F., Chung, C. N., Taranenko, N. I., Allman, S. L., Martin, S. A., Haff, L. and Chen, C. H. (1996). The study of 2,3,4-trihydroxyacetophenone and 2,4,6-trihydroxyacetophenone as matrices for DNA detection in matrix-assisted laser desorption/ionization time-of-flight mass spectrometry. *Rapid Commun Mass Spectrom* **10**, 383-8.

9 Appendix

9.1 Abbreviations

[BMIM][(CF₃SO₂)₂N]	1-butyl-3-methyl-imidazolium-bis-trifluoromethane-sulfonimide
[BMIM][BF₄]	1-butyl-3-methyl-imidazolium-tetrafluoroborate
[BMIM][OctSO₄]	1-butyl-3-methyl-imidazolium-octylsulfate
[BMIM][PF₆]	1-butyl-3-methyl-imidazolium-hexafluorophosphate
[MMIM][(CH₃)₂PO₄]	1,3-dimethyl-imidazolium-dimethylphosphate
A	analyte
ATP	adenosine 5-triphosphate
BSA	bovine serum albumin
CCA	α-cyano-4-hydroxycinnamic acid
CE	capillary electrophoresis
Da	dalton
DAAO	D-amino acid oxidase
DHB	2,5-dihydroxybenzoic acid
DMAPA	3-dimethylamino-1-propylamine
DMED	N, N-dimethylethylenediamine
DNA	deoxyribonucleic acid
ESI	electrospray ionization
FA	4-hydroxy-3-methoxycinnamic acid, ferulic acid
FAB	fast atom bombardment
FWHM	full width of half-maximum
GC	gas chromatography
H/D exchange	hydrogen/deuterium exchange
HPLC	high performance liquid chromatography
IL	ionic liquid
ILM	ionic liquid matrix
InAA	3-indoleacrylic acid
IR	infrared
IS	internal standard
LMW	low molecular weight

LOD	limit of detection
M/A	matrix-to-analyte ratio
MALDI	matrix assisted laser desorption/ionization
MI	1-methylimidazole
Na/K-adduct	sodium/potassium-adduct
NAD	nicotinamide adenine dinucleotide
NHS-acetate	N-hydroxysuccinimid-acetate
NMR	nuclear magnetic resonance
ODN	oligodeoxynucleotide
PMF	peptide mass fingerprint
Py	pyridine
RSD	relative standard deviation
SA	3,5-dimethoxy-4-hydroxycinnamic acid
SDS	sodium dodecyl sulphate
TBA	tributylamine
TEA	triethylamine
TFA	trifluoroacetic acid
UV	ultraviolet

9.2 Publications

1. Zabet-Moghaddam, M., Heinzle, E. and Tholey, A. (2004). Qualitative and quantitative analysis of low molecular weight compounds by ultraviolet matrix-assisted laser desorption/ionization mass spectrometry using ionic liquid matrices. *Rapid Commun Mass Spectrom* **18**, 141-8.
2. Zabet-Moghaddam, M., Kruger, R., Heinzle, E. and Tholey, A. (2004). Matrix-assisted laser desorption/ionization mass spectrometry for the characterization of ionic liquids and the analysis of amino acids, peptides and proteins in ionic liquids. *J Mass Spectrom* **39**, 1494-505.
3. Zabet-Moghaddam, M., Heinzle, E., Lasaosa, M. and Tholey, A. (2006). Pyridinium-based ionic liquid matrices can improve the identification of proteins by peptide mass-fingerprint analysis with matrix-assisted laser desorption/ionization mass spectrometry. *Anal Bioanal Chem* **384**, 215-24.
4. Tholey, A., Zabet-Moghaddam, M. and Heinzle, E. (2006). Quantification of peptides for the monitoring of protease-catalyzed reactions by matrix-assisted laser desorption/ionization mass spectrometry using ionic liquid matrixes. *Anal Chem* **78**, 291-7.

Eidesstattliche Versicherung

Hiermit versichere ich, Masoud Zabet Moghaddam, an Eides statt, dass ich die vorliegende Arbeit selbständig und ohne Benutzung anderer als der angegebenen Hilfsmittel angefertigt habe. Die aus anderen Quellen oder indirekt übernommenen Daten und Konzepte sind unter Angabe der Quelle gekennzeichnet.

Die Arbeit wurde bisher weder im In- noch im Ausland in gleicher oder in ähnlicher Form in einem Verfahren zur Erlangung eines akademischen Grades vorgelegt.

Saarbrücken, 2006

Masoud Zabet Moghaddam

Curriculum Vitae

First Name Masoud
Family Name Zabet Moghaddam
Birth Date/Place 10. Feb. 1974, Tehran, Iran

Educations

1992 High School Degree, Mashhad, Iran

1992-1996 Chemistry Department, Islamic Azad University of Mashhad, Iran
Bachelor of Science (B.Sc.)
Major: Chemistry

1999-2001 Chemistry Department, Pune University, India
Master of Science (M.Sc.)
Major: Biochemistry
Master Thesis: Immobilization of Acid Phosphatase Enzyme from
Erythra Indica

2002-2006 Technische Biochemie, Saarland University, Germany
Doctoral Degree (Ph.D.)

2006-Present Texas Tech University (TTU), Texas, USA
Postdoctoral Research Associate